Organometallic Vapor Phase Epitaxy of ZnSe with Novel Zn and Se Sources

by

JEUNG-SOO HUH

B.S. Metallurgy, Seoul National University (1983)
M.S. Metallurgy, Seoul National University (1985)

Submitted to the Department of Materials
Science and Engineering in Partial Fulfillment
of the Requirements for the Degree of

DOCTOR OF PHILOSOPHY

at the

MASSACHUSETTS INSTITUTE OF TECHNOLOGY

February 1994

Signature of Author _____
Department of Materials Science and Engineering
January 7, 1994

Certified by _____
Klavs F. Jensen
Professor, Department of Chemical Engineering and Materials Science
Thesis Supervisor

Accepted by _____
Carl V. Thompson II
Professor of Electronic Materials
Chair, Departmental Committee on Graduate Students

Organometallic Vapor Phase Epitaxy of ZnSe with Novel Zn and Se Sources

by
Jeung-Soo Huh

Submitted to the Department of Materials Science and Engineering
on January 7, 1994 in partial fulfillment of
the requirements for the degree of
Doctor of Philosophy in Electronic Materials

ABSTRACT

Organometallic vapor phase epitaxy (OMVPE) of high quality ZnSe has been investigated with particular emphasis on three critical issues; (1) reduction of prereaction between organometallic Zn and Se sources, (2) microwave plasma doping, and (3) organometallic Se replacements of H_2Se. The growth and nitrogen doping of ZnSe by low pressure OMVPE were investigated in a vertical downflow reactor equipped with a laser interferometer for *in-situ* growth rate measurements, and a microwave plasma cavity for precracking of ammonia for nitrogen doping. Particular emphasis was placed on understanding growth characteristics and reducing the prereaction in the gas phase through the use of a new adduct source, dimethylzinc:triethylamine ($DMZn:NEt_3$), instead of dimethylzinc (DMZn). At higher temperatures and pressures, growth results obtained with $DMZn:NEt_3$ are similar to those obtained using DMZn with the morphology exhibiting familiar hillock-shaped features. At lower temperatures ($< 300^oC$) and pressures (< 30 Torr), growth rates are higher with the adduct source and the surface morphology is improved relative to films synthesized with DMZn. Hall measurements and photoluminescence spectra of the grown films demonstrate that DMZn and $DMZn:NEt_3$ produce materials with comparable electronic and optical properties. Microwave plasma decomposition of ammonia was investigated as a possible approach to increasing nitrogen incorporation in ZnSe. Photoluminescence spectra indicated increased nitrogen

doping relative to conventional ammonia doping. The electrical conductivity was, however, still low 10^{15} cm^{-3}, presumably because of H passivation of N acceptors.

The growth of ZnSe was also investigated with dimethylzinc-triethylamine (DMZn:NEt_3) and several organometallic Se sources, specifically *tertiary*-butyl allyl selenide (tBASe), 2-selena-3-(1-methylethyl)-bicyclo[2.2.1]hept-5-ene (bCpSe), diallyl selenide (DASe) and diisopropyl selenide (DIPSe). These reagents are potential replacements of H_2Se for low temperature growth of ZnSe. Epitaxial ZnSe layers were grown at temperature as low as 350°C with a reasonable growth rate (~1μm/h). Surface morphology, crystalline and interface quality of ZnSe films on (001) GaAs were confirmed by scanning electron microscopy, double crystal diffractometry and Rutherford backscattering spectrometry. The 4K Photoluminescence showed good near-band-edge excitonic spectra. Secondary ion mass spectrometry (SIMS) revealed negligible carbon incorporation in ZnSe films grown from tBASe, bCpSe and DIPSe even at high VI/II ratios, in contrast to a carbon concentration of 10^{21} cm^{-3} in ZnSe films grown from DASe. Of the sources investigated, tBASe showed the best materials characteristics.

Thesis Supervisor : Professor Klavs F. Jensen
Title : Professor of Materials Science and Chemical Engineering

Contents

Lists of Figures

Lists of Tables

Acknowledgments

The most rewarding part of this thesis is the interactions I have had with many people, who not only contributed scientifically but also touched personally. The following acknowledgements constitute only a small fraction of those who helped me to finish this thesis.

First, I thank my thesis advisor, Professor Klavs F. Jensen for the guidance, encouragement and support which he has offered me. I will always appreciate his patience, his generosity with his time and his insightful ideas throughout this work. I am also grateful to Professors L.A.Kolodzeijski, A.Witt and K.Kolenbrander for serving on my thesis committee and for helpful suggestions and advices during the preparation of this dissertation.

Dr. Don Heiman of Francis National Magnet Laboratory, without whose help and suggestions a great part of this thesis would never have been possible. I really thank for guiding me optical processes in semiconductors and letting me use so promptly his photoluminescence equipment.

I can not forget about Dr. John Melngailis for expanding my background upto submicron lithography with his focused ion beam equipment. I always remember his positive attitude and generosity.

Professor Harry Gatos and Dr. Jacek Lagowski gave me an insight about electronic materials at the first stage of MIT.

I am grateful to our OMVPE group fellow members like A.Annaparaganda, C.Brian, M.Danek, J.Han, T.Merchant, S.Ngiam, S.Patnaik and S.Salim, and members of Korean materials science graduate students. Special thanks to J.Nando for proofreading this document.

My warmest thanks go to Gate Bible Study members, especially Drs. P.Jang, H.Park, D.Rhee, C.Oh, S.Lee and Mr. J.Ahn and J.Lee, and Korean Hope Church members, who have supported me physically, emotionally and spiriually during the whole life of MIT.

Special thanks, hugs and kisses to my lovely wife, Jeong-Ok, who is always present to provide me with joy and happiness and who has had a

abundant supply of love and patience to calm and soothe me when times were rough. And my wonderful son, Seyoung, for love and a big smile. I also extend my love to my parents, parents-in-law, sisters, brothers, sisters-in-law and brothers-in-law for their continuous encourgements from a long distance.

Chapter 1

Introduction

1.1. Zinc Selenide and Growth Techniques

ZnSe has long been recognized as one of the most technologically promising II-VI semiconductors for optoelectronic devices, specifically light-emitting diodes and visible laser diodes in the blue spectral region for use [Kukimoto, 1989; Bhargava, 1989] in optical memories, printers and short range communication via polymer fibers. The potential arises from its direct band-gap energy of 2.67 eV at room temperature and its expected high luminescence efficiency. In order to realize device applications that rely on carrier injection through a p-n junction, it is essential to control the carrier type and concentration by extrinsic impurity doping without causing any degradation of the luminescent properties. Many attempts [Neumark, 1989a; Cheng *et al.*, 1989; Shibata *et al.*, 1988; Yodo and Yamashita, 1989] have been made to obtain well-controlled and low-resistive n-type epilayers under appropriate growth conditions.

Organometallic Vapor Phase Epitaxy (OMVPE) is a low temperature crystal growth technique which is extensively employed for III-V device fabrication. The low growth temperature and non-equilibrium nature of the growth processes are expected to suppress self-compensation and native defect formation, which limits the formation of p-type ZnSe. This low temperature

growth technique has produced better quality samples which display photoluminescence spectra with dominant near-band-edge and weak deep-level emissions [Giapis, 1989a]. Even though the samples grown by Molecular Beam Epitaxy (MBE) or OMVPE were superior to those grown by bulk crystal growth techniques, nearly all (doped and undoped) samples were still found to be n-type [Fan and Williams, 1985; Fujita *et al.*, 1984]. The reason for the difficulty in growing p-type ZnSe is not completely understood, but it is believed to be related to the unintentional incorporation of shallow- or deep-donor defects. It is unclear, however, whether these defect levels are due to the incorporation of chemical impurities or native defects (or some combination of both). The identification and control of these unwanted defects and the controllable incorporation of dopants is essential if ZnSe is to be used as optoelectronic materials. It is thus apparent that the investigation of doping effect on ZnSe is needed for the understanding of the optical and electronic properties of ZnSe.

1.1.1. II-VI Compound Semiconductors

II-VI compound materials were the earliest materials used on a large industrial scale for the production of semiconductors. They were primarily used as luminescent coatings for color television tubes from the late sixties.

The II-VI compounds compromise a group of semiconductor materials having a great variety of properties for exploitation: the direct energy band gap vary from a negative 0.3 eV for Hg-based compounds to nearly 3.7 eV for ZnS. Figure 1.1 shows a map of energy gap versus lattice constant for various semiconductors. Moreover, they luminesce efficiently throughout the visible spectrum under electrical and optical form of stimulation. Most of these

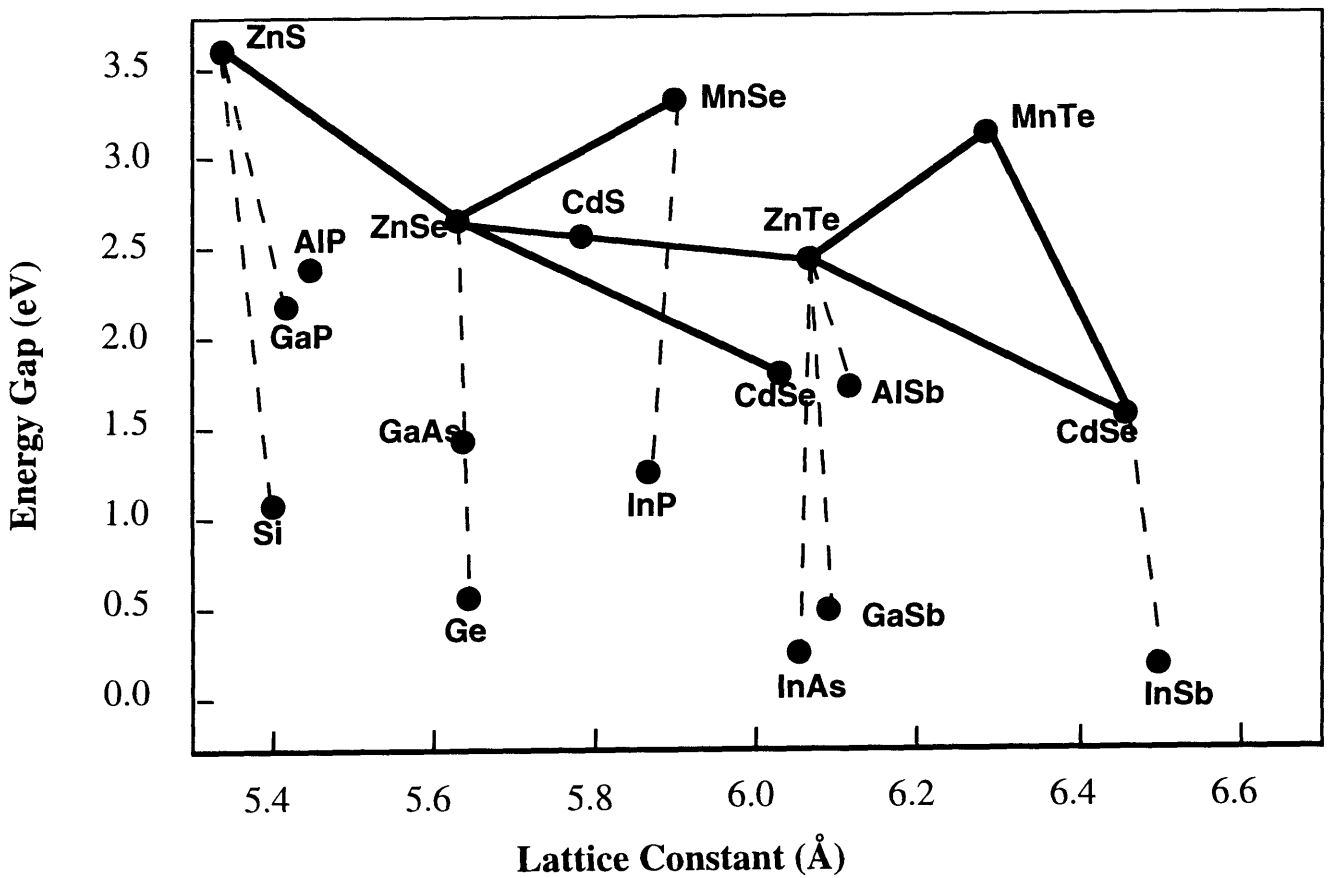

Figure 1.1 Lattice constant and energy bandgap for different group VI, III-V and II-VI semiconductor compounds

compounds are readily miscible allowing the whole visible spectrum to be covered by a continuous variation of the bandgap [Hartmann *et al.*, 1982]. However, growth of bulk crystal, single crystalline layers and epitaxial layers is more complex and costly than for Si, Ge and III-V compounds. Less is known about control of native defects and impurities as well as their electrical and optical property. The bonding in compound, formed by reaction of elements of group II with those of group VI, has a rather high degree of ionic character leading to a relatively wide energy gap between the valence and conduction band and direct gaps. These characteristics in turn result in high optical transition probabilities for absorption and luminescence. Effective masses of electrons and holes are substantially higher in II-VI compounds than in elemental and in III-V compound semiconductors. In addition, the radiative lifetime is smaller, because of the high dipole transition probabilities, and consequently diffusion lengths have upper limits and much shorter than those of III-V compounds (Table 1.1).

With respect to gap energies, mobilities and lifetimes, the technological well developed elemental and III-V semiconductors Ge, Si, GaAs and GaP are complemented by the wide gap II-VI compounds, ZnSe, ZnTe and ZnS. Despite their technological potentials, the II-VI compounds have had only a modest impact on our lives compared to elemental and III-V compounds. With the possible exception of the narrow-band-gap alloys of HgCdTe utilized in the infrared sensors, advances in II-VI technology have not followed the pace set by III-V materials'. This discrepancy between the two major classes of compound semiconductors may be viewed as a reflection of the difficult nature of the semi-ionic II-VI's as well as the superior properties of the III-V's for many applications.

Table 1.1

Comparison of technologically important semiconductors and II-VI compounds

Materials	Energy gap (eV:RT,4K)	Transition	Mobility (cm/Vs)	Effective mass (hh, lh)	Ionicity	Lifetime (s)
Ge	0.67, 0.74	ID	4000	1.58, 0.08	0	10^{-3}
Si	1.11,1.166	ID	1500	0.98, 0.19	0	10^{-3}
GaAs	1.43, 1.5195	D	9000	0.34, 0.085	0.31	10^{-8}
ZnTe	2.25, 2.39	D	100	0.68, 0.15	0.61	10^{-7}
ZnSe	2.67, 2.82	D	200	0.78, 0.15	0.63	$<10^{-8}$
ZnS	3.66, 3.8	D	150	0.28	0.62	$<10^{-8}$

Since 1960, many efforts have been made to shorten the wavelength of optoelectronic devices by exploiting wide band gap II-VI compound semiconductors. The research has been driven by potential applications in particular high density optical memories, medical diagnostics, and communications through sea water and ice. The original idea was to use direct-bandgap recombination in wide II-VI semiconductors like ZnSe, ZnS and ZnTe, There were two principal problems were, however, encountered (1) achieving electrical control of the semiconductors by doping and (2) reducing the substantial defect density within the bandgap caused by unintentional impurities and defects. Doping further often directly contributed to the generation of defects. It was easy to make some compounds p-type, specifically ZnTe and others n-type specifically ZnSe, ZnS, but it was difficult to obtain low resistivity in both polarities in a given compound. Thus, the formation of a p-n junction has not been feasible. Meanwhile the defects and imperfections meant that the radiative yield of blue-green photons was very poor even when electrons and holes were introduced by external excitation with light or electron beams.

In optoelectronics there is a weak competition of GaP which served well as a light emitter from the red to yellowish green range with II-VI compounds (Figure 1.2). The GaP-LED is a compromise between the high injection efficiency of a p-n junction and the very low radiative recombination efficiency of an indirect gap material with an insufficiently wide energy gap. Thus the wide band gap II-VI compounds would be good candidates in blue light-emitting diodes if either a structure could be invented to replace the p-n junction or a p-n junction could be produced. The III-V semiconductor light emitting diodes are commonplace, but can only access the longest wavelengths in the visible range.

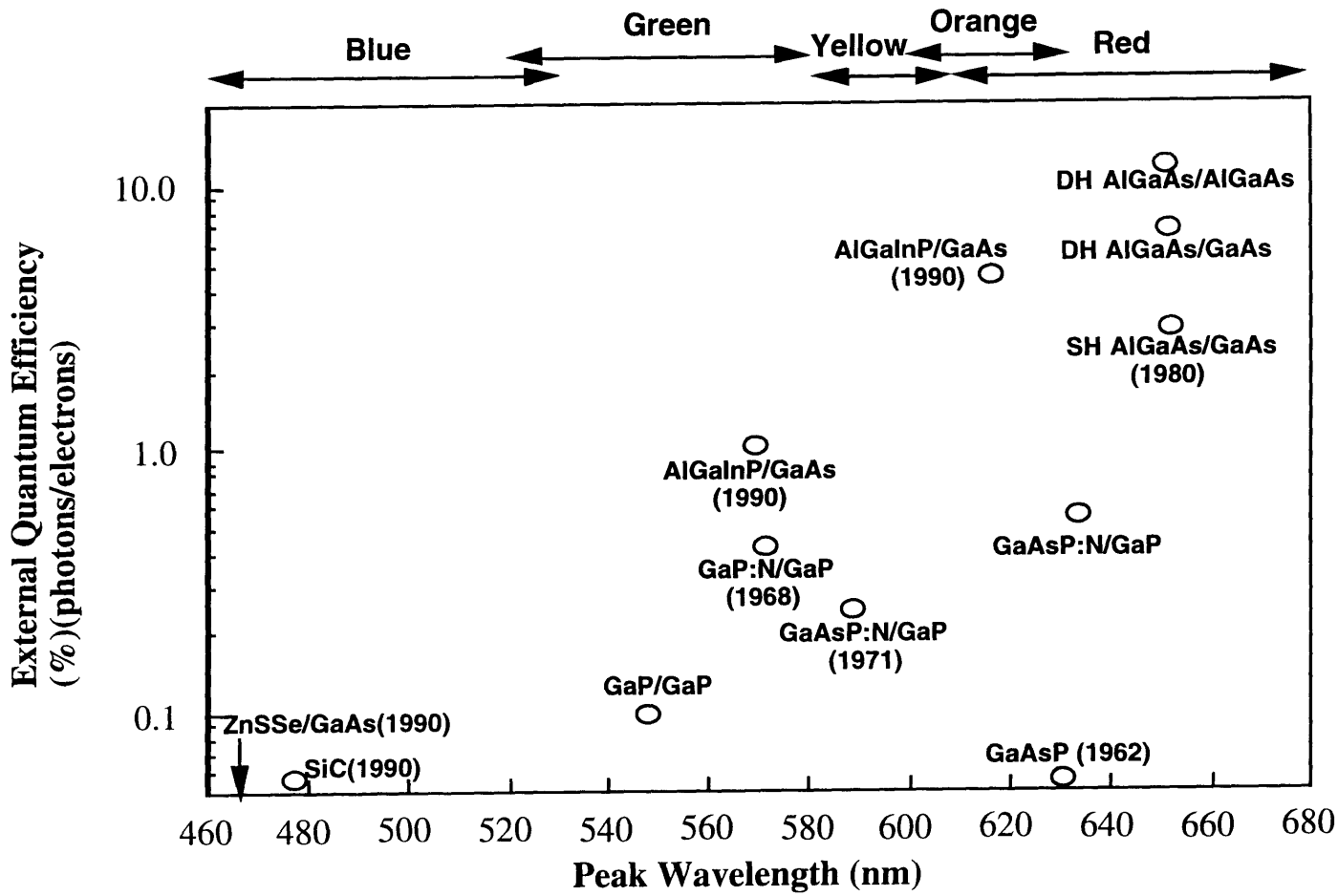

Figure 1.2 External quantum efficiency as a function of peak emission wavelength for III-Vand II-VI LED technologies

II-VI compounds have opened the blue-green region of the spectrum and a range of novel applications. Blue light emitting and laser devices can be produced with II-VI compounds like ZnSSe or ZnCdSe [Xie *et al.*, 1992].

1.1.2. Growth Techniques for II-VI Compounds

The classical methods of growth for II-VI compounds have been melt growth, solution growth and vapor phase growth. The large dissociation pressures developed near the stoichiometric melting points make melt growth difficult. As a result of chemical reactions between the melt and the silica or graphite crucible, impurities can be introduced into the growing boule. The possibilities for crystal growth of II-VI compounds by solution, flux and hyperthermal methods are also limited. Generally, the substances have a relatively low liquidus solubility in molten melts at high dissociation pressures. In solution growth, the solvents are invariably incorporated into the crystals grown and consequently affect the final electrical and optical properties. Liquid Phase Epitaxy (LPE) presents low solubility problems in II-VI semiconductor compounds.

Crystal growth from the vapor phase appears to have fewer limitations than synthesis from the melt. Elemental transport of the II-VI components was early on a preferred route for growth because of high volatility of the elements involved. However, the vapor phase epitaxy (VPE) approaches usually required growth temperatures within the range 600-900°C [Lilley *et al.*, 1982]. It has been increasingly recognized [Neumark, 1989c] that growth at these temperatures thermodynamically favors the formation of a multitude of defect structures, in

particular, defect or impurity-defect pair complexes. Thus, films grown by VPE often exhibit insulating rather than semiconducting properties.

Non-equilibrium growth techniques, molecular beam epitaxy (MBE) and organometallic vapor phase epitaxy (OMVPE), have developed into the most promising techniques achieving high quality epitaxy of II-VI compound semiconductors. The primary reason for the emergence of these two epitaxial growth techniques is the requirement of low growth temperature (<500°C) and improved control of stoichiometry as well as impurities [Cockayne and Wright, 1984; Yao *et al.*, 1983]. At this point MBE has produced blue light emitting devices while OMVPE so far has not yielded high p-type conductivity.

In the OMVPE technique, at least one of the film precursor is carried to reaction zone as an organometallic compound. The process retains the advantages of VPE, but supersaturations are very large. Vapor phase chemical reactions take place at room temperature forming condensed phases before the vapor streams reach the heated substrates. The growth conditions are kinetic-controlled. As compared to MBE, common advantages [Ludowise, 1985] are the low processing cost, multiple wafer throughput, source versatility and controllability of materials purity and overall quality.

1.2. ZnSe Precursors for OMVPE

The ideal source reagents for ZnSe growth would have the following characteristics [Hails and Irvine, 1991; Jones, 1991, 1993; Mullin *et al.*, 1990] :

(a) The source must be sufficiently volatile to permit gas-phase transport to the reactor without excessive heating of the lines which could cause

decomposition. Liquids with vapor pressures of 1 -100 Torr at room temperature are preferred.

(b) The reagent must be pure. Two types of purity are required. First, the compound must be of high chemical purity to insure that the vapor pressure of the source remains constant during sample use. Second, the sample must be of high elemental purity - a function of the synthetic pathways and purification processes employed in its production.

(c) The source's toxicity should be as low as possible to minimize containment costs.

(d) The source reagent must decompose efficiently in the reactor at low temperature to deposit only the desired element without incorporation of impurities into the product film.

(e) The reagent should not undergo undesirable side reactions such as polymerization or premature reaction with the other source reagent.

(f) The reagent must be stable during room temperature storage for extended periods in bubblers.

Chemical and elemental purity in the source can in principle be controlled by appropriate synthesis and purification. Volatility, pre-reaction, stability and decomposition characteristics are controlled by the structure and reactivity of the precursors. The purity of organometallic precursors has been greatly improved in recent years. This advance is largely due to the improvements in synthesis and purification techniques such as "adduct purification" (Figure 1.3) together with increasingly sensitive analytical techniques like direct injection inductively coupled plasma emission spectroscopy (ICP-ES) [Jones, 1993]. As a result routine production of commercial organometallic precursors with total metallic impurity

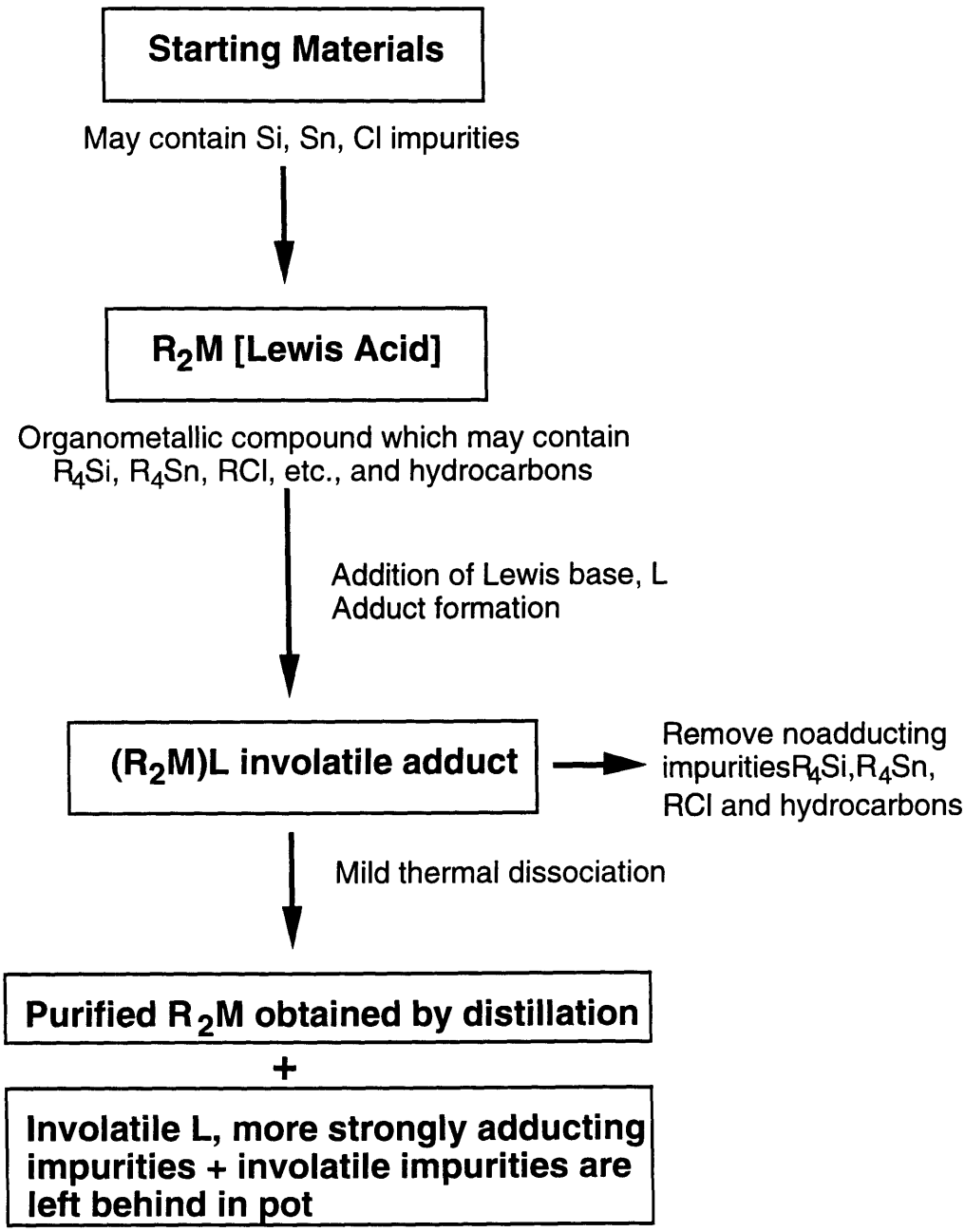

Figure 1.3 Principles of adduct purification [Jones, 1993]

levels of less than 1ppm is now available. The absence of extrinsic dopant metal impurities in organometallic precursors has allowed the identification of intrinsic impurities, which result from the incorporation of alkyl fragments, specifically carbon, generated in the pyrolysis of organometallic precursors. In addition, a better understanding of precursors interactions in the gas phase of OMVPE has allowed variations in the uniformity and optical/electrical properties of the grown layers to be rationalized [Jensen *et al.*, 1991].

Growth of ZnSe by OMVPE has been carried out mainly by using organometallic compounds such as R_2Zn, where R=methyl, ethyl, ally etc., along with the hydride H_2Se [Wright *et al.*, 1989]. The most favored reaction is that between DMZn and H_2Se which has yielded layers of good structural quality with n-type conductivity and carrier concentrations in the range 10^{15}-$10^{17}cm^{-3}$ for nominal undoped materials [Giapis *et al.*, 1989a]. A major problem is the premature reaction between the group II precursor and group VI hydride, which leads to poor morphology.

1.2.1 Organometallic Selenium Sources

In order to limit this prereaction effect between DMZn and H_2Se, a number of alternative group VI precursors without acidic hydrogen atoms have been investigated. These include dimethyl selenide [Mitsuhashi *et al.*, 1986], diethyl selenide [Sritharan and Jones, 1984a,b], and methylallyselenide [Giapis *et al.*, 1989c] as well as heterocyclic molecules such as selenophene (C_4H_4Se) [Wright *et al.*, 1984]. Unfortunately, although this approach limits prereactions, it invokes the penalty of higher growth temperatures. For DESe these growth temperatures are as high as 450 -550°C compared with the optimum temperature

of 280°C reported for ZnSe grown using DMZn and H_2Se [Fujita *et al*, 1984]. At these higher growth temperatures the optical properties of ZnSe layers often degraded due to the increased incorporation of impurities and increased occurrence of native defect-impurity complexes.

In an effort to lower the ZnSe deposition temperature, Se sources containing the allyl ligand (CH_2=CH-CH_2-) [Giapis *et al.*, 1989c] have been investigated. The allyl radical is thermodynamically more stable than methly or ethyl radicals due to electron resonance stabilization of the radicals (CH_2 ⟷ CH ⟷ CH_2). Consequently, methylallylselenide (MASe) and diallyl selenide (DASe) pyrolyse at lower temperatures than DMZn or DEZn. However, the use of MASe and DASe with DMZn led to ZnSe layers containing high levels of carbon. Decomposition of allyl- based selenium sources [Patnaik *et al.*, 1993] indicated that this arise from an intramolecular re-arrangement of the allyl group during pyrolysis which leads to a moiety containing a Se=C bond. Ditertiary butylselenide ($(tBu)_2Se$) [Stazl *et al.*, 1993] has also employed to lower the growth temperature. In another approach, methylselenol (MeSeH) [Hirata *et al.*, 1990: Fujita *et al.*, 1988] and tertiary-butyl selenol (tBSeH) [Nishimura *et al.*, 1993], which contains the weak Se-H bond, has been used to grow ZnSe without significant prereaction at 300°C.

1.2.2. Organometallic Zinc Sources

DMZn has been the most used Zn source in the growth of ZnSe even though there are problems associated with its synthesis. DMZn is usually prepared by the reaction of methyl-iodine or methyl-bromide with a freshly prepared zinc-copper couple [Price and Trotman, 1957]. Although, after

repeated distillation, this method apparently gives relatively pure dimethylzinc, there is concern that copper and halogen contamination may occur.

An alternative approach is to modify the group II source so as to reduce its susceptibility to pre-reaction with the group VI hydride by employing adducts of DMZn, and thereby decreasing its reactivity [Wright *et al.*, 1990, 1989, 1987; Yates and Williams, 1991]. Wright *et al.* [1987] used the adduct formed between DMZn and a chelating ether (1,4-dioxan) to form a stable complex, which retained sufficient volatility for transport to the deposition zone. They showed that an adduct, DMZn:(1,4 dioxan), had potentially advantageous properties as a zinc source, particularly with respect to ease of use, low growth temperature (as low as 250°C) and minimization of prereaction during the growth of ZnSe.

A significant advance was made by the use of the nitrogen donor adduct, dimethylzinc triethylamine, DMZn:NEt_3 [Wright *et al.*, 1990]. One reason for the improved purity in layers grown using this adduct appears to be the removal of halogen elements, particular iodine which is an n-type donor in ZnSe, by the adduct purification process. DMZn:NEt_3 has a convenient vapor pressure of ca. 37.2 Torr at 21°C for OMVPE application. This permits the use of more convenient source temperature and carrier gas flow rates than is the case for the more volatile DMZn (vapor pressure, 194 Torr at 0°C). Moreover, the premature reaction with H_2Se appears to be significantly suppressed.. This effect has been attributed to the presence of a stable adduct in the gas phase which can prevent premature coordination and reaction between DMZn and H_2Se (to be discussed in section 3.3.1).

1.2.3. Organometallic Bubbler

The organometallic precursor is generally introduced into a reactor by bubbling a carrier gas through the liquid organometallic reagents contained in a stainless steel container. The flow rate of reagent is calculated by assuming that the carrier gas is saturated with the organometallic source after passing through the liquid. There are several cautions associated with the use of bubblers [Yoshikawa *et al.*, 1984]. These may be summarized as follows.

(a) Saturation of the carrier gas with the organometallic source materials is influenced by the flow of the gas since mass transfer changes with the flow rate of the gas. Consequently, the partial pressure of the organometallic source in the carrier gas tends to be lower than that predicted from equilibrium calculations.

(b) Temperature fluctuations of the bubbler affects the organometallic source vapor pressure, and the temperature must then be accurately controlled to maintain a constant organometallic source flow rate.

(c) The total amount of organometallic source remaining in the cylinder also affects the partial pressure in the carrier gas since the length traveled by the bubblers changes with the liquid level in the bubbler. Thus the flow rate of organometallic source might decrease with time even if both the flow rate of the carrier gas and the temperature of the cylinder are accurately controlled.

(d) Estimation of the amount of organometallic source remaining in a cylinder is difficult.

(e) When many organometallic sources are used in a growth system, a large number of valves and tube-fittings as well as temperature controllers for the bubbling cylinders must be used, complicating gas-flow control and increasing the possibility of leak-points.

1.3 Materials and Growth

1.3.1. High quality ZnSe layer

An undoped epitaxial layer of ZnSe may be considered as being of high quality when all of the following criteria are satisfied.

(a) The film shows sharp double crystal X-ray rocking curve (the FWHM of the film is lower than 300 arcsec).

(b) The film exhibits a channeling spectrum in Rutherford Backscattering spectrometry.

(c) The film has good surface morphology without any features such as hillocks, pinholes or twins, as evidenced by SEM (at least 10,000X magnification)

(d) The film yields strong near-band-edge photoluminescence (PL) emission at room temperature as well as low temperatures (10K).

(e) At 77°K, the total carrier concentration is around $5X10^{15}$ cm^{-3} and the corresponding electron mobility higher than 3000 $cm^2/Vsec$.

(f) The film shows undetectable intrinsic impurity concentrations, as set by the detection limit of SIMS (~ 10^{17} $atoms/cm^3$).

Many efforts made in Japan, England and US towards heteroepitaxial growth of ZnSe/GaAs by OMVPE have resulted in good quality materials with dominant near-band-edge and reduced deep-level emission to a degree where meaningful optical and electrical measurements can be performed. However, even with the low temperature growth offered by OMVPE, the fundamental problem of p-type doping to high concentration still remains. P-type conversion has been realized in MBE grown materials through the use of radio frequency

plasma nitrogen source [Park *et al.*, 1990: Haase *et al.*, 1991a: Xie *et al.*, 1992]. This MBE achievements has yet to be mirrored by OMVPE, which has significant long term advantage as a manufacturing process.

There are several problems that must be addressed to realize p-type doping in the OMVPE process.

(a) Self compensation Effect. Because ZnSe has a wide band-gap and relatively strong ionic characteristics, compensation problems are difficult to avoid. Lack of good p-type conductivity in ZnSe has been blamed on the strong energy incentives for compensation, resulting in a strong tendency for the introduction of native defects [Kroger, 1964]. The self-compensation of the intentionally added donor or acceptor impurities is caused by the intrinsic lattice defects, i.e., vacancies or native interstitials (e.g., $[V_{Zn}]^{++}$ in chlorine doped ZnSe or self-interstitial) [Marfaing, 1981], of the opposite conductivity type. Hydrogen incorporation has in particular been identified as a problem by passivating the N acceptor of OMVPE grown ZnSe:N [Wolk *et al.*, 1993].

(b) Ohmic Contacts to p-type ZnSe. Very little information is known about good ohmic contacts to p-type ZnSe. DePuydt *et al.* [1989] showed via rectification studies that In does not provide an ohmic contacts to Li-doped p-type ZnSe epilayer, whereas In has commonly been used in the last decade to provide ohmic contacts for electrical measurements in n-type ZnSe. Au does not form ohmic contacts to n-ZnSe (Schottky barrier formation at Au/ZnSe interface was extensively investigated by Anderson *et al.* [1989]). Lansari *et al.* [1992a,b] suggested epitaxial layer of semimetal HgSe as a new ohmic contacts for p-type ZnSe films in order to decrease the interstitial energy barrier, valence band offset, to about 0.6 eV .

(c) OMVPE chemistry. There are few researches about the chemistry involved in the OMVPE growth in ZnSe. If the high quality materials are to be grown, the reaction pathways leading to growth of epitaxial materials as well as assisting or inhibiting impurity incorporation must be understood. *In-situ* diagnostics, indispensable in understanding complex chemistries, have not been employed in the growth of ZnSe by OMVPE.

1.3.2. ZnSe and ZnS_xSe_{1-x} Epitaxy

Substrates play a critical role in high-quality epitaxial deposition, particularly in light-emitting epitaxial structures, where stable, long lifetime operation is necessary. Ideally, the substrate and epitaxial layers should have closely matched lattice constants and thermal expansion coefficients, in order to minimize the strain in the active region. In addition, the substrate material should be available in the form of relatively large area, high-quality single crystals. Most of the work in the literature [Ohmi *et al.*, 1987; Fujita *et al.*, 1985] has focused on ZnSe epilayers on GaAs substrates. The use of GaAs has the advantage that bulk-grown wafers are relatively inexpensive, readily available and have reasonably low dislocation density. There is presently no established commercial source of ZnSe substrates.

The combination of epitaxial ZnSe on GaAs forms a polar or reactive heterojunction [Tu and Kahn, 1985]. The bonding at the interface may influence the properties of the grown ZnSe films. If stoichiometry is not completely maintained at the interface, there may be enhanced diffusion of Ga into ZnSe and/or Zn into GaAs. Ga is known to enter the ZnSe epitaxial layer, a consequence of the relative ease of diffusion in the high concentration of

mismatch dislocations in the interfacial region. The extent of this dislocated region and the temperature of deposition are crucial parameters in the depth of gallium penetration. The lattice mismatch of 0.26% at room temperature between the epilayer (ZnSe, a=5.6676Å) and the substrate (GaAs, a=5.6533Å) further leads to the generation of a number of dislocations or defects [Williams *et al.*, 1984].

One approach to circumvent these problems is to grow the lattice-matched ternary alloy, ZnS_xSe_{1-x} on GaAs. Reduced Ga contamination and excellent thermal stability was found in the lattice-matched $ZnS_{0.06}Se_{0.94}$/GaAs interface [Ohmi *et al.*, 1987]. Cockayne *et al.* [1989] found a significant reduction in gallium penetration into the interfacial region (0.25μm) when the ZnS_xSe_{1-x} was appropriately matched. From the annealing at an elevated temperature of 600°C of nearly lattice-matched x composition range of $0.045<x<0.075$ was found to be highly stable, while for the composition outside of this region the Ga donor related peak increased abruptly after 5 hour annealing [Kanda *et al.*, 1988].

1.3.3. Plasma Assisted Growth

Plasma enhanced growth of ZnSe has the advantage of a various freedoms for exciting molecules chemically by means of plasma, afterglow and atomic ions. The possibility of growing high quality sample at temperatures as low as 200°C yields a potential route for producing a variety of artificial materials with pseudomorphic structure. However, in order to eliminate deep level defects several problems like ion bombardment and substrate damage should be solved.

Plasma-assisted OMVPE of ZnSe was tried by Mino *et al.*, [1986] to reduce growth temperature and increase chemical reactivity The intensity of the self-

activated emission band, whose peak was at 606 nm, was more dominant than those of the near-band-gap emission peaks since the film contains a large number of defects. Matsumoto *et al.*, [1986] also employed hydrogen plasma to enhance the quality of the ZnSe films. Hydrogen radical enhanced chemical vapor deposition through the utilization of atomic hydrogen generated by microwave plasma was developed by Goto *et al.*, [1992, 1991, 1990] for the purpose of lowering the growth temperature. Even though alternate gas supply were tried to suppress adduct formation between sources and to avoid ion bombardment to reduce defect density, the films still showed deep level emission at 2.1 eV.

1.4. Doping

Impurities must be incorporated into any semiconductor in order to achieve electrical properties required for different device applications. The nature of the semiconductor and the solubility of the dopant in the semiconductor host are the two most important factors in determining the type and magnitude of the conductivities. For example, in order to obtain a particular level of n-type conductivity, it is necessary to have first, a sufficient solubility of the donors, and second, a sufficient small energy separation between the donors and the band so that the donors are readily ionized.

1.4.1. n-type ZnSe

As-grown, normally undoped ZnSe by bulk or epitaxial growth technique is typically n-type, sometimes even well-conducting (*i.e.*, material with conductivity greater than $1\Omega^{-1}cm^{-1}$), because of high concentrations of persistent

extrinsic donors [Besomi and Wessels, 1980]. The n-type doping of epitaxial ZnSe films have been achieved with group III and group VII donors, such as Al [Kamata *et al.*, 1986], Ga [Skromme *et al.*, 1989], In [Matsumoto *et al.*, 1990], Cl [Cheng *et al.*, 1989] and I [Shibata *et al.*, 1988]. The photoluminescent properties of Al- or Ga- doped layers show a marked degradation when the carrier concentration exceeds $10^{17}cm^{-3}$. Among these donor elements, it has been reported that group VII elements are superior to group III elements with respect to controllability in electrical and photoluminescent properties of the films [Kamata *et al.*, 1988]. Cl produces highly conducting films (up to $10^{19}cm^{-3}$) which exhibits strong blue near-band-edge emission with suppressed deep level emission, but the high reactivity of Cl atoms could potentially lead to surface morphology degradation and impurity contamination.

1.4.2. p-type ZnSe

Group I_a elements and group V_b elements have been intensively studied as acceptor impurities. The best results have been obtained within nitrogen as an intentional dopant because this element is known to produce shallow acceptor levels. High conductivity p-type ZnSe was first reported by 3M Corporate Laboratory for MBE grown ZnSe materials N-doped by a radio frequency plasma source in MBE system [Park *et al.*, 1990]. Proof-of-concept demonstrations of blue-green semiconductor lasers and lighting emitting diodes has been done by several groups [Qiu *et al.*, 1991: Yu *et al.*, 1992: Xie *et al.*, 1993]. However, this advance has not yet been mirrored by OMVPE. Therefore, OMVPE research efforts should be focused on enhancing nitrogen incorporation and understanding the electrical and optical properties of ZnSe:N. Incorporation of

other group V elements, such as phosphorus and arsenic has also been explored, but there is no conclusive report on the electrical and optical activity of P and As in ZnSe [Bhargava *et al.*, 1979: Yao *et al.*, 1986].

On the other side of the periodic table (Group I elements), Li has attracted much attention as a useful shallow acceptor in ZnSe. Li has the following peculiar features as an acceptor impurity in ZnSe compared with nitrogen: (a) the solubility of Li in ZnSe may be higher than that of nitrogen, leading to Li being a preferable acceptor, but (b) since Li is an amphoteric and mobile impurity in ZnSe, interstitial lithium is easily introduced into the films, making Li an unfavorable compensation center in ZnSe. Li has the further disadvantage of moving under an applied bias [Neumark and Herko, 1982] and having a very high diffusivity in ZnSe [Cheng *et al.*, 1988]. These limitations cast doubt on the applicability of this otherwise promising dopant.

Na could be another dopant of choice, since its acceptor behavior in ZnSe has already been established [Tews *et al.*, 1979, Kosai *et al.*, 1988]. Incorporation of the cation site could be particularly advantageous with the introduction of excess Se, leading to Zn vacancies and thus, offering an additional incentives for preferential incorporation of Na on the substitutional site (instead of the interstitial site). Several attempts to produce p-type material with Na have been unsuccessful [DePuydt *et al.*, 1989; Yamada and Taguchi, 1990]. It is not clear whether this problem is inherent to Na or simply related the low purity of Na doping sources.

To provide further perspective on the problems associated with p-type doping of ZnSe past OMVPE results are reviewed in the following.

Stutius [1982] firstly reported nitrogen incorporation in ZnSe on GaAs by using NH_3 in OMVPE. Even though a strong peak of I_1^N (2.7916eV) was observed in the photoluminescence spectrum, electrical conductivity could not be measured to give a direct proof of p-type behavior. Yasuda *et al.* [1988] reported that co-doping of Li and N of ZnSe grown by OMVPE resulted in highly conducting p-type ZnSe with carrier concentration of up to $9x10^{17}$ cm^{-3}. Of concern was, however, the claim that ohmic contacts to p-ZnSe were obtained by In, which was disproved by Cheng *et al.* [1988]. Another controversial point is that no decrease in carrier concentration with decreasing temperature is obtained for a sample with $n_{298K} = 6X10^{17} cm^{-3}$. This may be attributed to the formation of a degenerate impurity band, related to the metal-insulator transition. However, this degenerate impurity band is expected to occur at $n_c = 1X10^{20} cm^{-3}$, a value of two order of magnitude higher than the observed value [Neumark, 1989]. Stuecheli and Bucher [1989] have reported p-type ZnSe in vapor phase transport growth with iodine. This is a peculiar result since iodine is expected to be a donor (on the Se site). Indeed, it was found in the works of Yoshikawa *et al.*, [1988a] and Shibata *et al.*, [1988] that iodine can be incorporated at as high a concentration as $1x10^{19}$ cm^{-3}, resulting in very low resistivity n-type ZnSe, with resistivity down to 0.002 Ωcm. Yodo and Yamashita [1988] reported Li-ion doping of ZnSe grown by OMVPE. They also observed dominant I_1 acceptor-bound excitonic emission with weak donor-acceptor pairs, but did not report any electrical measurements. Yoshikawa *et al.* [1988a,b] grew Li-doped ZnSe film with cyclopentadienyl lithium (C_5H_5Li) as a dopant source. Cp-Li is a solid source but it has advantages of not containing oxygen in its structure, and having a fairly high vapor pressure. They confirmed Li as a shallow acceptor with an

activation energy of about 101-118 meV. The second promising lithium dopant is fine powder of Li_3N [Yasuda *et al.*, 1988]. The advantage of Li_3N is that lithium and nitrogen impurities are together codoped as p-type dopants. The ZnSe layers exhibits a lower resistivity up to 0.2 Ωcm and a carrier concentration of $9X10^{17}$ cm^{-3} together with Hall mobility of 40 $cm^2/Vsec$. The dopant source Li_3N was heated to 400°C and carried by H_2 gas into the deposition chamber. The decomposition of Li_3N into N_2 and LiH is suspected. Ohki *et al.*, [1988] have reported p-ZnSe/GaAs, using N from NH_3 as a dopant. The authors obtained conducting p-type ZnSe by increasing the flow rate of NH_3. At high temperatures (>400°C), the crystallinity of the films deteriorated and very weak NBE(near-band-edge) transitions were observed. A reduction of sticking coefficient of the N-bearing species (which includes N incorporation) at higher growth temperatures is possibly contributing to this effect. They used Au-Sb alloys as electrodes to p-ZnSe (evaporated on the surface of the ZnSe layers). Prior to the growth of ZnSe:N epilayers for Hall measurement, they grew an undoped ZnSe buffer layer of very high resistivity to electrically separate the N-doped layer from the GaAs substrate. They tried to have high concentration of nitrogen incorporation in ZnSe with NH_3 [Ohki *et al.*, 1990]. Above the concentration of $1X10^{18}$ $/cm^3$, the films degraded significantly, which degradation can be relieved by thermal annealing. A prime problem with this study is that the p-ZnSe layers with measurable conductivity had low temperature PL spectra dominated by donor-acceptor pair emission with very weak near-band-edge emission which is usually an indication of highly resistive material, with high compensation. Ohki *et al.* [1991] proposed acceptor compensation model. They found the existence of defect levels, which reveals as

donor defects in photo-assisted Hall measurement, in nitrogen doped ZnSe films. Suemune *et al.* [1991, 1988] employed NH_3 as a N dopant source in a ZnSe/ZnSSe periodic structure with a S mole fraction of 0.08 corresponding to an average composition lattice matched to the GaAs substrate. They found that the I_1 intensity was sensitively dependent on the S mole fraction. The electrical properties of the corresponding lattice-matched $ZnS_{0.06}Se_{0.94}$ layer was p-type with a carrier concentration of $7X10^{15}cm^{-3}$. Nakanishi *et al.* [1991] observed high output power from photopumped ZnSe/ZnSSe blue laser operating at room temperature. The structure was prepared with DEZn, DESe and DES at 515°C. Parbrook *et al.* [1993] demonstrated ZnCdSe-ZnSe multilayers with DMZn, DMSe and DMCd as reactants at 475°C. However, they did not achieve atomically abrupt interface because of the relative high growth temperature. Tertiarybutylamine [Zhang and Kobayashi, 1992], dimethyl aminolithium [Yanashima *et al.*, 1992], dimethyl hydrazine [Yoshikawa *et al*, 1990] and phenylhydrazine [Akram *et al.*, 1993] have also been tried as dopants. The studies showed a slight increase in nitrogen incorporation into ZnSe according to PL measurements, but the carrier concentrations were still below $3X10^{15}/cm^3$. Taskar and Shahzad [1993] recently explored a flow modulation epitaxy and a new rapid thermal annealing technique for enhancing the activation of nitrogen acceptors. They reported net acceptor concentration of $3X10^{16}/cm^3$, as measured in C-V profiling, in p-type ZnSe grown with NH_3 as dopant. They employed Au dot to p-type ZnSe as Schottky contacts, which has large energy barrier [Lasari *et al.*, 1993]. Wolk *et al.* [1993] recently observed H incorporation to N acceptors in ZnSe:N samples grown by OMVPE. They assigned a new N-H stretching vibration mode at 3194 cm^{-1} and a N-H wagging vibration mode at 783 cm^{-1}.

Hamada *et al.* [1993] reported p-type ZnSe grown by plasma-assisted epitaxy in nitrogen-based plasma. While hydrogen improve the electronic properties of ZnSe layers, excessive hydrogen may have an effect of reducing doping efficiency of shallow-acceptor nitrogen. The excessive nitrogen gas flow rate increases incorporation of inert nitrogen in ZnSe films and consequently produce deep complex defects.

To provide perspective on the OMVPE research it is worthwhile to briefly summarize key MBE observations.

Akimoto *et al.* [1990,1991] have reported on the growth of oxygen-doped ZnSe p-n junctions. Oxygen is an isoelectronic impurity in ZnSe, when substituting on the Se site. However, the authors claimed that oxygen in ZnSe acts as an acceptor with an acceptor level of about 80 meV measured by photoluminescence. They suggested that the acceptor-like behavior of oxygen may be caused by charge transfer from the host lattice to oxygen, due to its large electronegativity. Isoelectronic impurities have been observed experimentally [Hopfield *et al.*, 1966] to behave as donor-like or acceptor-like traps and a theoretical treatment of these observations has already been proposed [Faulkner, 1968]. However, they were unable to confirm p-type behavior via Hall measurements, due to the unstableness of the Hall voltage. Instead, they relied on evidence from the low-temperature photoluminescence spectra of ZnSe:O films, which indicated existence of a claimed weak very shallow acceptor-bound excitonic emission I_1, the position of which shifted from 2.7938 to 2.7926 eV with the oxygen concentration. However, the spectra were dominated by donor-acceptor pairs, consistent with high resistivity of the films. Helms [1993] proposed oxygen interstitial acceptor model coupled with the passivation of

excess Se or Zn defects. Researchers at 3M reported p-type ZnSe with free radical nitrogen beam doping through radio frequency plasma process in MBE for the first time [Park *et al.*, 1990]. Net acceptor concentrations as large as $3.4X10^{17}$ cm^{-3} were measured by several characterization techniques [DePuydt *et al.*, 1989, Haase *et al.*, 1990b and Park *et al.*, 1991]. LED based on ZnSe:N/ZnSe:Cl p-n junctions exhibited dominant blue emission at room temperature. Subsequent studies led to p-type ZnSe with a net acceptor concentration up to $1X10^{19}$ cm^{-3} and the demonstration of the first laser diodes fabricated from ZnSe [Qiu *et al.*, 1991]. These devices emitted coherent light as a wavelength of 490 nm when pulsed at 77K [Haase *et al.*, 1991a]. Ohkawa *et. al.* [1991a,b,c and 1992] reported N-ion doping during MBE growth of ZnSe and obtained films with photoluminescence spectra dominated by the I_1, acceptor-bound exciton, whose intensity was 40 times greater than the donor-acceptor pair emission. However, they were unable to perform Hall measurements due to the high resistivity of the films. The Purdue group [Jeon *et al.*, 1992a,b, 1991a,b; Xie *et al.*, 1992a,b,c,; Gunshor *et al.*, 1992] has shown blue-green injection lasers and light-emitting diodes based (Zn, Cd)Se/ZnSe MQW system on GaAs or (In,Ga)As buffer layers. In pulsed operation, outpowers were measured exceeding 600mW at 77K from the typical devices of both polarities. Similarly, researcher at North Carolina State University [Ren *et al.*, 1992a,b, 1991a,b, 1990a,b; Yu *et al.*, 1993, 1992; Dreifus *et al.*, 1990] reported blue ZnSe and green $ZnSe_{0.9}Te_{0.1}$ light emitting diodes and fabricated ZnSSe-ZnCdSe quantum well structures which emit bright blue electroluminescence at 2.601eV (476nm) at room temperature. They proposed an epitaxial layer of semimetal HgSe as a new ohmic contacts for p-type ZnSe films [Lansari *et al.*, 1992a,b]. Recently, Gaines *et al.* [1993] described blue-green

Table 1.2 Summary of p-type ZnSe

Reference	Growth method	Acceptor Mobility	Net Carrier	p-n junction	Comments
Yashuda *et al.*(1988)	OMVPE	Li_3N	$9X19^{17}cm^{-3}$ ~$40cm^2/Vs$	Yes	Not reproducible
Ohki *et al.*(1989)	OMVPE	NH_3	$10^{14}cm^{-3}$ $50cm^2/Vs$	No	$p>10^{14}cm^{-3}$ difficult
Akimoto *et al.* (1990)	MBE	O	$1.2X10^{16}cm^{-3}$	Yes	LED (77°K)
Park *et al.*(1990)	MBE	N_2 plamsa	$3.4X10^{17}cm^{-3}$	Yes	LED(RT)
Haase *et al.*(1991)	MBE	N_2 plasma	$1X10^{19}cm^{-3}$	Yes	LD(490nm, 77K)
Jeon *et al.* (1992)	MBE	N2 plasma	$1X10^{18}cm^{-3}$	Yes	LD(600mW)
Huh *et al.*(1993)	OMVPE	NH_3 plasma	$1X10^{15}cm^{-3}$	No	
Taskar *et al.*(1993)	OMVPE	NH_3	$3X10^{16}cm^{-3}$	No	RTA with capping

injection lasers containing ZnMgSSe cladding layers to improve optical confinement. The devices showed low threshold current density ($500A/cm^2$) and high pulsed output power (500mW) at 516nm at room temperature.

Based on the above literature review (Table 1.2), best results in p-type doping experiments have been obtained with nitrogen plasma in MBE. In order to follow the success of p-type ZnSe in OMVPE, research activity should be emphasized in enhancing nitrogen incorporation into ZnSe and understanding the electrical and optical properties of ZnSe:N. Since OMVPE offers a flexibility of source manipulation, new sources of nitrogen and new methods to crack down the nitrogen compounds into radicals can be investigated.

1.5. Objective and outline of this thesis

The objective of this research has been to provide an overall understanding of the problems associated with OMVPE growth and doping as summarized above. In particular, the thesis has addressed the following issues.:

(a) reduction in gas phase prereaction through the use of Zn adducts

(b) microwave plasma doping of ZnSe.

(c) use of alternate organometallic Se sources

The thesis is organized as follows. The growth of ZnSe by OMVPE is reviewed in chapter I. Chapter II describe the design of the OMVPE reactor used for ZnSe growth and molecular beam mass spectroscopy system used for decomposition studies. Among the reactor features described are a laser interferometer for *in-situ* growth rate measurement and a microwave plasma

cavity for precracking of ammonia for nitrogen doping. Safety issues are also discussed.

Chapter III details growth characteristics obtained with H_2Se and the Zn adduct source, dimethylzinc:trimethylamine (DMZn:NEt_3), as compared to those obtained with H_2Se and DMZn. Gas-phase pyrolysis studies of Zn sources and H_2Se also included. Finally, microwave plasma decomposition of ammonia is investigated as a possible approach to increasing nitrogen incorporation in ZnSe.

Chapter IV concerns the growth of ZnSe with dimethylzinc:triethylamine (DMZn:NEt_3) and several organometallic Se sources, specifically tert-butylallylselenide (tBASe), 2-selena-3-(1-methylethyl)-bicyclo[2.2.1]hept-5-ene (bCpSe), diallyl selenide (DASe) and diisopropyl selenide (DIPSe). These reagents are potential replacements of H_2Se for low temperature growth of ZnSe. The growth investigations are complemented with mass spectroscopy investigation of precursor pyrolysis. This thesis results are summarized in Chapter V along with directions for future research.

Chapter 2

Experimental System and Characterization

2.1. OMVPE Reactor System

2.1.1. System Evolution

The growth of high quality epilayers by Organometallic Vapor Phase Deposition (OMVPE) requires, in addition to an understanding of the growth process itself, a well-engineered reactor. A well-engineered reactor produces materials of good quality and continues to do so in spite of having been subjected to such difficulties as component failures, precursor changes and normal maintenance procedures. This OMVPE system was originally built in 1987 by Giapis (1990b) and has been modified to achieve the objective of this thesis, but the fundamental reactor characteristics remain the same. The reactor may be categorized as a load lock-equipped, vertical, stagnant point flow, resistance heated, microwave assisted OMVPE reactor with laser interferometer.

The first modification was to supply H_2Se gas directly to the reactor system instead of using the *in-situ* H_2Se generation chamber. When operating the *in-situ* H_2Se generation chamber for a while, deposits of Se_n(n=2,3,5~8) by-products were generated in the condensation zone. These particles could be the another source of contamination and they also blocked the Millipore filter in the

gas manifold so that the pressure of the H_2Se gas line became progressively unstable. A new gas chamber (Airgas Technologies) with 8-valve purge assembly was installed to store high purity H_2Se (99.999%, Solkatronic Chemicals Inc.). The second modification was to attach another gas manifold for doping to make p-type ZnSe. High purity of NH_3(99.999%) and N_2(99.999%, Matheson Gas Co.) were employed as p-type doping sources. The third modification upgraded the gas manifold of Zn source from manual operation to semi-automatic operation in order to stabilize the bubbler pressure with automatic pressure controller. The fourth redesigned the quartz nozzle reactor chamber with optical window for laser interferometer and special tube for accommodating the microwave cavity system. The fifth installed laser interferometer for obtaining *in-situ* layer thickness and growth rate information and attached microwave plasma cavity system to make active nitrogen radicals by cracking dopant sources.

2.1.2. System Description

An OMVPE reactor for II-VI materials must be capable of producing with low background impurity level, good surface morphology, reasonable growth rate, abrupt junctions and uniform thickness, composition and doping. The satisfaction of each of these requirements is dependent to some extent upon the reactor design and maintenance. The major components of the system are the reactor and load lock chamber, gas handling system, exhaust system, laser interferometer, and microwave plasma cavity shown in Figure 2.1.

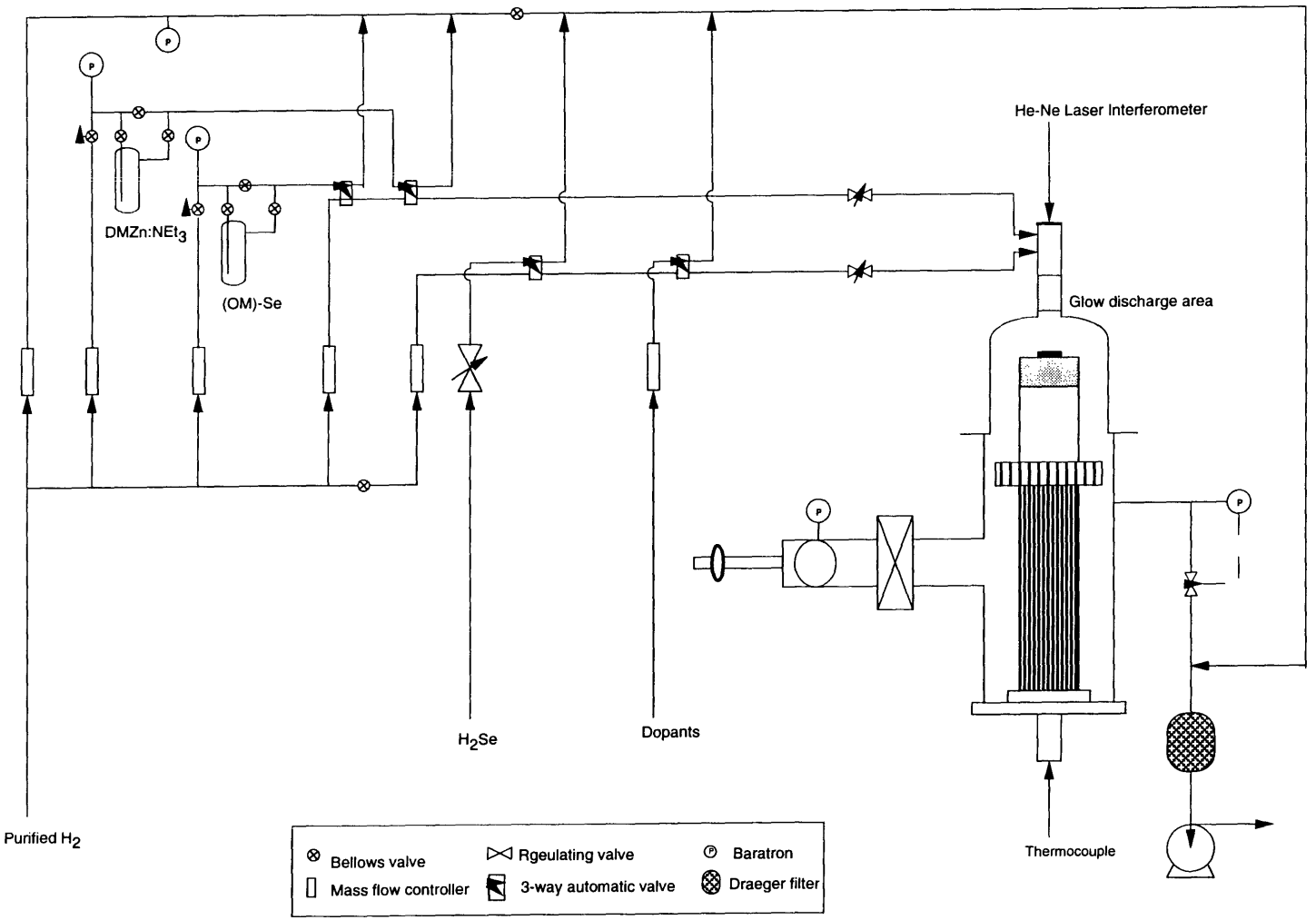

Figure 2.1 Schematic Diagram of OMVPE reactor

2.1.2.1. Reactor and Loadlock Assembly

The reactor is of the vertical down-flow configuration. The reactor enclosure consists of four basic components (a) quartz nozzle and reaction chamber, (b) load lock assembly, (c) heating stage, (d) precise positioning assembly.

(a) Quartz Nozzle and Reaction Chamber

The reaction chamber, where the deposition takes place, is a quartz bell-shaped custom made piece (G.Finkenbeiner Inc). The reason for using a quartz chamber, instead of performing the deposition process inside the lower stainless steel part of the reactor, is the ease of removing dangerous deposits from the quartz reactor walls. The inlet nozzle is specially designed for effectively mixing the reactants by reducing premature reactions and for providing uniform flow.

(b) Load Lock Assembly

Another key feature of this system is the loadlocked sample introduction chamber so that the growth chamber is not exposed to atmospheric contamination when loading or unloading substrates. In this way, downtime between runs is considerably minimized and an important source of uncontrolled impurities is effectively eliminated. Furthermore, the importance of not exposing the operator to the toxic absorbents of the reaction chamber walls should not be underestimated. The wafer transferring mechanism is a simple rotary-linear motion magnetically coupled feedthrough with a "fork" shaped holder that carries the susceptor. When the substrate is loaded, the loadlocked chamber is pumped down quickly with a Leybold TMP 150 turbomolecular pump to a base pressure of 1×10^{-7} Torr. The gate valve is then opened in order

to transfer the substrate into the main reactor chamber, on top of the heating stage.

(c) Heating Stage

The heater should be efficient in order to minimize thermally induced outgassing and the resulting vacuum degradation. It must also, despite its efficiency, have a short thermal time constant so that the wafer can be rapidly heated and cooled. The heating ought to be uniform and reproducible. The main body of our heater is made of quartz. It is a "cup" shaped compact piece that are ground to an angle of 60° from the horizontal towards the inside, to form a sharper edge. The cover of the heater is a high purity molybdenum round plate, machined so as to mate with the sloped edge of the quartz body. It bears a shallow groove that will accept the wafer as well as a pair of symmetric side-foldings, so that can transfer the cover back and forth from the top of the heating stage to the load lock. The Mo susceptor can be effectively cleaned from ZnSe deposits in hot aqueous NaOH solution. The quartz body is perforated at appropriate positions for electrical feedthroughs as well as in the center for a thermocouple (type K, chromel-alumel). The electrical feedthroughs and the quartz tube(via a quartz-to-stainless steel transition) are welded on a stainless steel disk, especially shaped to hold the quartz body in a lock-in position, without creating virtual leak possibilities. The thermocouple is enclosed by a thin tube which serves to protect the thermocouple from the growing films. Another important feature is the accurate measurement and effective controlling of temperature through the use of automatic temperature controller. The exact temperature on the GaAs substrate was measured with another type-K thermocouple and calibrated since temperature difference between controller

thermocouple and substrate thermocouple became severe in the lower reactor pressure.

(d) Assembly for Precise Positioning of the Substrate

The heating stage, consisting of the susceptor, the quartz body with the heating elements inside, the stainless steel holder, and the base nipple, is placed on top of the positioning assembly. This is a moving pedestal that allows elevation of the substrate into the reaction chamber, precise (~0.1mm) positioning with respect to the gas mixing nozzle for the deposition, and retraction of the susceptor back into the main reactor enclosure for substrate unloading.

2.1.2.2. Gas Handling System

The gas manifold is built solely of seamless electropolished stainless steel tubing with welded VCR fittings. All valves, both manual and pneumatic, are bellow-sealed stainless steel valves. The gas handling system is built around three basic building blocks. The first one is organometallic bubbler assembly (Figure 2.2.), which is compromised of three bellow valves, two mass flow controllers, a capacitance manometer, a check valve, a temperature controlled refrigerated bath, and an automatic pressure controller with a control valve. By adjusting the amount of hydrogen flowing through the bubbler, assuming saturation at bath temperature, and stabilizing the bubbler pressure automatically, one expects to have control over the molar flow rate of the organometallic compound flowing into the reactor. The second building block is for the Group VI hydrides and their makeup hydrogen lines in Figure 2.3. Hydride lines essentially consists of two bellows valves, a pneumatic valve, two

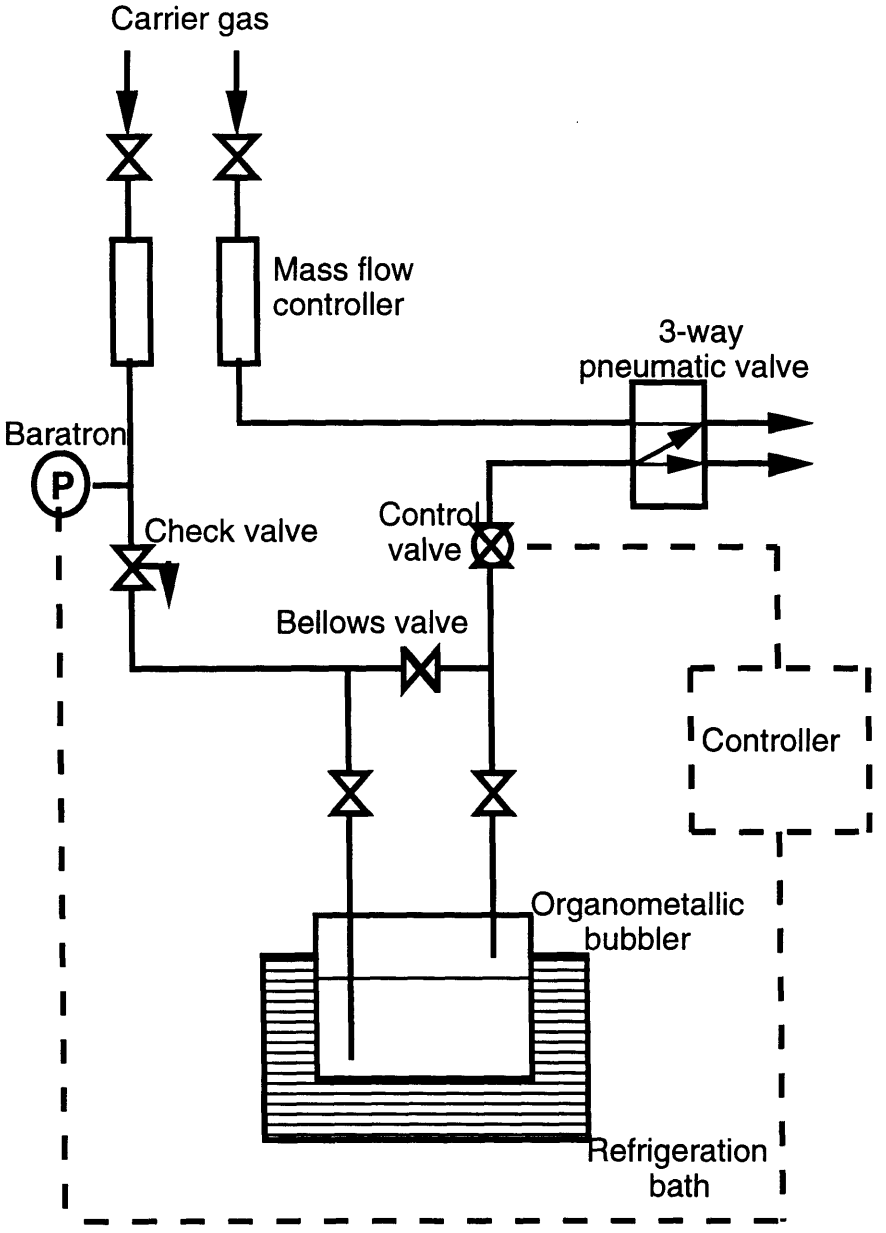

Figure 2.2. Schematc diagram of the organometallic bubbler assembly

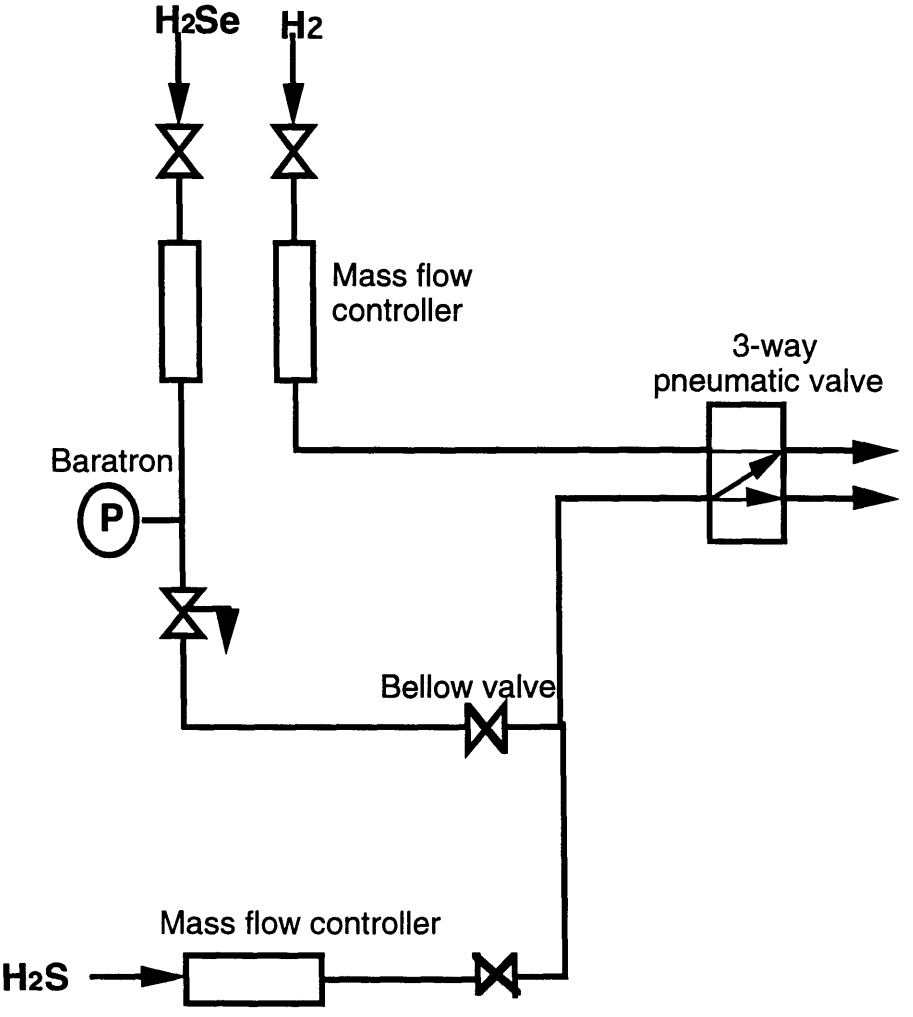

Figure 2.3. Schematc diagram of the group hydride

mass flow controllers, a Millipore filter and a capacitance manometer. There is also a makeup hydrogen line, meeting the hydride/H_2 affluent, downstream of the H_2Se cylinder for adjusting the hydride concentration as desired. The third building block is the reactant gas injection manifold, consisting of a series of pneumatic valves in a closed packed arrangement to eliminate extra tube lengths, and positioned right before the reactor (upstream). The pneumatic valves are custom-made 3-way valves with an extra port for continuos purge with H_2. The pneumatic valves are arranged according to the VENT/RUN principle where one port is the reactant line leading to the reactor and the other port is connected to the dump line. Flipping the appropriate switch sends the reactants from growth to dump or vice-versa.

2.1.2.3. Exhaust System

This system has two separate pumping systems; a reactor pumping system and a load lock pumping system which is also used for residual gas analyzer. A high capacity Trivac D60 rotary vane mechanical pump serves as the reactor pumping system. The downstream lines of the reactor are made of 1.5" diameter stainless steel tubing. Larger cross-section lines are important in order to avoid substantial pressure drop downstream. For ZnSe OMVPE in particular, where hydrogen selenide is involved, this exhaust issue is of primary concern. A Draeger activated charcoal filter has been installed upstream of the mechanical pump. This filter was found to withhold efficiently all undesirable toxic reaction by-products and, when frequently replaced (every approximately 30 runs), no H_2Se contamination of the pump oil was detected. Pressure balancing inside the reactor is achieved by a mechanical exhaust throttle valve and a throttle valve

controller in a closed-loop arrangement. An exhaust automatic pressure controller was selected because it works with all types of pumps, provides fast response, is tolerant of most effluent gases, and has moderate initial cost. It can easily be integrated in any process control scheme and it is expected to contribute significantly in minimizing pressure perturbations. The pressure of the reactor is monitored by two capacitance manometers (1000 Torr full scale and 10 Torr full scale) and an ionization gauge. The second pumping system is made of Leybold TMP150 turbomolecular pump backed by a rotary vane pump. This pump has been employed for evacuating the load lock and for cleaning the whole system. The base pressure of the system is $1X10^{-7}$ Torr. This pump is also connected through the right angle valve and sampling leak valve for sampling and monitoring the actual chemical reaction inside the reactor by Quadruple Mass Spectroscopy (QMS112, Balzers) in order to obtain high quality and reproducible ZnSe films.

2.1.2.4. Laser Interferometer

A He-Ne laser interferometer has been used to monitor thin-film thickness during OMVPE of ZnSe. The He-Ne laser beam (λ=6328Å) is directed at nearly normal incidence to the ZnSe film, and the reflected beam is detected by a silicon detector. The Si photodetector (Oriel 7504) is operated at zero bias photodiode mode so that the photocurrent is proportional to the intensity of the light collected. The output from the chart recorder is a trace representing intensity of the reflected light as a function of time. During the deposition the thickness of the layers and the growth rates were controlled *in-situ* by

monitoring the interference between beams reflected from the surface of the grown ZnSe layer and from the substrate-layer interface using a He-Ne laser.

The first step in applying interferometry to a OMVPE reactor is to choose and adapt the geometry of the light path to the physical limitations of the process. By employing a beam splitter to the system, the light strikes the film at 0° angle of incidence (normal to the surface). The laser, detector, and sample are oriented at right angles, as shown in Figure 2.4. This configuration keeps the light path inside a narrow tube leading from outside the reactor to the sample. Because the beam is split twice at the beamsplitter, only 25% of the light emitted by the laser reaches the photodetector, a significant loss of laser power. In addition, the splitter produces a double image in one of the split beams, so great care should be taken to direct the single-image beam to the sample. A alternate configuration without a beam splitter at some incidence angle was employed in studies with a gas nozzle designed to separate the group II and VI species.

2.1.2.5. Microwave Plasma Cavity

The purpose of the microwave cavity is to transfer power efficiently from the microwave power source to the static or flowing gas which is contained in a discharge tube. A resonant cavity is simply a hollow metal container having a shape and size which allow a standing electromagnetic wave to be established within or alongside it. Because the standing wave is at a microwave frequency (2.45GHz), the cavity dimensions will be on the order of several centimeters. The cavity is constructed from metal such as gold and copper which have a low skin depth to achieve a higher coupling efficiency. The Evenson 1/4-λ cavity system (Optos Instrument) used in this work is shown in Figure 2.5. The coaxial

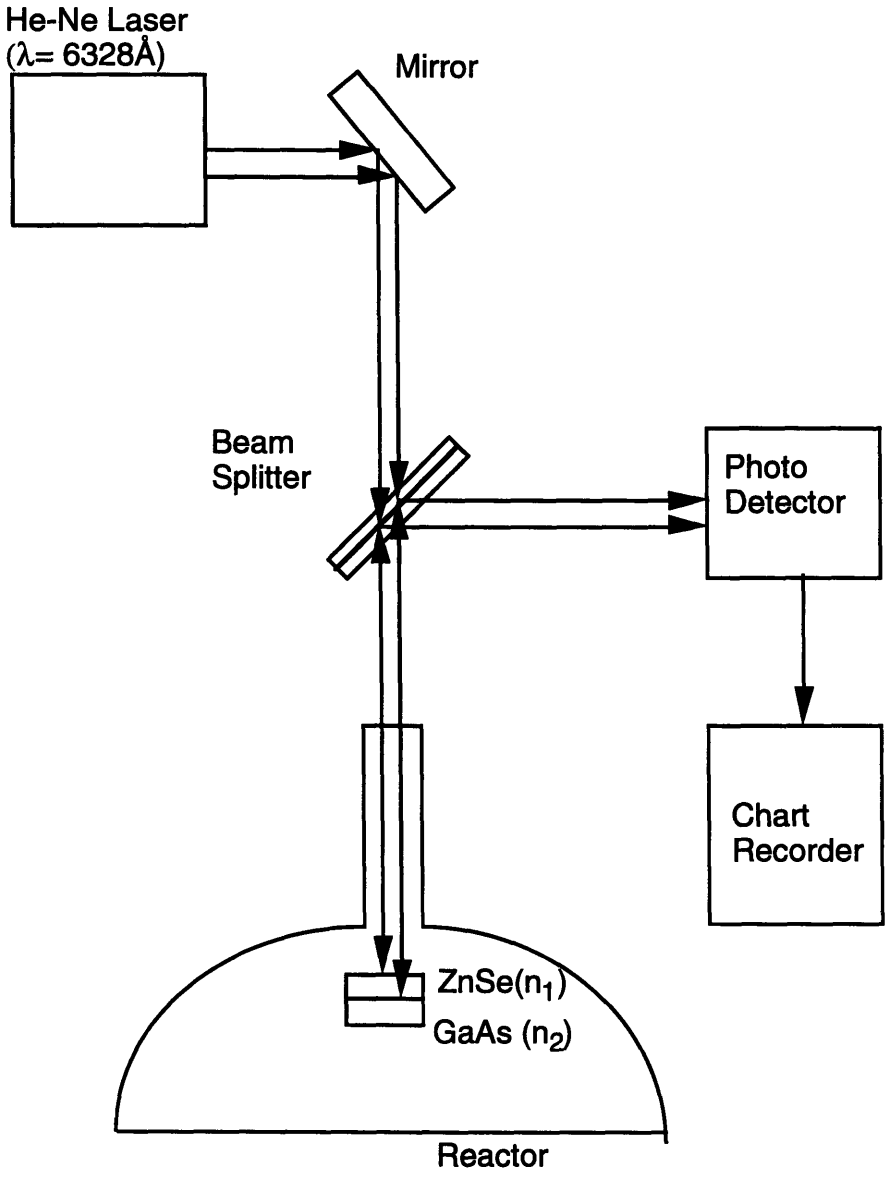

Figure 2.4 Schematic diagram of He-Ne laser interferometer

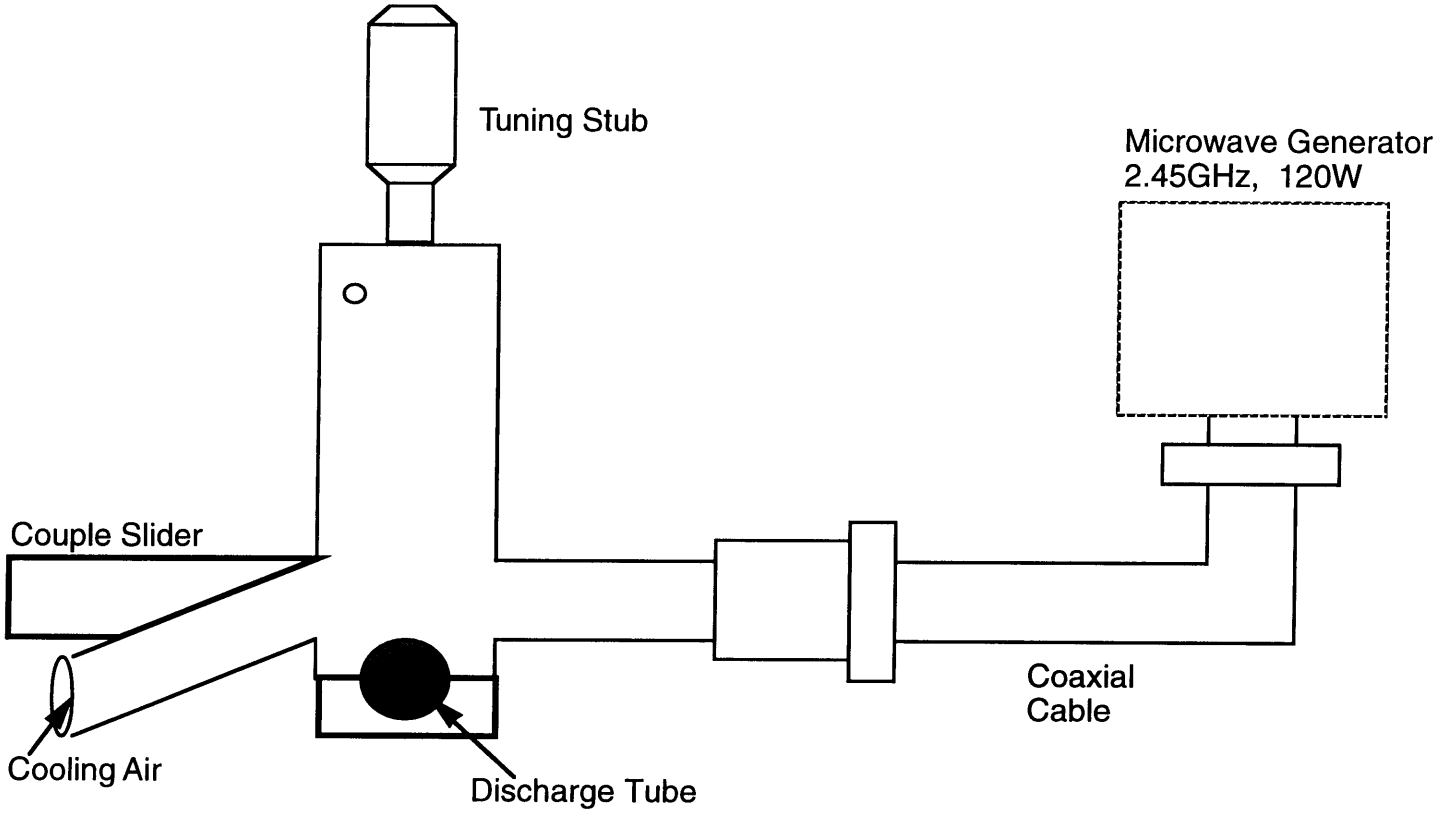

Figure 2.5 Evenson Cavity for use in microwave plasma generation [Optos, 1986]

transmission is terminated in the cavity by a fixed gap, and the discharge tube is placed perpendicular to the gap. The Evenson cavity is equipped with both a tuning stub and an adjustable slider on the body. The stub adjusts the resonance frequency which may be affected by the presence of the plasma in the charge tube. The slider is used to control the coupling. This cavity can excite discharge in both static and flowing gases at pressures ranging from a few mToor to several hundred Torr. However, tuning is critical to achieving this. The microwave plasma is initiated by providing "seed" electrons, with excitation by a Tesla coil.

2.1.3. Reactor Maintenance

Reactor maintenance is essential if the reactor is to remain safe and productive in the face of precursor changes and routine repairs. Preventing or minimizing the exposure of internal reactor parts to air is a particular concern. Any atmospheric contamination in OMVPE usually leads to unsuccessful epitaxial growth by affecting uncontrollably properties of the materials grown, by leading to polycrystalline growth, or sometimes by preventing completely the growth. This is particularly true for water vapor and oxygen. Water clings tenaciously to stainless steel surfaces and opening a section of tubing to air can result in a reactor recovery time on the order of days during which material quality is poor as this water is purged from the system. Baking air-exposed reactor parts can decrease this recovery time, but some parts such as mass flow controllers cannot be heated. It is thus critical that contact of internal reactor parts with air be minimized.

2.1.3.1. Reactor Purge Consideration

Even if a reactor is leak-tight, there are still two sources of contamination with which to contend. First, it is virtual impossible to completely remove water from the internal stainless steel surfaces of the valves and tubing. This residual water is constantly outgassing into the reactant pathways. Second, since no seal is perfectly leak free, there is an extremely small but steady stream of air entering the reactor at all times. If allowed to accumulate these contaminants will deteriously affect the epi-quality until they are purged from the system. As a preventative measure, all reactor lines were constantly purged with high-purity hydrogen (99.999%).

2.1.3.2. Inert gas purge capacity

In order to minimize air exposure when the reactor is opened, an inert gas can be purged into all reactor plumbing. The inert gas pressurizes any section of line that is to be opened, so that the flow of inert gas out of the opened line keeps air out. This is particularly important when the gas handling manifolds are opened during precursor change. A suitable gas for this purpose is Helium, which is effectively inert for our application, relatively inexpensive and easily available in high quality grade (99.9999%, Matheson Gas Co.).

2.1.3.3 Leak Test Capability

After system maintenance, the whole system should be leak-tight. The system was leak checked with He gas by using the Quadruple Mass Spectroscopy (QMS112, Balzers) after evacuating the system with Leybold TMP 150 turbomolecular pump up to $1x10^{-7}$ Torr. The leak test capability proved

indispensable not only for maintaining the reproducible cleanliness of the growth chamber but also in eliminating any potential leak danger of the toxic gas, H_2Se.

2.1.4. Safety Issues

Nothing can be compromised when it comes to the safety of the individuals working on the system and their laboratory partners. Every safety aspect was coordinated with the Industrial Hygiene Office and Safety Office at MIT. Safety considerations in a OMVPE laboratory center on the highly toxic and flammable properties of the chemicals used. A two pound cylinder of 100% H_2Se is installed in the laboratory. The cylinder is housed in a special vented gas cabinet with a purging system (Air Technology Co.). The metal hydrides like H_2Se are the most dangerous of these hazards because of their extreme toxicity [Lum *et al*,1986]. The H_2Se used in this reactor system has a Threshold Limit Value (TLV) of 50 ppb, and an Immediately Dangerous to Life and Health (IDLH) value of 2ppm [Sax, 1979]. The flammable precursors and gases are second in hazard ranking after the metal hydrides. A canister of activated charcoal filter (Draeger) was used to absorb and remove any hydride and/or unreacted organometallics.

The third danger is hydrogen explosion from an accumulation due to a plumbing leak combined with hood exhaust failure. The fabricated quartz reaction chamber and gas mixing nozzle are fragile and will not tolerate mechanical abuse of excessive pressure. We use hydrogen gas monitors outside the enclosure, which activate an alarm in case of a hydrogen leak. A sturdy aluminum enclosure was constructed to ensure lower pressure for the whole

reactor system. The pressure inside the lab is slightly lower than that of the outside corridor, thus minimizing the accidental dispersion of hazard gas to the outside.

The safety configuration of the lab are shown in Figure 2.6. The lab has an eight-point toxic gas monitor (Model PSM 8xt, MDA) where sampling points are assigned inside of the enclosure and gas chamber (*i.e.*, process points). Two other single-point hydride monitors (Series 7100, MDA) were installed to detect if any hydrogen selenide is in the lab room air. The first low level alarm is programmed to 25ppb (50% of TLV) and the second high level alarm to 50ppb (100% of TLV). If the concentration of toxic gases becomes greater than the first level, the toxic gas monitor triggers an audible alarm together with a yellow emergence light at the entrance of the lab and if the concentration is greater than the second level a fire alarm in the building sounds in order to prompt evacuation of the building. The emergency signal goes to Physical Plant Operations, who notifies a list of laboratory personnel in case of trouble. Standard safety equipments, including SCBA gear and gas masks, are available within reach for everybody in the first floor of Building 66. Other comprehensive safety interlock systems and the gas handling system for designing an OMVPE lab are reviewed in the references [Johnson, 1984].

An operator can cause serious damage to the system even if a reactor is well designed. Operator errors can occur during maintenance when evacuating or pressurizing lines. Such errors might be avoided by having the state of each valve, including those that are hand or automatically operated, indicated on an easily interpreted status-board.

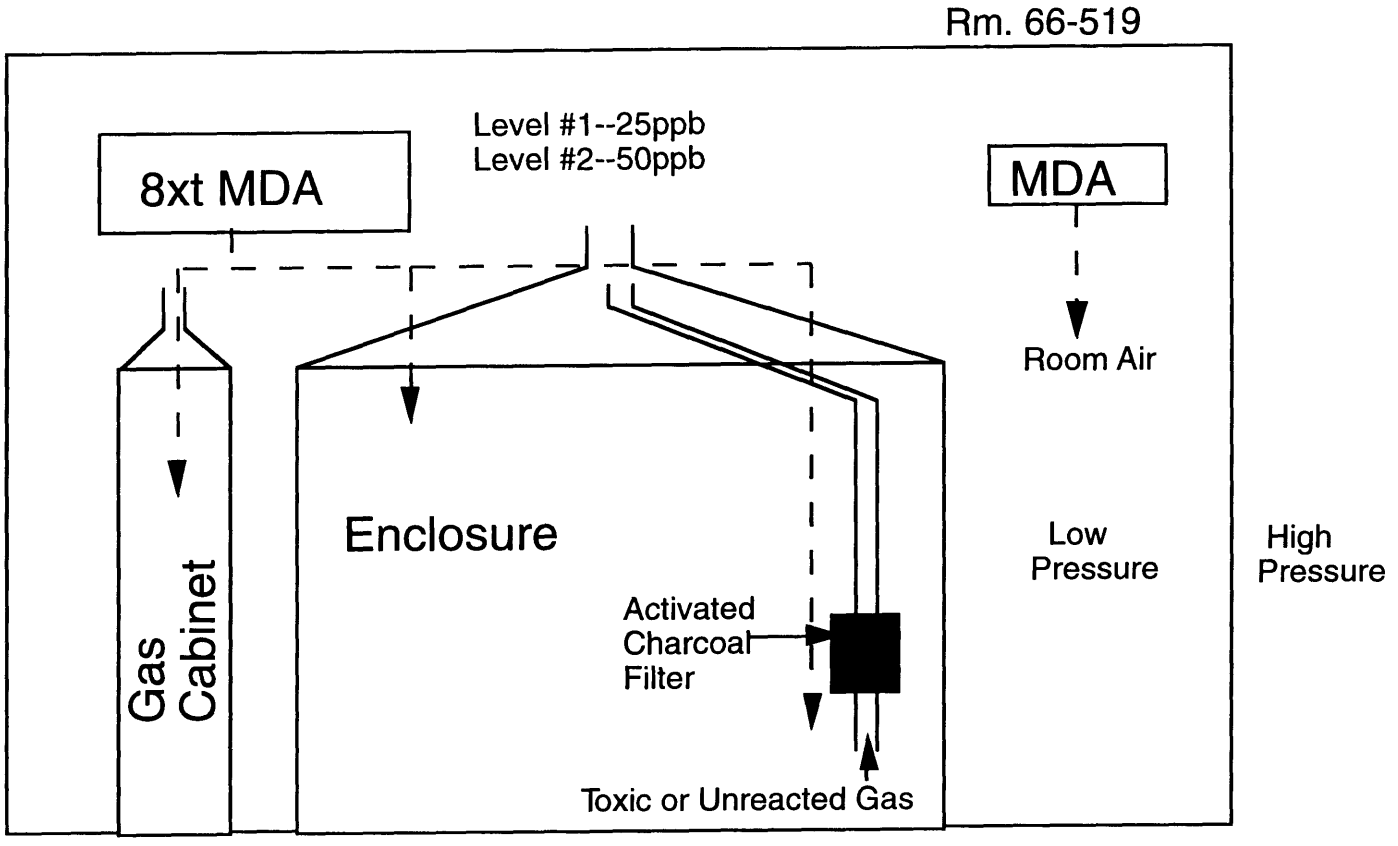

Figure 2.6 Schematic of toxic gas monitoring system

2.2. Molecular Beam Mass Spectrometry

Figure 2.7 shows a schematic of the molecular beam mass spectrometry system (MBMS) used to investigate the gas-phase pyrolysis of Zn and Se reagents. The MBMS system consists of a reactor stage and two differentially pumped stages. Gas phase precursors are introduced from the top of the reactor through a quartz gas distributor at which different reactants are mixed. The reactor is kept at 30-50 Torr so as to maintain a continuum source. A graphite susceptor is heated resistively and its temperature is measured by a type-K thermocouple cemented to the susceptor surface. During gas sampling at high temperatures (>250°C) the reactor wall is cooled with cooling water to avoid reactions induced by hot walls. Gas phase reactants are sampled through a Fenn type orifice (diameter ~100μm) to the first vacuum stage. The first vacuum stage is pumped by a Leybold TMP 450 turbomolecular pump, which provides a typical background pressure of 10^{-6} to 10^{-5} Torr during sampling. The sampled gas continues to expand before it transforms to a free molecular jet.

A 400μm conical skimmer is located downstream of the transition surface to further sample the beam to a second vacuum stage, which is pumped by Leybold TMP 360 turbomolecular pump. The operating pressure of the second stage is in the range of 10^{-8} to 10^{-7} Torr. The skimmer collimates the beam toward a Blazers 311 quadruple mass spectrometer equipped with two rhenium filaments as the cross beam sources. The analyzer is mounted with a 90° off axis secondary electron multiplier which provides an extra amplification of 10^5 to 10^6. In order to reduce beam attenuation effects such

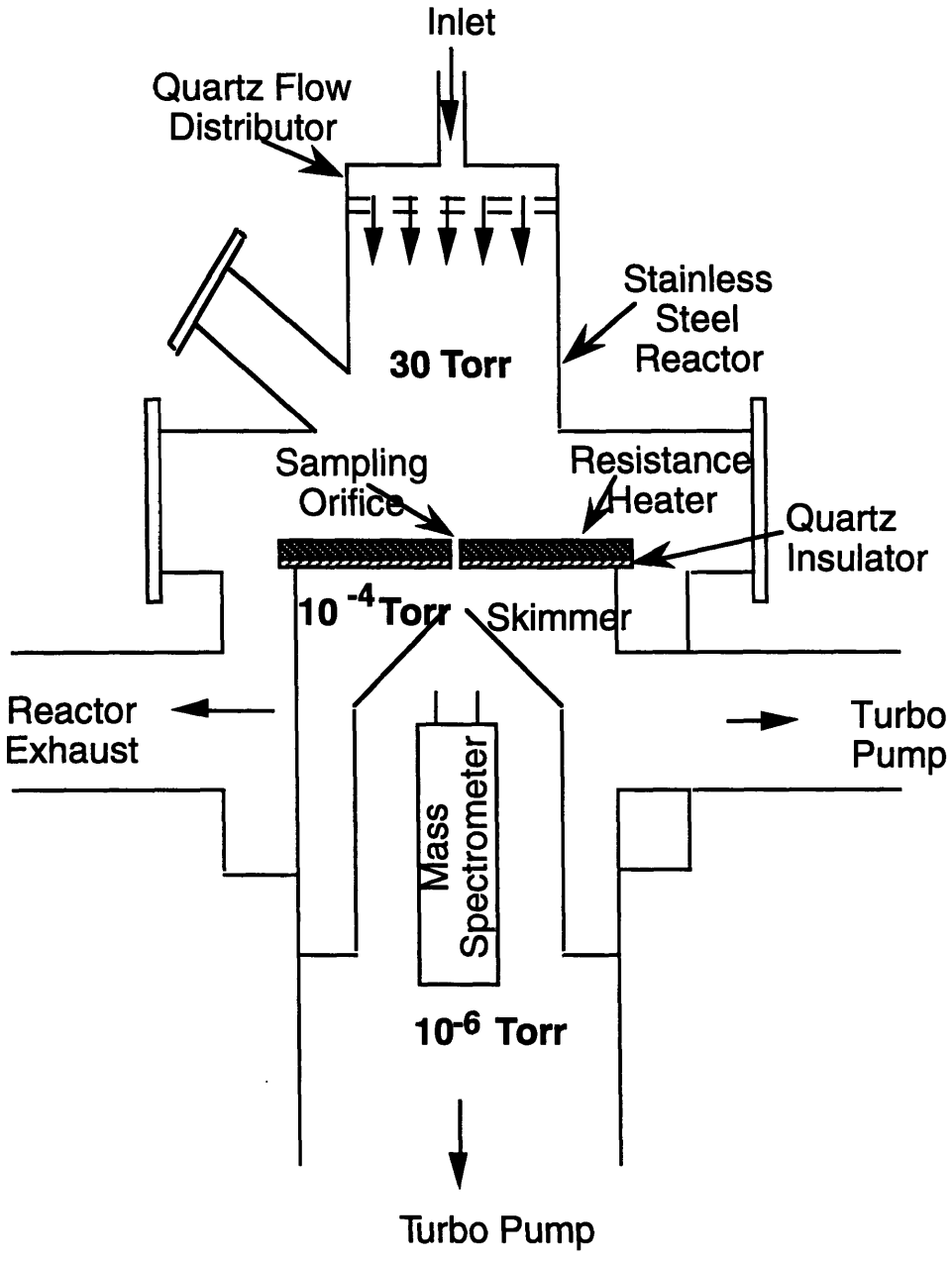

Figure 2.7 Schematic diagram of Molecular Beam Mass Spectrometric System

as Mach number focusing, the quadruple analyzer is located immediately below the skimmer entrance. In this way, the bulk gas phase species extracted over the growth surface are quenched and analyzed with minimal perturbations.

2.3. Characterization Techniques

2.3.1. *In-situ* Process Characterization Techniques

2.3.1.1. Mass Spectroscopy

The reactor is equipped with a quadruple mass spectrometer (QMS 112) and sampling system designed for residual gas analysis as well as for leak testing of the OMVPE system. The sampling point is located just below the molybdenum susceptor, when the system is in running position and the heating stage is placed inside the reaction chamber. This down stream mass spectrometer makes it possible to monitor gas phase composition, gross chemical effects and possible H_2O/O_2 contamination in the reactor. It is also used routinely to check if a particular gas composition has been reproduced successfully by monitoring the intensity of the particular peaks (for example, Se species).

2.3.2.2. Laser Interferometry

The growth rate was monitored during the whole growth to confirm whether there was unexpected equipment misfunction. During the deposition the thickness of the layers and the growth rates were controlled *in-situ* by

monitoring the interference between beams reflected from the surface of the grown ZnSe layer and from the substrate-layer interface using a He-Ne laser.

The principle of the laser interferometer is relatively simple. Figure 2.8 shows a laser beam traveling from the air through a thin film (n_1) into a substrate (n_2). Depending on the optical path difference between the beams reflected at interfaces A and B, alternate constructive and destructive interference occur as the film thickness (d) increases.

If the laser beam is linearly polarized in the direction perpendicular to the plane of propagation, the reflection coefficient r can be defined as

$$r = \frac{E^r}{E^i}$$

$$= \frac{r_1 + r_2 e^{-2\beta i}}{1 + r_1 r_2 e^{-2\beta i}}$$

where

$$\beta = \frac{2\pi}{\lambda} d n_1 \cos\phi_1$$

$$= \frac{2\pi}{\lambda} d \sqrt{n_1^2 - \sin^2\phi_0}$$

$$r_1 = \frac{\cos\phi_0 - n_1 \cos\phi_1}{\cos\phi_0 + n_1 \cos\phi_1}$$

$$r_2 = \frac{n_1 \cos\phi_1 - n_2 \cos\phi_2}{n_1 \cos\phi_1 + n_2 \cos\phi_2}$$

and E^r and E^i which are the magnitudes of the electric fields of the reflected and incident beams, respectively. The reflectance $\Re$ can be given by :

$$\Re = r^* \bullet r$$

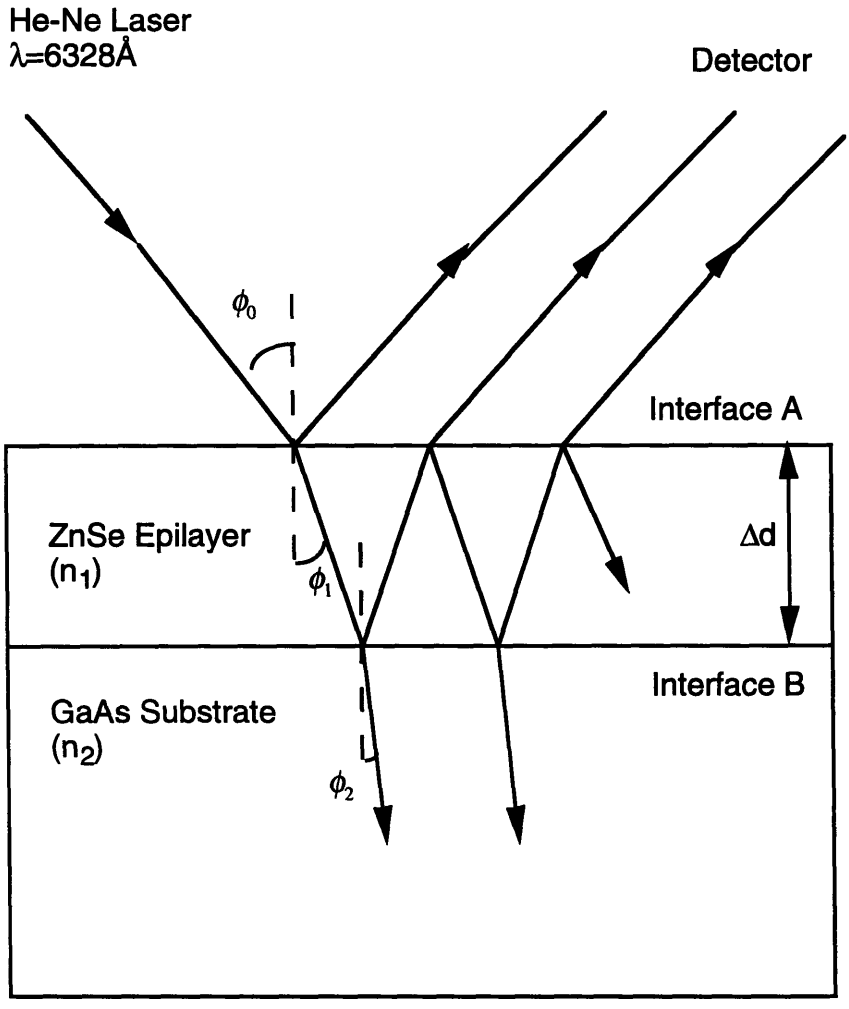

Figure 2.8 Basic Principle of Laser Interferometer

Since the period of $\Re$ is given by $2\beta = 2m\pi$, the consecutive constructive or destructive interferences are related to the change in the film thickness Δd by

$$\Delta d = \frac{\lambda}{2\sqrt{n_1^2 - \sin^2 \phi_0}}$$

The time between alternate maxima or minim represents a growth period τ. The growth rate during the period is computed from

$$\text{Growth rate} = \frac{\Delta d}{\tau} = \frac{\lambda}{2\tau\sqrt{n_1^2 - \sin^2 \phi_0}}$$

2.3.2. *Ex-situ* characterization Techniques

The as grown materials were characterized by a number of standard thin film characterization techniques. The procedures are briefly summarized below.

2.3.2.1. Impurity level

Secondary Ion Mass Spectrometry (SIMS) is a sensitive technique used to measure impurity concentration in the deposited layers [Vickerman, 1989]. In SIMS, the bombarding species are ions, and only the charged secondary species (ions) are detected and analyzed by a mass spectrometer. As the primary ions erode the sample, further depths of the sample can be analyzed. Hence, depth profile of the impurity species within the sample may be resolved as well. However, the bombardment caused by the primary ions introduce sample damage. Other potential problems arise from sample topography, preferential sputtering and sputter-induced mixing. A rough sample can lead to non-uniform sputter yields by the retrapping of ionized species in pores and crevices.

Preferential sputtering can occur on multi-element targets in which one or more of the elements under investigation sputter away more easily than others. This leads to an enrichment along the surface of elements that are sputtered less and a depletion of those that are sputtered most. While roughness can be monitored and ionization probability can be accounted for with the standards, sputter-induced mixing can be a more serious and complex problem. In essence, various transport processes can be initiated by each bombardment event. These include thermal diffusion, radiation enhanced diffusion, cascade mixing and thermal and/or radiation induced segregation. While the exact source is often difficult to pinpoint, the result is essentially the same: the distortion of abrupt concentration changes and gradients, particularly at interfaces.

Nevertheless, with proper calibrations, SIMS can provide very accurate concentrations of dopant and impurity atoms as a function of depth in ZnSe. With its high dynamic range, SIMS is also capable of covering changes of several orders of magnitude in a single depth profile.

Depthwise compositional analysis for thick ZnSe layers were performed by John Turner at Hewlett Packard with a Cameca IMS-4f Spectrometer. The primary bombarding ion was Cs^+ with an ion energy of 10keV and a beam current of 33nA, and the negative secondary ions were collected from a 100μm x 100μm detection region out of a 500μm x500μm raster area. C and N concentrations in ZnSe layers were quantitatively measured with the same sensitivity factor obtained in the instrument through the analysis of known ion-implanted standard samples. Depth scales for SIMS profiles were determined from measurements of the crater depths with a calibrated profilometer.

2.3.2.2. Surface morphology and crystalline quality

Film surface morphology was examined by scanning electron microscopy. The thicknesses of ZnSe epilayers on GaAs substrate were also determined by cross-sectional SEM. Film growth rates were obtained from the thickness measurements The instrument was Hitachi which provided a resolution of 500Å. All films were coated with ~200Å thick Pt-Au film prior to examinations to reduce charging effects.

Rutherford Backscattering spectrometry, located at Harvard University, was used to determine the depth information through energy loss and evaluating epi-quality through the channeling method [Feldman, 1986]. The RBS spectra obtained was plotted and analyzed with the Rutherford Universal Manipulation Program (RUMP), available at the RBS facility.

Double Crystal Diffractometry (DCD) was used to further assess the crystalline quality of the thin ZnSe films on GaAs in a nondestructive way. A double crystal diffractometer (model 300, BEDE Scientific, Inc) with a InP (001) reference crystal and Cu_{Ka} radiation from a rotating anode X-ray generator (Model RU-200, Rigaku) was employed. The sample geometry is shown in Figure 2.9. The search and optimization of a peak was done automatically by the instrument software. Symmetric ZnSe (004) rocking curves were recorded and full widths at half maximum (FWHM) were compared for quantitative analysis of the quality of epitaxial layers. Symmetric GaAs (004) peaks were also taken and the angular separations between ZnSe and GaAs were measured to analyze

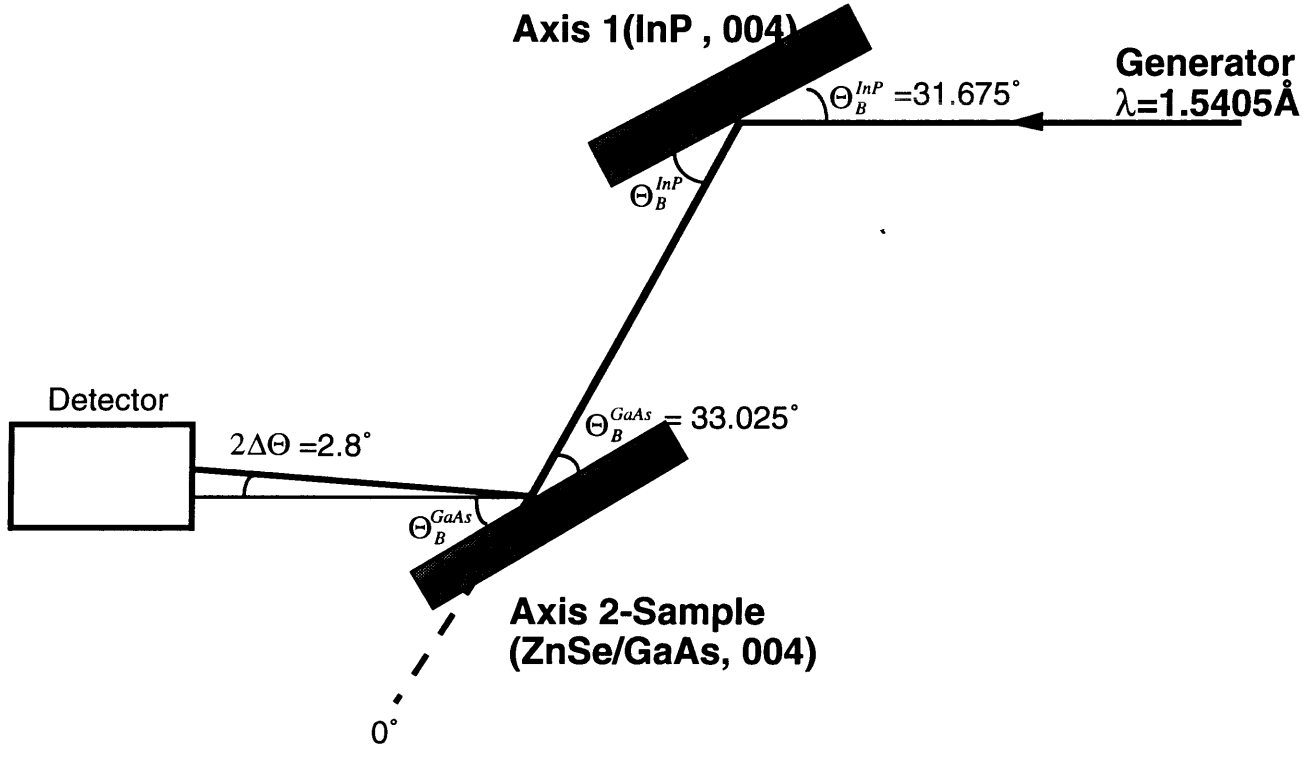

Figure 2.9 Schematic diagram of Double Crystal Diffractometer

the strain developed in the ZnSe layers and the relative misorientation between ZnSe and GaAs.

ZnSe film thickness was measured directly with a surface profilometer ("DEKTAK"). Before measuring the thickness using the surface profilometer a step need to be created by removing ZnSe down to GaAs on part of the sample.. This was accomplished by slicing the sample into a 5mm by 5mm piece, then coating half of the piece with photoresist using a Q-tip. The coated half of the piece was hard baked at 120°C for around 15 minutes, then dipped into an acid mixture (400ml H_2O +5ml HNO_3 +0.2g $K_2Cr_2O_7$) at 55°C to etch a ZnSe layer. The photoresist was stripped in a developer solution. After stripping photoresist, the thickness of ZnSe films was measured by the surface profilometer.

2.3.2.3. Electrical and optical properties

The Van der Pauw method was used to measure Hall mobilities, surface carrier concentrations, and conductivity type of the epitaxial layers. The measurement imposed no restrictions upon the shape of the sample. The only requirements were that small contacts be made at the circumference of the samples and the layers be uniformly thick and continuous [Van der Pauw, 1958].

Ohmic contacts were fabricated in a simple procedure which did not involve any photolithography or etching. Indium dots were pressed upon the corners of degreased samples. The samples were subsequently placed in an annealing furnace. The annealing chamber was evacuated by means of a mechanical pump and backfilled with either forming gas (5%H_2 + N_2) or pure hydrogen gas to a pressure of 200mTorr. The sample was then annealed for

three minutes at 300°C; the ramp up time, from room temperature, was approximately 3 minutes. Formation of ohmic contacts was verified using a curve tracer. A Bio-Rad HL 5200 Hall system was employed to measure Hall mobility, surface carrier concentration and conductivity type of epilayer at 77°K as well as at room temperature.

Photoluminescence is perhaps the most widely employed technique in characterizing semiconductors and their alloys of all optical techniques. PL is used both to understand the fundamental recombination processes in the semiconductor as well as to characterize its quality [Pankove, 1971]. The purity and quality of the grown epilayers were examined on the basis of photoluminescence(PL) spectra obtained at 4°K by using He-Cd laser (λ=325nm) at low power density (<10mW/cm^2) in the system shown schematically in Figure 2.10. The spectra were collected with a 0.85m SPEX 1403 double monochrometer and photon multiplier tubes. Spectral resolution in the range of interest was better than 0.5cm^{-1}.

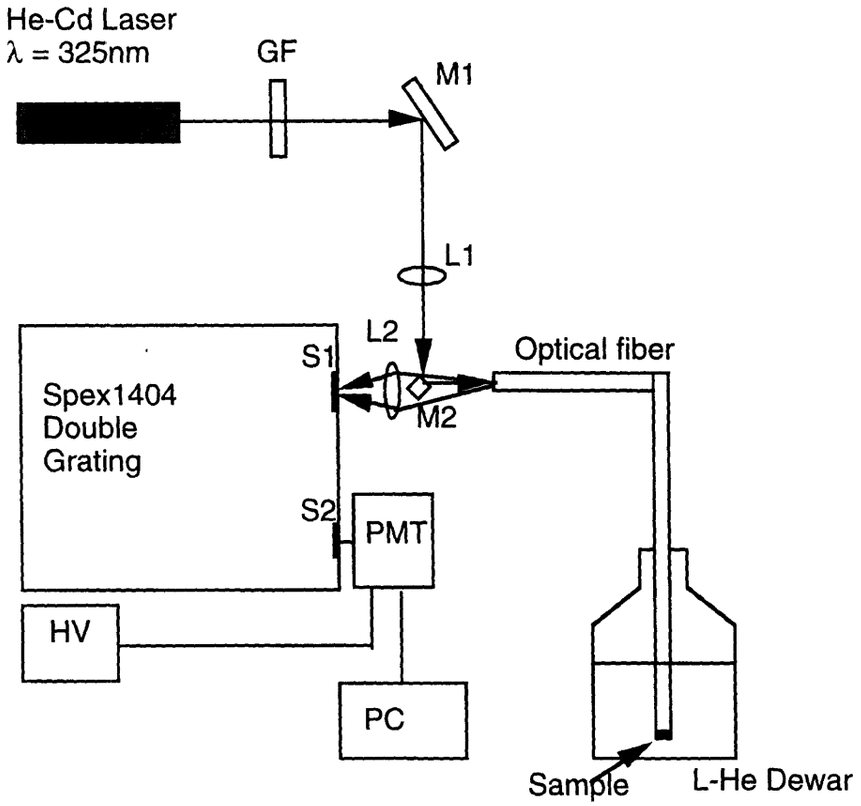

HV : High Voltage(1650V) Power Supply
GF : Movable Grating Filter
M1,M2 : Mirrors
L1, L2 : Lenses
S1, S2 : Slits
PMT : Photo Multiplier Tube
PC : Computer Console

Figure 2.10 Photoluminescence Measurement Set-up

Chapter 3

Investigation of ZnSe Growth with Hydrogen Selenide and Dimethylzinc-Triethylamine

3.1 Introduction

Organometallic Vapor Phase Epitaxy (OMVPE) is playing an important role in the epitaxial growth and doping of ZnSe since the underlying chemistry and, hence, the film properties can be controlled by altering the structure of precursor species. The OMVPE growth of ZnSe has two major problems which are less of concerns in the growth of III-V materials. First, there is a premature reaction between Zn alkyl and H_2Se and second native defects such as Zn- and Se-vacancies tend to be formed at high growth temperatures. The first problem leads to non-uniform thickness and poor surface morphology, and it may be addressed by using an appropriate source combination. The second problem seems to be inherent to wide bandgap semiconductors containing relatively high vapor pressure elements. It is necessary to reduce the growth temperature as low as possible so that the generation of native defects is minimized. Reducing the growth temperature may also be achieved through the use of appropriate reagents.

The use of H_2Se as the selenium source in combination with dimethyl zinc (DMZn) for OMVPE of ZnSe results in films with good electro-optical properties

at 325°C [Giapis *et al., 1989*]. However, this process is plagued by the aforementioned premature gas phase reaction which occurs between the group II alkyl and group VI hydride causing ZnSe layers with poor morphology and thickness uniformity as well as variable optical and electrical properties [Stutuis, 1978; Blanconnier *et al.*, 1978]. The use of Lewis bases(NEt_3), such as triethylamine complexed with Zn source (*i.e.*, DMZn:NEt_3), in conjunction with the group VI hydride, has been employed successfully to reduce prereaction and to improve surface morphology, whilst still retaining the advantage of low-temperature growth and good electrical properties [Wright *et al.*, 1989; Jensen *et al.*, 1991].

The use of the DMZn:NEt_3/H_2Se source combination for reducing growth temperature and limiting prereaction is explained in this chapter. The growth and characterization studies are complemented with molecule beam mass spectroscopy investigations to identify decomposition pathways and explain the effect of different Lewis basis on the premature reactions.

3.2 Experimental

The growth of ZnSe by reduced pressure OMVPE was investigated in the low pressure vertical down-flow OMVPE reactor and decomposition studies of the Zn precursor are carried out separately in the molecular beam mass spectrometric sampling system. Both system were described in Chapter 2.

3.2.1. Experimental Procedures

ZnSe was grown in a load lock equipped OMVPE reactor. Two concentric quartz tubes were mounted in the gas inlet nozzle to deliver the reactants separately until they were very close to the heated substrate. The free cross-sectional area ratio $[S_i]/[S_o]$ of the inside $[S_i]$ over the outside $[S_o]$ tube was found to greatly affect thickness uniformity and electrical properties. The flow was balanced so that the average gas velocity at the exit of both tubes was the same. Typically, flow rates of DMZn:NEt_3 and H_2Se were kept at 15μmol/min and 120μmol/min respectively when $[S_i]/[S_o]$=1/4 or 1/10. The substrates were semi-insulating GaAs (100), misoriented 2° towards <110> and were prepared according to standard cleaning procedure [Stutuis, 1978]. The GaAs wafer was placed on a Mo susceptor inside the loadlock and pumped down to a base pressure of $1X10^{-7}$ Torr. It was then transferred into the main reactor chamber where it was heat-treated at 600°C for 10min in 0.4 slm (standard liters per minute) H_2 flow with Se overpressure (150μmol/min H_2Se) to prevent As evaporation. The reactor pressure was kept at 30 Torr. This growth initiation procedure was critical to get good quality of epi-layers by removing oxide layers on GaAs. The samples discussed below were grown at temperature range from 250 to 350°C, pressures in the interval from 100 Torr to 0.5 Torr, and nozzle to susceptor distances in the range of 20-30mm. A mass spectrometer system, with a sampling port immediately downstream of the susceptor, was used to monitor stable reaction by-products. The film thickness was measured *in-situ* by laser interferometer using He-Ne laser.

3.2.2. Molecular Beam Mass Spectrometer

Experimental procedures for gas phase pyrolysis studies were similar to those for film growth experiments except that the reactor pressure was restricted to 30-50 Torr in order to maintain a continuum source. Before each experiment, the reactor was purged with pure hydrogen and the heater was cleaned by heating it to high temperatures. Mass spectra were acquired to ensure that the background was clean. The susceptor was then allowed to cool to room temperature. Carrier gas and makeup gas flowrates were typically in the range of 20-40 sccm and 5-10 sccm respectively. Organometallic sources were carried into the reactor by either pure H_2 or He gas. The delivery rate of the organometallic sources, controlled by mass flow controllers, was about 20μmol/min. When steady state was reached mass spectra were acquired as a function of the heater temperature. Background pressures in the two stages were expected to decrease as the temperature increased. For this reason, high-purity Ar was induced at a rate of 0.1-0.3 sccm so that the Ar^+ signal could be used to compensate for the variations in ion currents due to temperature ramping. The mass spectra were recorded on a personal computer interfaced to the spectrometer system. After each experiment, the reactor was purged with the hydrogen at high temperatures to remove unreacted precursors.

3.2.3. Film Characterization

All layers investigated in the present study were single crystalline and showed features common to ZnSe, *i.e.*, hillocks parallel to the (011) cleavage plane [Stutuis, 1981]. Film thickness and growth rate were measured *in-situ* by He-Ne laser interferometer and confirmed by cross-sectional Scanning Electron

Microscopy (SEM) and Rutherford Backscattering Spectrometry (RBS). Surface morphology was characterized by SEM. The structural property and lattice mismatching were monitored with double crystal diffractometry using Rigaku200. The purity and quality of the grown epilayers were examined on the basis of photoluminescence(PL) spectra obtained at 4°K Electrical properties were evaluated by Hall effect measurement (See section 2.3.2.3).

3. 3 Results and Discussion

3.3.1. Prereactions

Figure 3.1 shows the degree of gas-phase decomposition of DMZn as a function of heater temperature along with the decomposition products, CH_4 and C_2H_6. DMZn starts to decompose around 250°C and CH_4 and C_2H_6 are generated. 50% conversion of DMZn occurs at ~370°C and pyrolysis is completed at 450°C. The decomposition of DMZn occurs by a bond homolysis followed by free radical reactions. The key reactions are :

$$CH_3\text{-}Zn\text{-}CH_3 \longrightarrow \cdot Zn\text{-}CH_3 + \cdot CH_3 \quad (1)$$

$$\cdot CH_3 + H_2 \longrightarrow CH_4 + \cdot H \quad (2)$$

$$\cdot CH_3 + \cdot CH_3 \longrightarrow C_2H_6 \quad (3)$$

The overall reaction between DMZn and H_2Se can be expressed in the form

$$DMZn + H_2Se \longrightarrow ZnSe + 2CH_4 \quad (4)$$

and it is known that CH_4 is produced during OMVPE growth, but the actual mechanism by which growth proceeds is not known. The prereaction between DMZn and H_2Se is complete even at room temperature [Khan *et al.*, 1989].

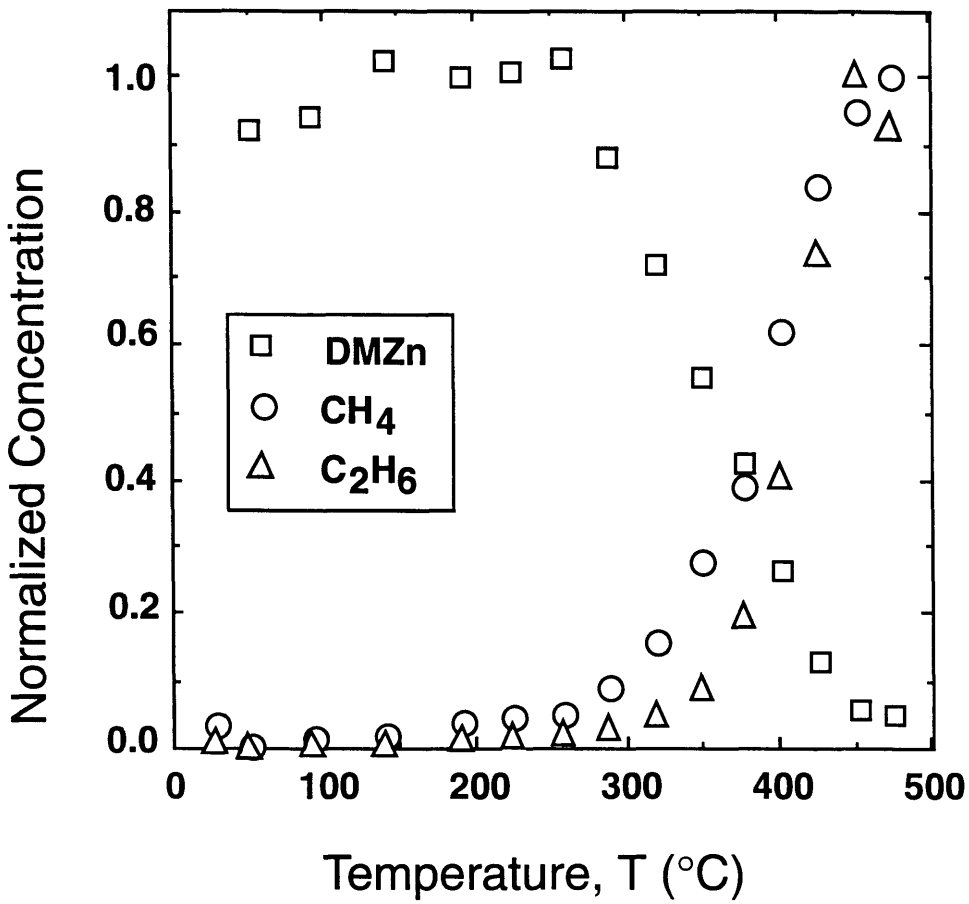

Figure 3.1 Decomposition profiles for DMZn and its products (CH_4 and C_2H_6)

Extensive deposition of ZnSe is often observed on the reactor walls well before the heated substrate (250-350°C), where the gas mixture is close to room temperature and certainly less than 100°C. At these temperatures each reactant, in the absence of the other, can be transported in the carrier gas to the hot deposition zone of the reactor without undergoing any breakdown. Hence, the prereaction is unlikely to involve the pre decomposition of either constituent.

To investigate the interaction of the Lewis base trimetylamine (NMe_3) with DMZn/H_2Se mass spectra of the individual Zn and Se components and mixtures were collected with and without NMe_3 present. Figure 3.2 (a) to (d) reveals that Lewis bases do not interact with DMZn or H_2Se alone. When DMZn and H_2Se were reacted together, the presence of NMe_3 lead to higher signal indicating a reduced prereaction (Compare Figure 3.2 (e) and (f)).

The interaction of Lewis bases with DMZn/H_2Se at 30 Torr is further evaluated in Figure 3.3. The increase in the Se mass spectrometer signal with Lewis base addition is taken as a measure of the strength of the interaction. The ability of Lewis bases to block the premature reaction is expected to increase according to Lewis basicity, NEt_3>NMe_3>NH_3, and decrease with temperature as also observed in Figure 3.3(a) and (b) respectively. The interaction of pyridine is stronger than expected from its basicity and it is most likely due to a steric effect.

The interaction of the Lewis bases with the DMZn/H_2Se growth is further evidenced in Figure 3.4, which displays the effect of [Lewis base]/[Zn] on the growth rate of ZnSe. The growth rate enhancement becomes greater as the basicity of the Lewis base (NR_3) complex is increased. The growth rate of ZnSe with the H_2Se/DMZn:NEt_3 combination is increased while the growth rate does

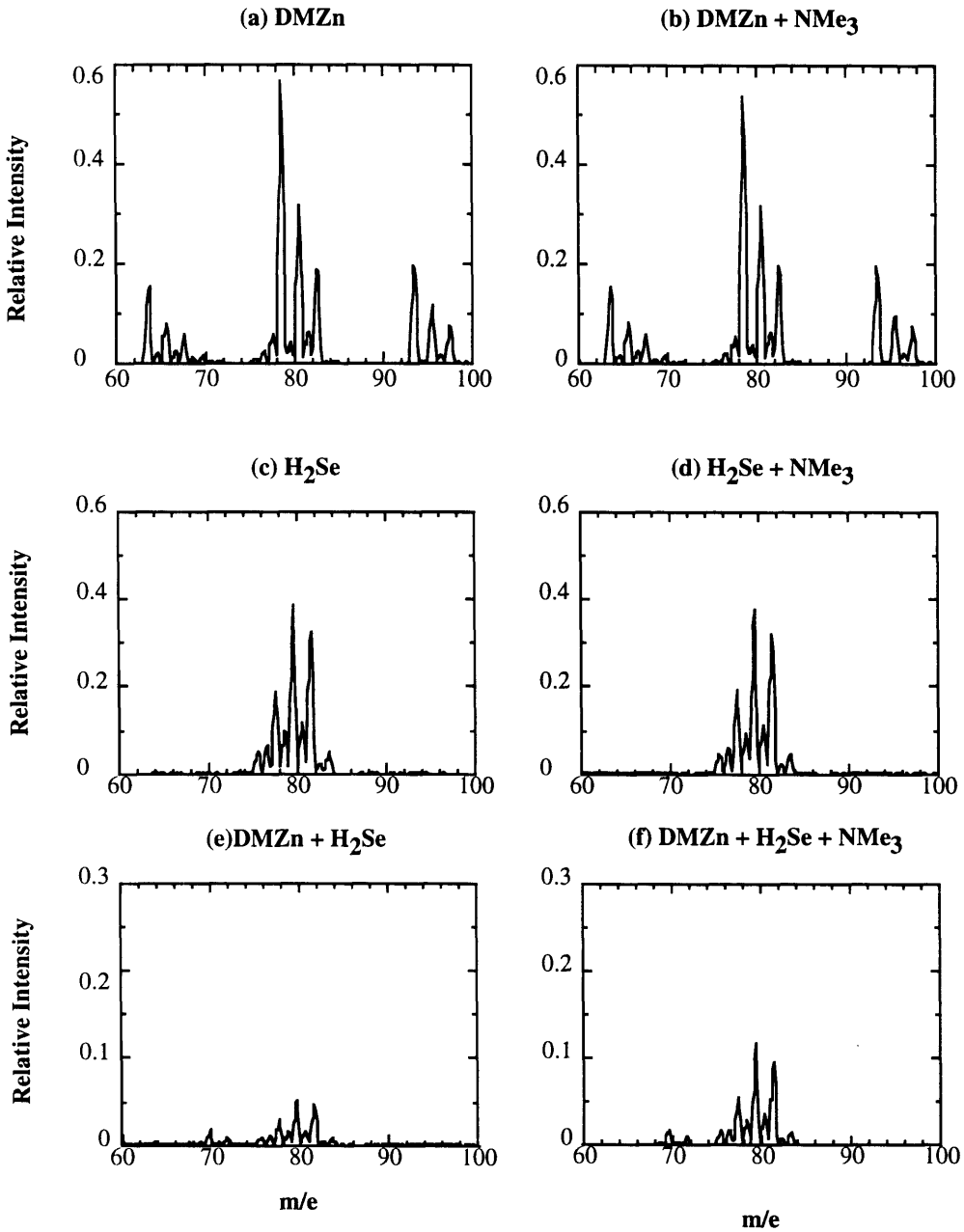

Figure 3.2 The interaction of NMe_3 with $DMZn/H_2Se$ at T=24°C and P=30Torr

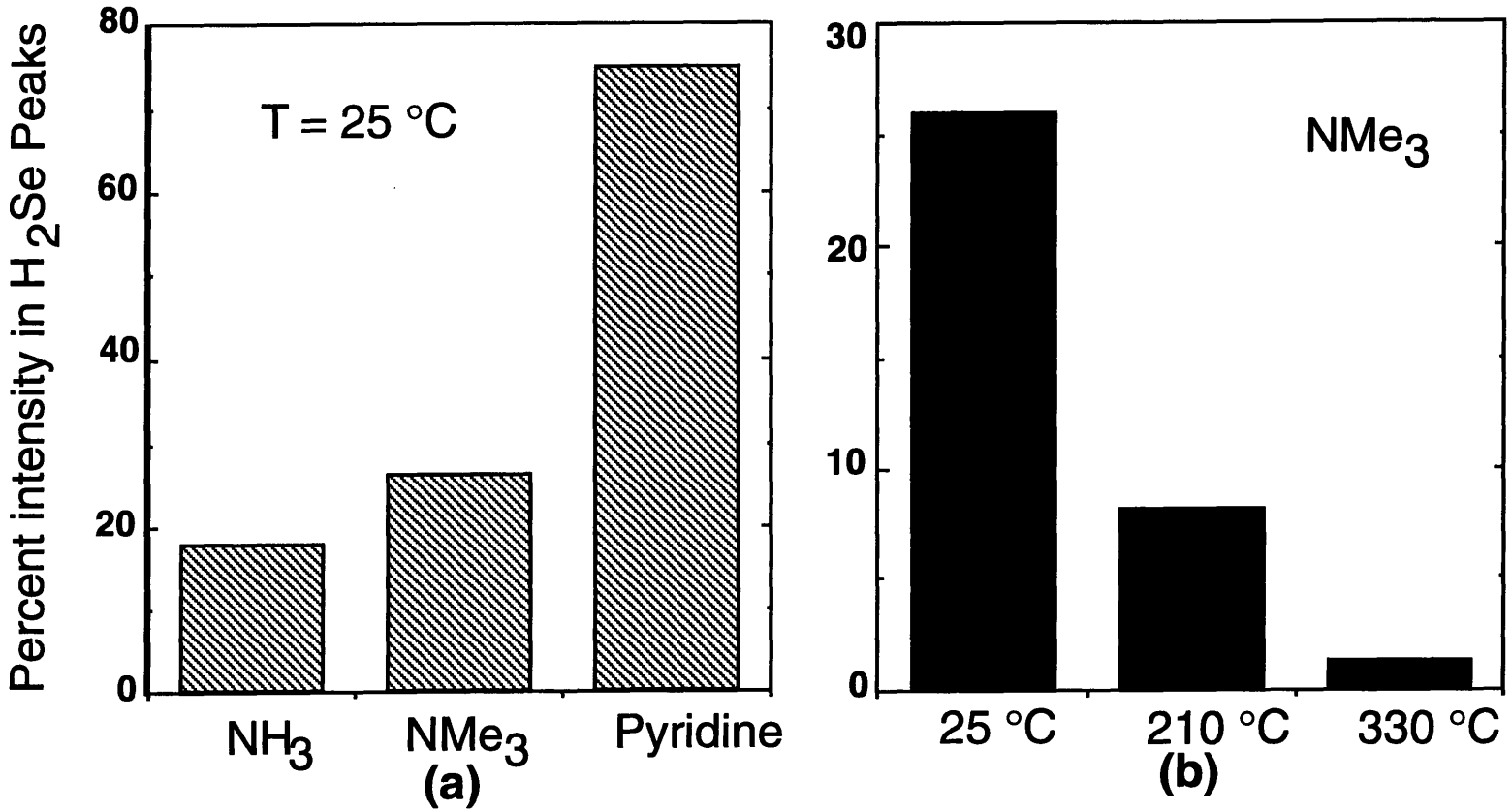

Figure 3.3 The interaction of Lewis base with DMZn/H_2Se at 30Torr (a) different basicity (b) different temperature

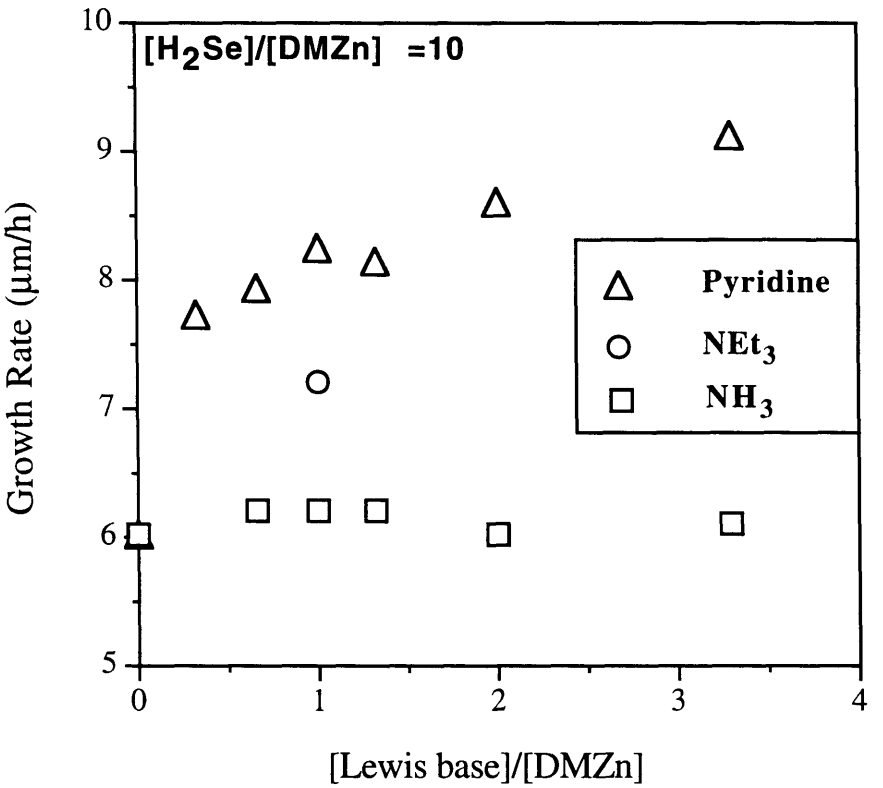

Figure 3.4 The effect of [Lewis base]/[DMZn] on the growth rate of ZnSe (T_G=250°C, P_R=30Torr, $[S_O]/[S_i]$=10, DMZn = 15 μmol/min)

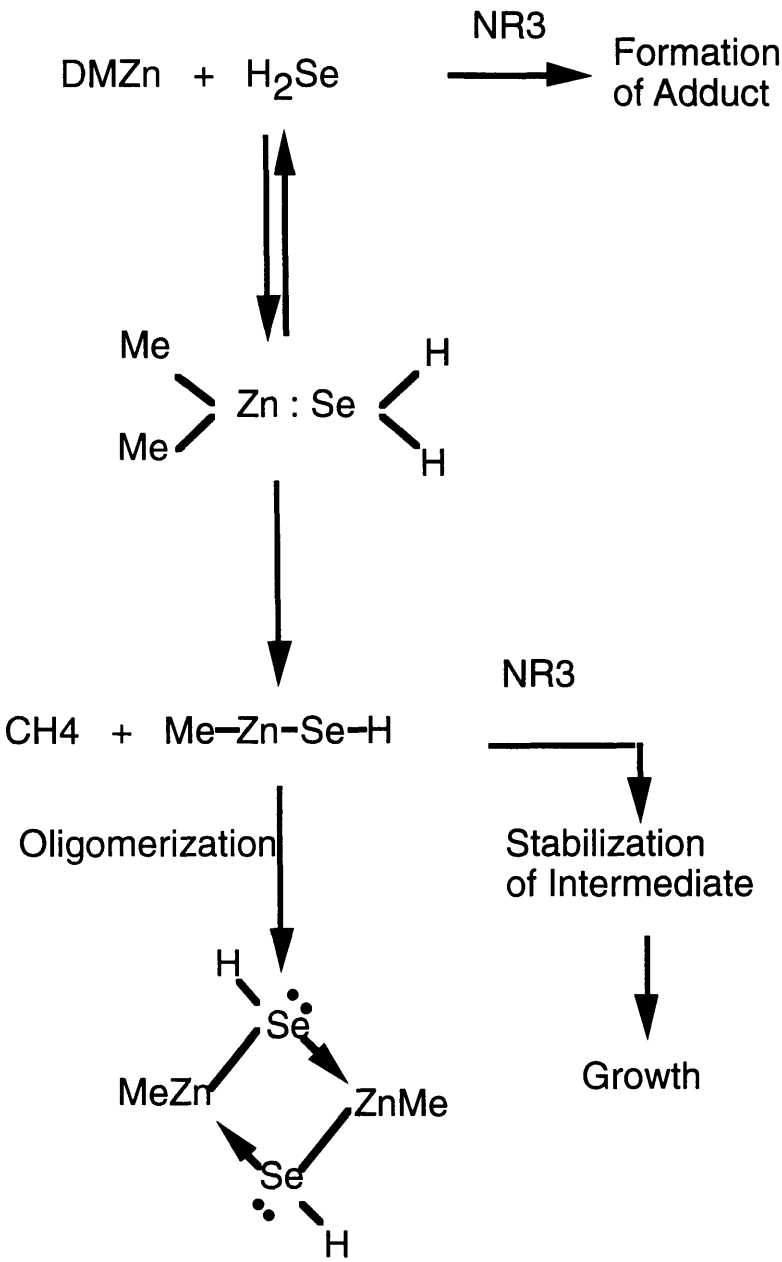

Figure 3.5 Reaction Mechanism of DMZn/H_2Se and NR_3

not change much with NH_3. Pyridine addition gives the largest growth rate enhancement in agreement with the gas-phase result in Figure 3.3.

According to Figure 3.5, the parasitic reactions may be attributed to adduct formation of the Lewis base, H_2Se, and the Lewis acid, DMZn, followed by elimination of CH_4 and subsequent oligomerization to larger clusters. The effect of Lewis base addition could be attributed to stabilization of the intermediate product and a correspondingly reduced oligomerization and parasitic prereaction. Adduct precursors have shown to be effective in blocking or, inhibiting homogeneous pre-reaction. Simple blocking of the reaction by the formation of the Lewis acid-base adduct in the vapor phase can be ruled out, however, since dissociation of adducts is likely to be extensive at the elevated temperature used for growth.

3.3.2 Growth rate

Figure 3.6 compares measured growth rates for the different source combinations; DMZn, DMZn:NEt_3 and DMZn+pyridine as a function of growth temperature. The growth rate appears to be limited by some process at low temperature and *decreases* exponentially at higher temperatures, in sharp contrast to the standard OMVPE growth behavior displayed by organometallic selenium reagents (see Figure 4.13). The unusual decline in ZnSe growth rate observed for DMZn/H_2Se with increases in temperature is consistent with a competitive parasitic reaction having a lower activation energy than the growth process and becoming dominant at high temperature.

Use of the Lewis base addition increases the deposition rate at low temperatures, but has no effect at higher temperatures. This behavior is

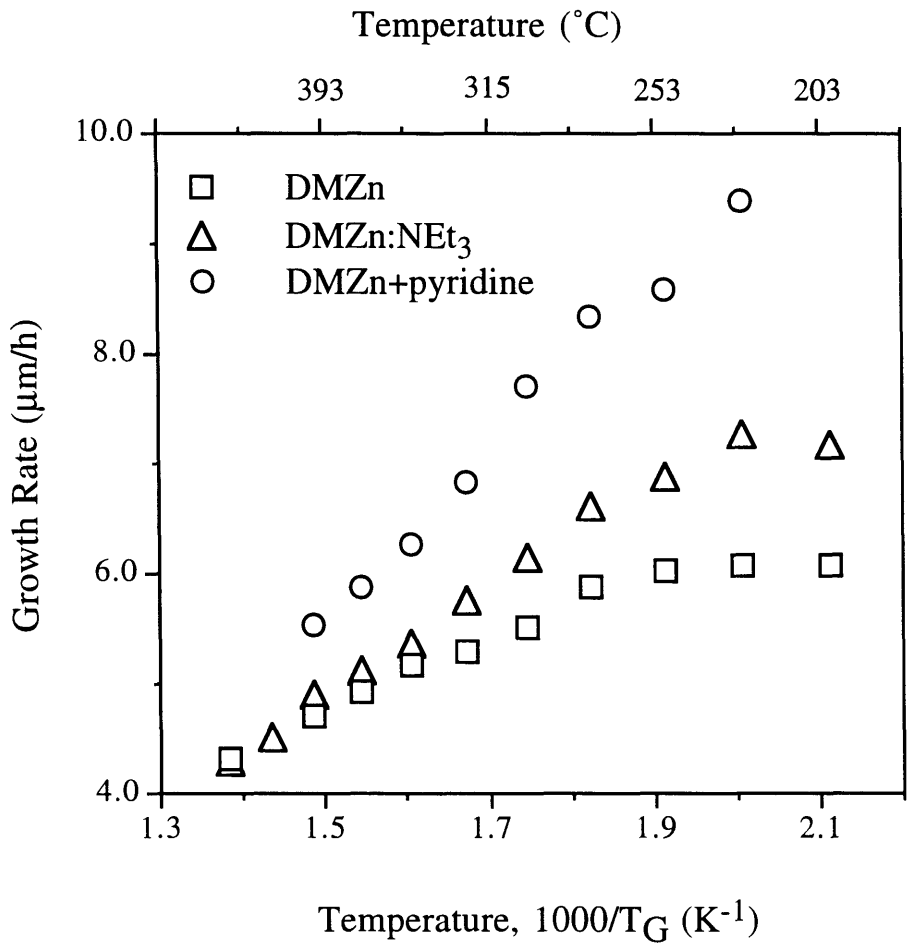

Figure 3.6 The effect of growth temperature on the growth rate of ZnSe (P_R=30Torr, $[S_o]/[S_i]$=10, VI/II=10, H_2Se = 150 µmol/min)

consistent with the relatively low energies involved in the adduct formation and stabilization (~10 kcal/mol) compared to those required to break chemical bonds (~40 kcal/mol). Thus, at high temperatures the adduct is dissociated, and stabilization of any intermediate formed is no longer possible. It is apparent that there are no clear kinetic or mass transfer limited regimes, which would be another indication of parasitic prereactions occurring between H_2Se and the Zn source.

Figure 3.7 illustrates the effect of reactor pressure on the growth rate of ZnSe. Growth at a higher pressure (>200 Torr) resulted in enhanced premature reactions with further reduction in the growth rate. The variation in growth rate with pressure shows a significant enhancement of the deposition rate at low pressures when DMZn:NEt_3 is used while this effect is not present with pyridine. Concerning that surface reactions play a significant role at the lower pressures, this effect suggests that surface reactions also participate in the improved growth characteristics. Within experimental accuracy, the DMZn:NEt_3 and DMZn yield the same growth rates at high temperatures and pressures indicating that the ethylamine has no effect under those conditions where the adduct is dissociated. Addition of pyridine has a strong effect as also reported by Wright *et al.* [1991].

At low temperatures (~250°C), where the complex appears to reduce prereactions, the adduct precursor DMZn:NEt_3 yields higher deposition rates than those obtained with DMZn over a wide range of hydrogen flows (Figure 3.8). The increase in growth rates for both precursor systems with increasing flow rates of hydrogen is consistent with the higher mass transfer expected at high flow rates [Fotiadis *et al.*, 1990]. It is interesting that the ratio of the growth

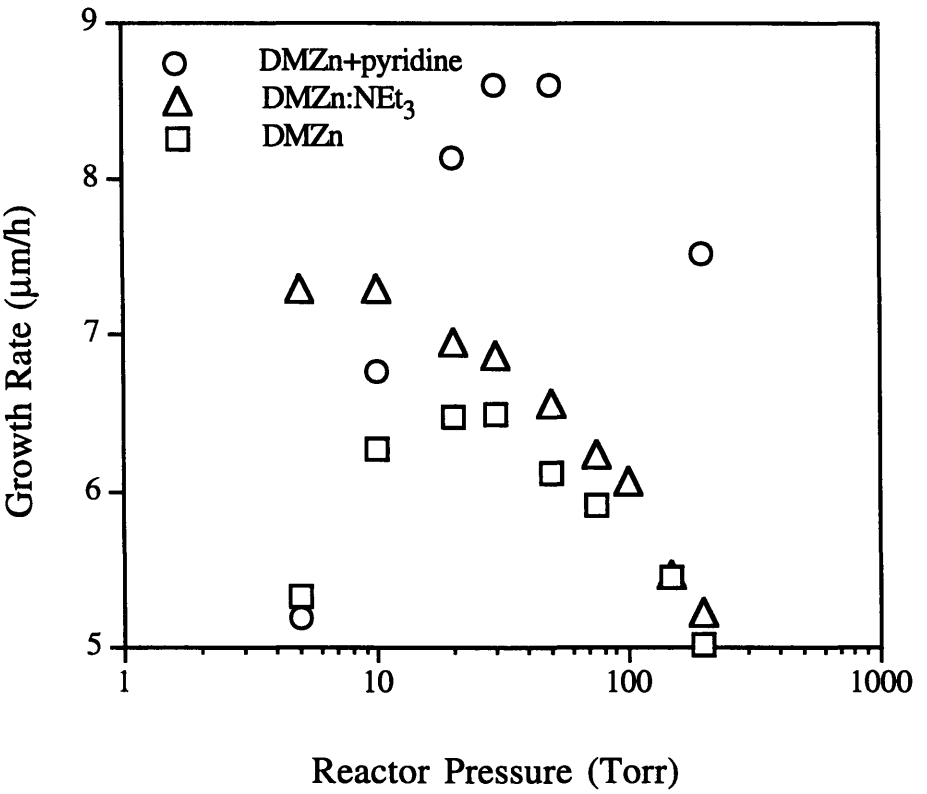

Figure 3.7. The effect of reactor pressure on the growth rate of ZnSe (T_G=250°C, $[S_O]/[S_i]$=10, VI/II=10, H_2Se = 150μmol/min)

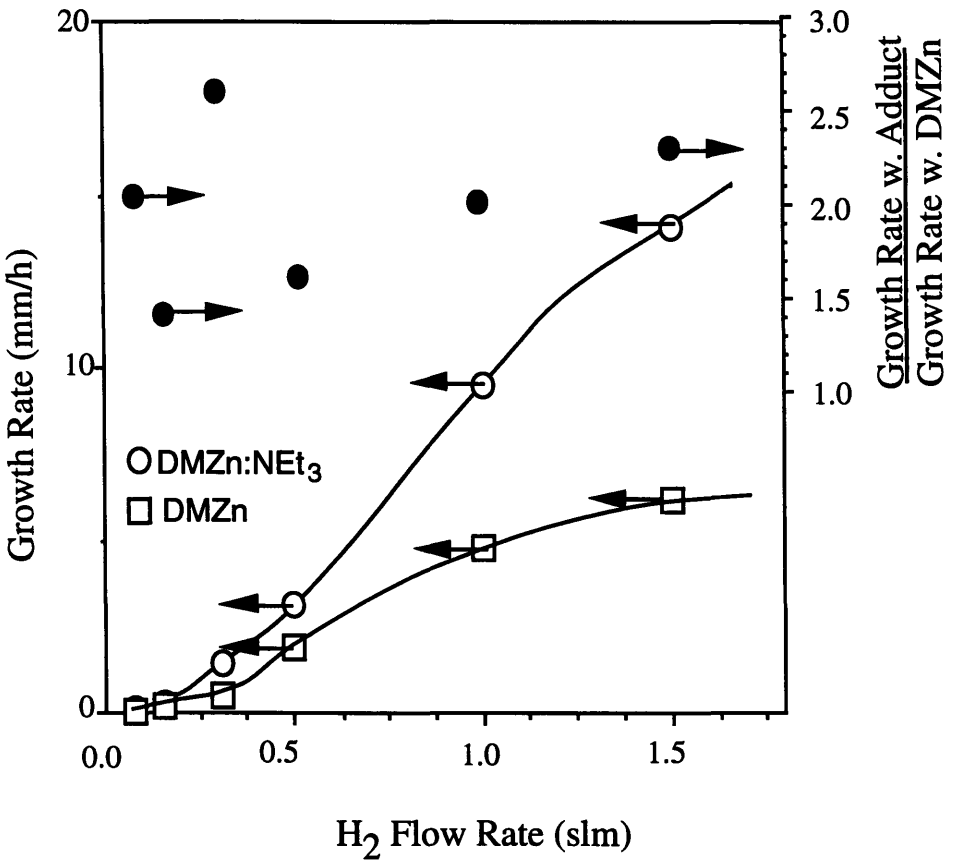

Figure 3.8. The effect of hydrogen flow rate on the growth rate and ratio of growth rate (P_R=30Torr, T_G=250°C, VI/II=10, H_2Se =150μmol/min)

rate obtained with the adduct, to that measured for DMZn, shows no significant variation over the range of flow rates investigated. If the "blocking" reaction had been a purely gas-phase effect it would have been more dominant at low flow rates, where the residence time is large. The scatter in the ratio data at low flow rates may be attributed to decreased accuracy of the film thickness measurements for very thin films (~0.3μm).

The effect of susceptor-nozzle distance on the growth rate is shown in Figure 3.9. An increase in the nozzle-to-substrate distance from 20mm to 25mm results in a reduction of the growth rate of about 1/5 from that observed at 20mm as expected from mass transfer analysis [Fotiadis *et al.*, 1990]. The growth rate increases linearly with the DMZn:NEt_3 delivery rate (Figure 3.10) while it is nearly independent of the H_2Se delivery rate at two different growth temperatures (Fig 3.11). Thus, the Zn source delivery rate appears to limit the growth rate. Finally, Figure 3.12 shows the carrier gas effect on the growth rate of ZnSe. There is no significant change of growth rate between H_2 and He carrier gas. This behavior is consistent with the similar thermophysical properties of the two gases.

3.3.3. Surface Morphology

The surface morphology of the ZnSe epilayers was determined from SEM measurements. Since epilayer crystallinity and morphology greatly depend on the growth temperature, SEM photomicrographs of films grown between 275°C-375°C are given in Figure 3.13. Surface morphologies of ZnSe films prepared with DMZn and the adduct, DMZn:NEt_3, are compared. In agreement with previous reports [Stutius, 1981], ZnSe layers grown with H_2Se and DMZn exhibit

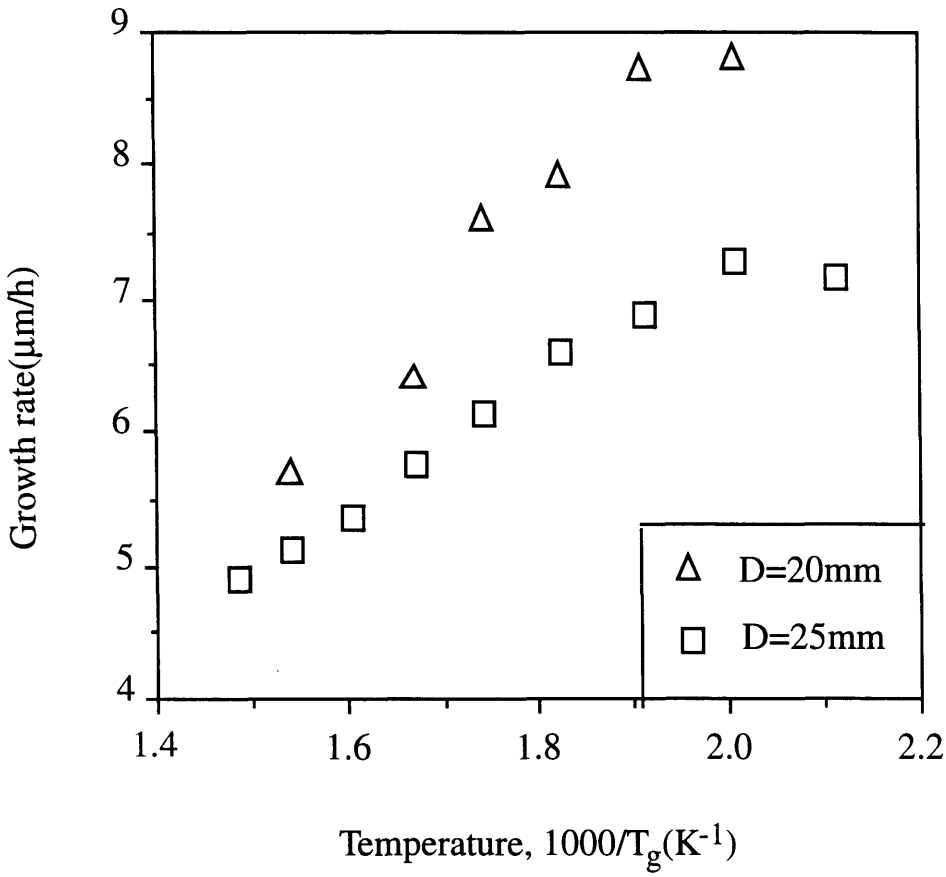

Figure 3.9. The effect of susceptor-nozzle distance on the growth rate (P_R=30 Torr, $[S_o]/[S_i]$=10, VI/II=8, DMZn:NEt_3 = 30 μmol/min)

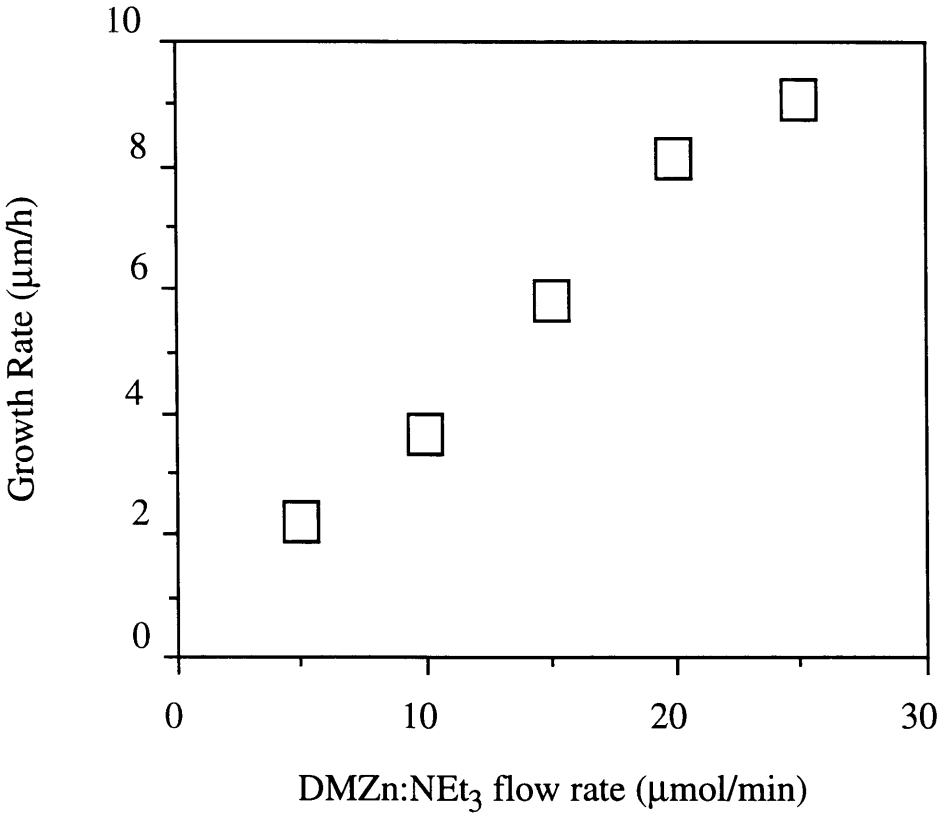

Figure3.10. Growth rate dependence on the DMZn:NEt_3 flow rate (T_G=250°C, P_R=30 Torr, $[S_o]/[S_i]$=10 and VI/II=8)

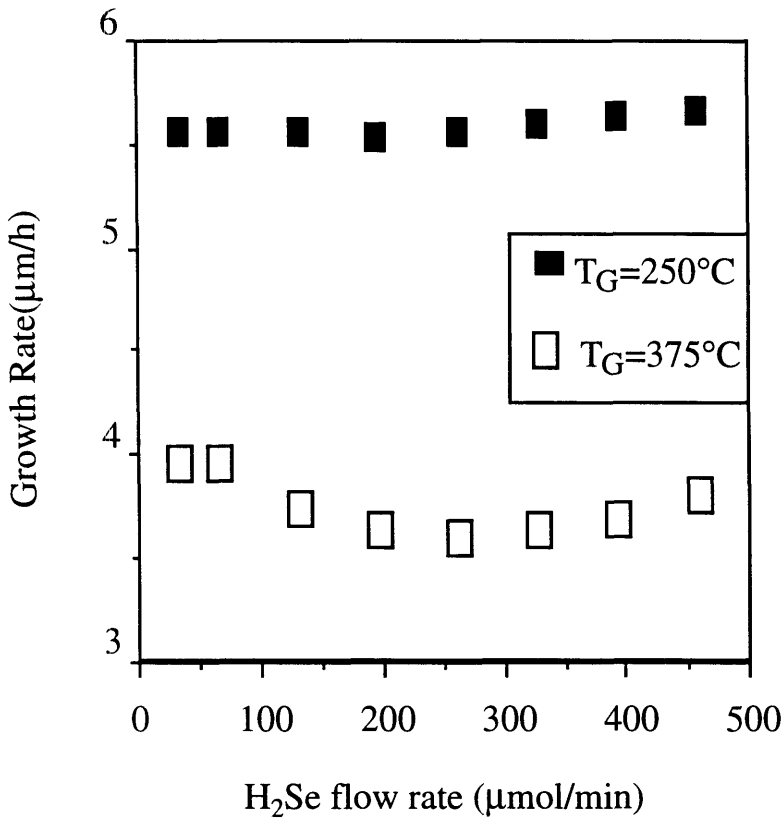

Figure 3.11. Growth rate dependence on the H_2Se flow rate at 2 different T_G (P_R=30 Torr, $[S_o]/[S_i]$=10, and DMZn:NEt_3 =15 μmol/min)

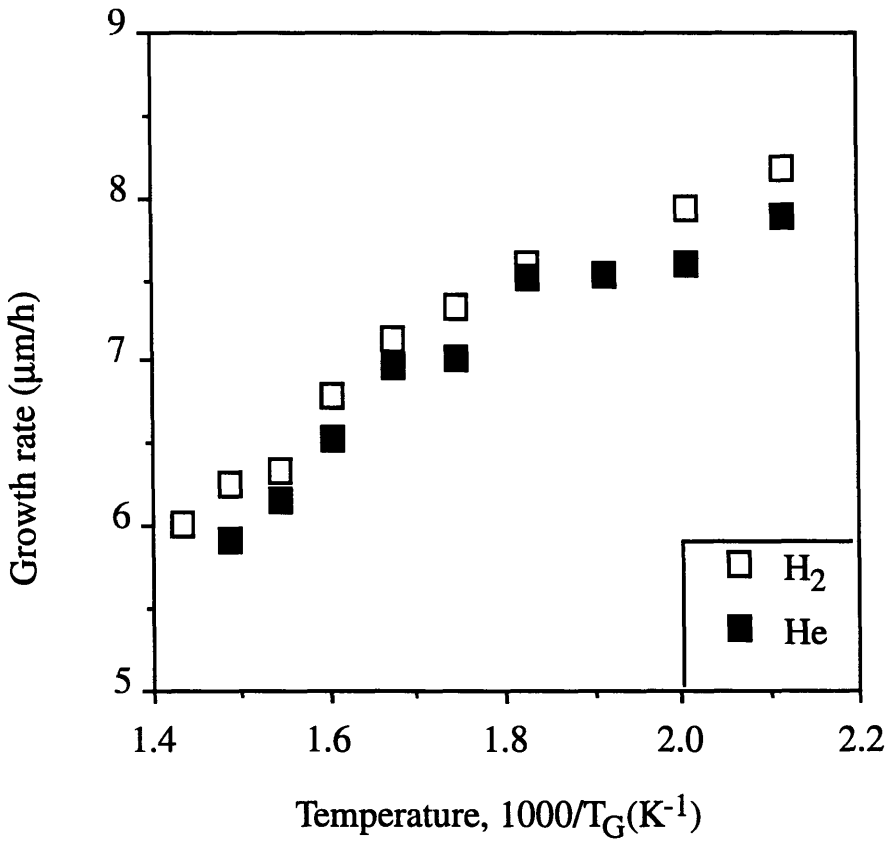

Figure 3.12. The effect of carrier gas on the growth rate of ZnSe (P_R=30 Torr, $[S_o]/[S_i]$=10, VI/II=8, DMZn:NEt_3=30μmol/min)

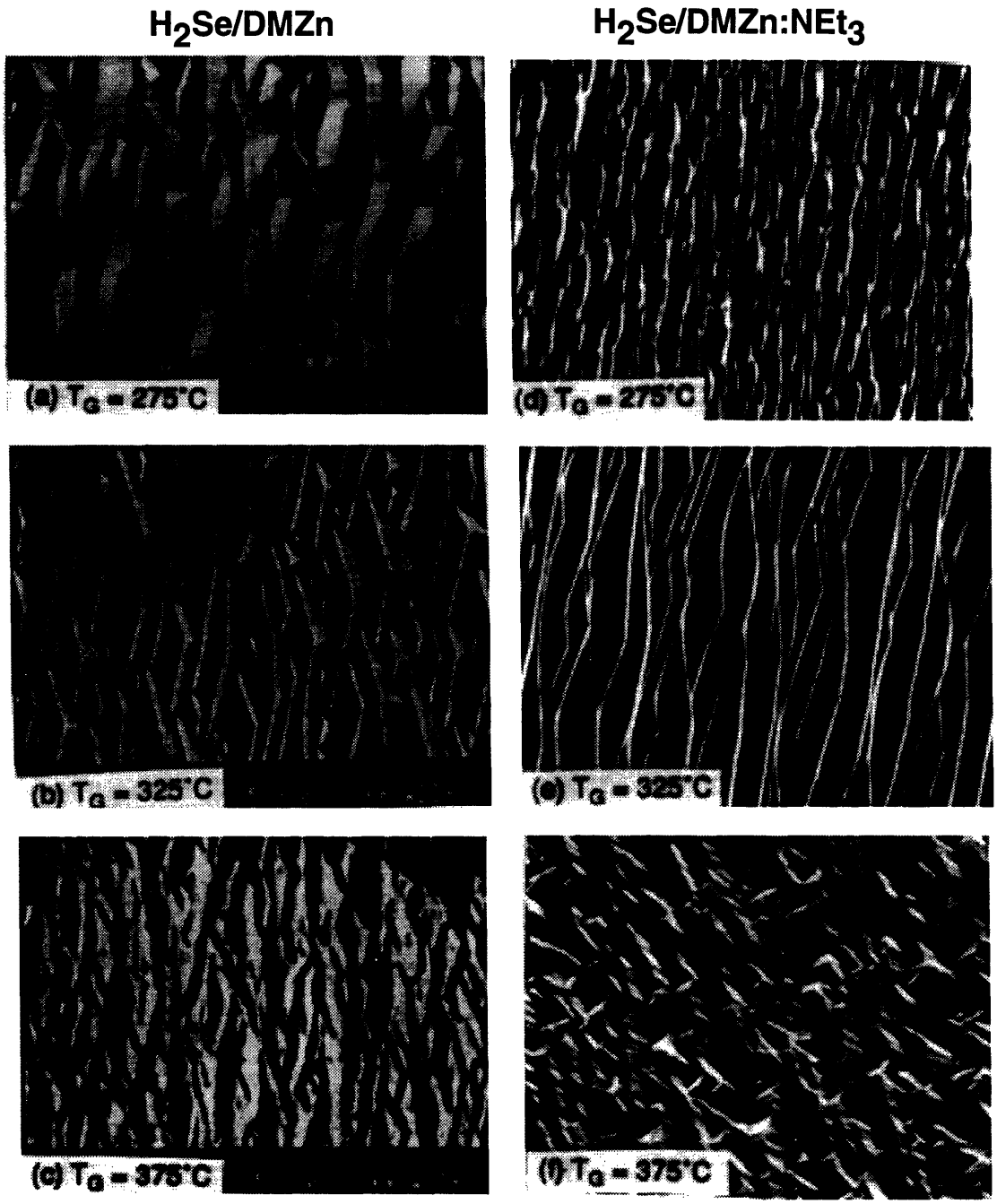

Figure 3.13 SEM microgrphs of ZnSe grown with H_2Se and either DMZn (left side) or DMZn:NEt_3(right side). Growth condition : [VI]/[II]=10, P_G=30 Torr.

a ridge-shaped hillock structure, parallel to the (011) cleavage plane. Films synthesized with DMZn:NEt_3 display a similar surface morphology at high temperatures (325°C), whereas at reduced growth temperatures (275°C) the surface becomes smoother than that obtained with DMZn. This improvement in surface morphology at lower temperatures is consistent with the reduction in parasitic reactions shown in Figure 3.6 and discussed above. At 375°C the hillocks have lost their sharp, well-defined edges. Higher growth temperatures resulted in further coarsening of the surface.

3.3.4. Electrical properties

Electrical properties of selected ZnSe films grown from H_2Se/DMZn:NEt_3 are shown in Table 3.1. All samples measured were n-type with 300K net carrier concentrations ranging from $1.7X10^{14}$ to $2.3X10^{16}cm^{-3}$. The 77K mobility value of 4309 cm^2/Vsec is relatively high for ZnSe films from H_2Se/DMZn:NEt_3 since the purity of the DMZn:NEt_3 source is not pure enough to compare with commercially pure DMZn at the present time. The Hall electron mobility *vs.* carrier concentration at 77°K is shown in Figure 3.14. The solid lines were produced from the theoretical work on electron transport in ZnSe by Ruda [1986]. His model works well at 77°K, where ionized impurity scattering becomes the dominant mechanism limiting electron mobility. In order to estimate N_A, N_D and the compensation ratio q from experimental values of 77°K mobility and carrier concentration, the Brooks-Herring equation [Brooks, 1955] has been employed. In our films from the H_2Se/DMZn:NEt_3 combination, compensation ratio q falls between 0.7-0.95 in agreement with the calculation by Ruda [1986] as can be seen in Figure 3.14. The Hall electron mobilities were

Table 3.1 Experimental and calculated electrical properties of undoped ZnSe. n and μ are the net carrier concentration and mobility at the corresponding temperature. N_A and N_D are the total acceptor and donor concentrations, θ is the compensation ratio.

Run #	Thickness μm	n_{300} ($10^{15}cm^{-3}$)	n_{77} ($10^{15}cm^{-3}$)	μ_{300} ($cm^2/Vsec$)	μ_{77} ($cm^2/Vsec$)	N_A ($10^{15}cm^{-3}$)	N_D ($10^{15}cm^{-3}$)	θ
212	8	0.5	0.27	152	4309	5.83	6.16	0.94
214	5.7	1.2	0.43	100	3610	7.35	7.83	0.92
216	7	12	3.4	230	2878	11.2	14.6	0.77
219	5.9	1.4	1	201	4102	7.1	8.14	0.87
225	7.52	4	1.8	211	1722	3.43	3.89	0.88
239	7.66	2.1	1.3	187	2193	13.9	15.2	0.91

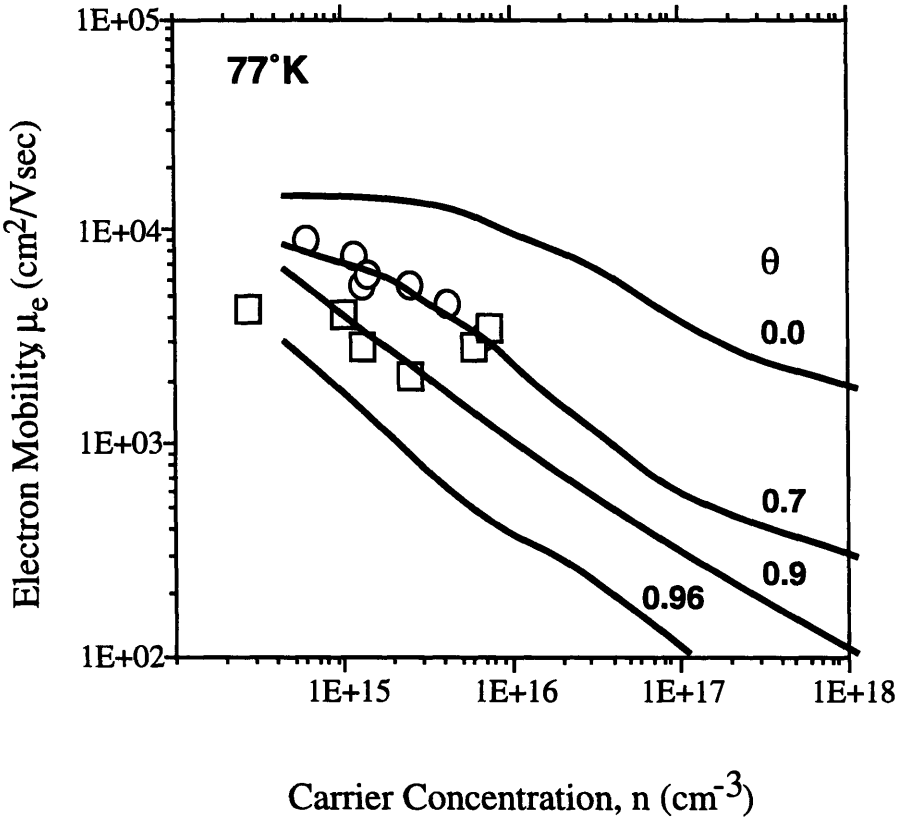

Figure 3.14 Comparison of the Hall electron mobility vs. carrier concentration at 77°K for ZnSe films grown from H_2Se/DMZn:NEt_3 (□) and H_2Se/DMZn(o).The solid curves represent the calculated values of mobility vs carrier concentration for different compensation ratios, reproduced from the work of Ruda,1986

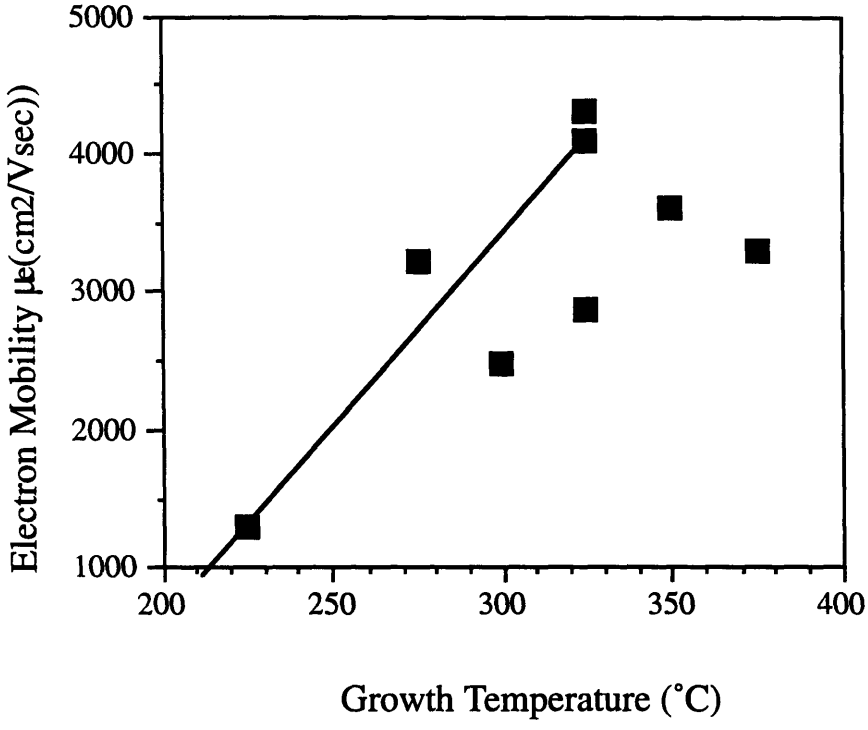

Figure 3.15 The 77K Hall electron mobility (μ_e) on the growth temperature of ZnSe films grown from H_2Se/DMZn:NEt_3

expressed as a function of growth temperature in Figure 3.15. The Hall effect mobility at 77°K increases with temperature up to approximately 375°C, at which point the films become resistive. The origin of this change in electrical characteristics is not known but it is attributed to a thermally activated defect generation mechanism, causing the concentration of carrier traps and deep levels to increase dramatically.

3.3.5. Photoluminescence Characteristics

A typical low-temperature (4K) photoluminescence (PL) spectrum of normally undoped ZnSe samples, grown at the optimal condition on GaAs substrates, is shown in Figure 3.16. An expansion of near-band-edge emission is given in the inset of the figure. This sample was grown at 325°C, 30 Torr and VI/II ratio of 8. The spectrum is composed of a strong near-band-edge (NBE) emission, while the broad emission at smaller energies (deep levels) is weak. The 4K spectrum (inset of Figure 3.16) is dominated by an intense and narrow peak at 2.7954eV (I_X^{lh}). This is due to a radiative recombination of an exciton bound to a neutral donor, identified as chlorine [Giapis *et al.*, 1990] which can explain the n-type conductivity of these films. A second dominant peak is clearly defined at 2.7970eV (I_X^{hh}) and has been attributed to recombination of excitons bound to the same shallow extrinsic neutral donor [Shahzad, 1988, Skromme *et al.*, 1988]. There are also two peaks due to free exciton recombination: the very intense E_X^{lh} at 2.8002eV and , on the high side, the E_X^{hh} at 2.8026eV. The samples are ~3μm thick. Even though there is little lattice-mismatch induced strain affecting the position of the peaks, there exists residual thermal expansion coefficient

mismatch between GaAs and ZnSe, which leads to a small but clearly observable splitting of the free- and bound-exciton peaks [Ohkawa *et al.*, 1988].

At lower energies two more emissions can be observed. The peak at 2.7732eV (I_V) was suggested as recombinations involving selenium-site defects (V_{Se}) [Shahzad *et al.*, 1989]. The peak at 2.7694 is the I_X -1LO replica. At even lower energies, Y_o peak (~2.605eV) and S band have been associated with complex dislocation tangles and other extended defects in ZnSe [Myhajlenko *et al.*, 1984]. The weak intensity of Y_o is an indication of good crystalline quality of the films. Since there is no discernible I_1^d line in PL spectrum, which usually appears at 2.782eV and is attributed to Zn vacancies [Isshiki *et al.*, 1985,] or Cu impurities [Robbins *et al.*, 1986], it is believed that our materials are very close to being stoichiometric. Another manifestation of the purity of our films comes from the two to three orders of magnitude smaller deep level (DL) emission (E<2.5eV), as compared to the NBE dominant peak. The DL emission appears as a weak broad Cu-green emission at approximately 2.3 eV [Grimmeiss *et al.*, 1979].

Figure 3.17 shows the near-band-edge photoluminescence spectra for ZnSe grown with H_2Se/DMZn:NEt_3 at different temperatures. The spectra are similar to those previously reported for DMZn [Giapis *et al.*, 1990], and display no sign of nitrogen incorporation from the amine portion of the adduct. The intensity of the donor-bound exciton peak, I_x^{lh} (2.7954 eV), decreases relative to that of the free exciton peak, E_x^{lh} (2.8002 eV), with increasing growth temperature. A similar behavior has been observed for growth with DMZn and attributed to a decreased halogen impurity incorporation at higher growth temperatures.

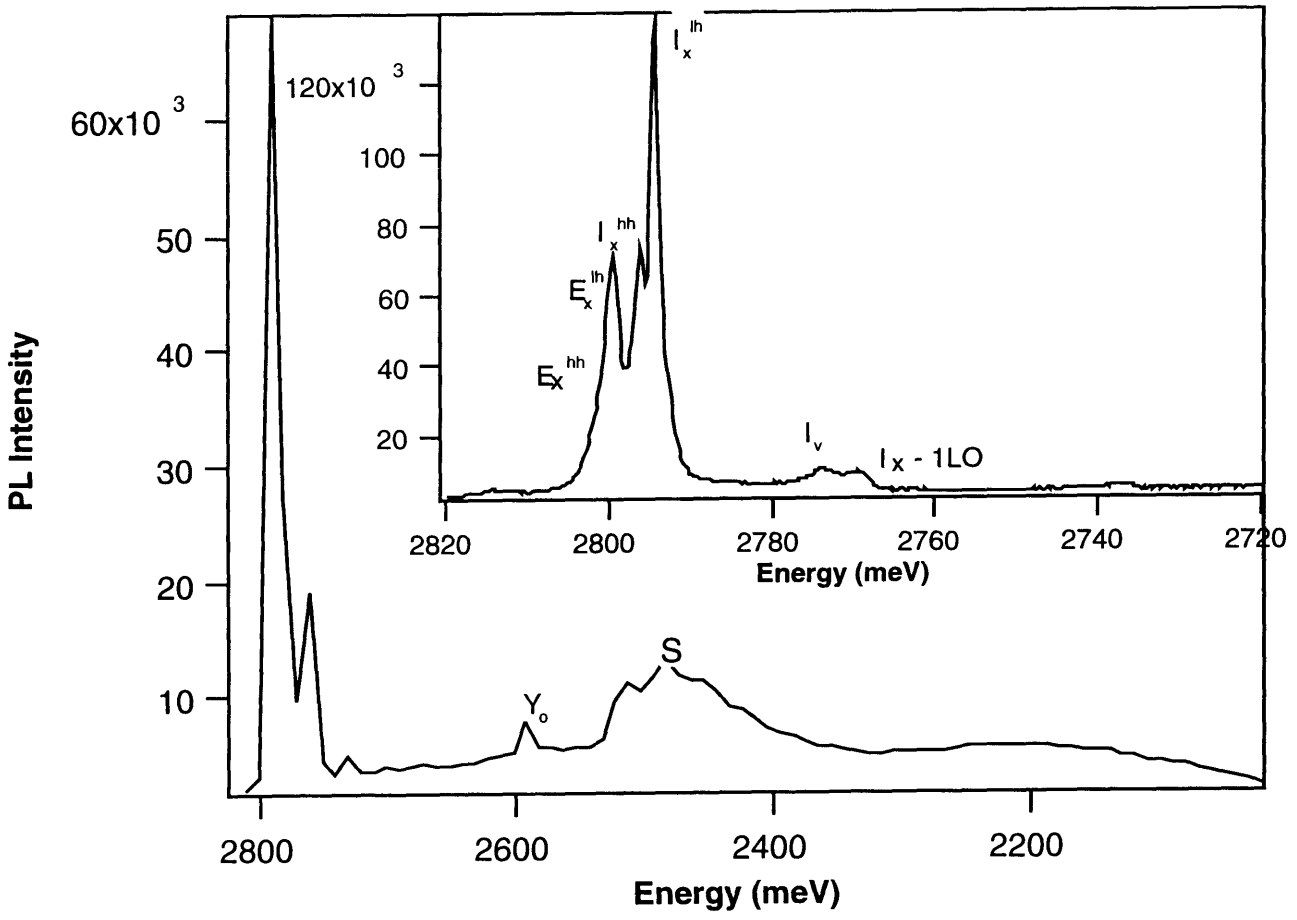

Figure 3.16. The photoluminescence spectrum of ZnSe from H_2Se and DMZn:NEt_3. The inset of the figure is an enlargement of the near-band-edge luminescence spectrum

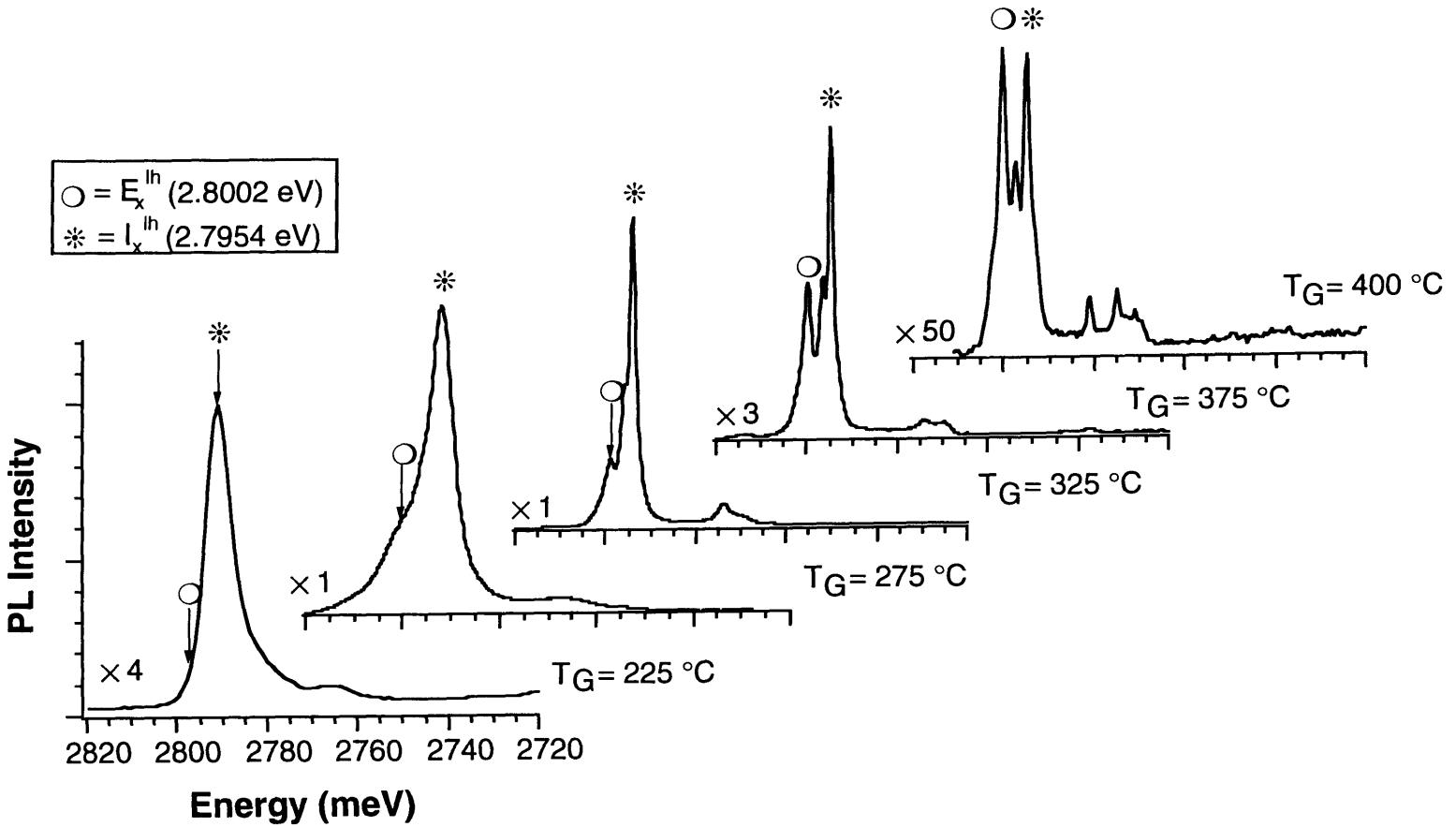

Figure 3.17 Variation in near-band-edge photoluminescence spectra of ZnSe films with deposition temperature. E_x^{lh} :○; I_x^{lh} :✳. Films deposited with H_2Se and DMZn:NEt_3 at 30 Torr and VI/II=10

3.3.6. Thermoelastic Strain and Misorientation Analysis

Since ZnSe epilayers were grown on 2° off (100) GaAs substrate toward <110> direction, meaning that the stepped substrate surface was vicinal to the (100) plane, two rocking curves were needed to obtain the lattice mismatch of the epilayer, $(\Delta\alpha/\alpha)_{\perp}$. The two rocking curves were measured per sample, one with [110] direction of the substrate facing the X-ray source and the second after it was rotated aximuthally by 180 degrees. From these two rocking curves information on the epilayer quality and the strain of the ZnSe epilayer could be obtained. Figure 3.18 shows typical rocking curves obtained for a 3μm thick ZnSe layer on GaAs substrate. The angular separation ($\Delta\theta$) between the GaAs substrate peak and the ZnSe epilayer peak allows the ZnSe lattice constant to be measured accurately. The $\Delta\theta$ is defined as :

$$\Delta\theta=\theta_{GaAs} - \theta_{ZnSe} \qquad (5)$$

If the angular tilt is denoted as $\Delta\Phi$ and introduces another angle, azimuthal rotation of the sample, α, (*i.e.*, rotation axis normal to the sample), then the separation of the apparent Bragg peaks can be expressed as a function of azimuthal angle α [Nagai, 1974]. For any given azimuthal angle some fraction η of $\Delta\Phi$ contributes to $\Delta\theta$. The two rocking curves give

$$\Delta\theta_1 = \Delta\theta + \eta\Delta\Phi \qquad (6)$$

$$\Delta\theta_2 = \Delta\theta - \eta\Delta\Phi$$

and the (004) lattice spacing of ZnSe is determined by the average angular separation $\Delta\theta$, which is defined as :

$$\Delta\theta = \frac{\Delta\theta_1 + \Delta\theta_2}{2} \qquad (7)$$

Since the bulk lattice constants of ZnSe (5.6684Å), GaAs (5.6532Å) in an unstained state, and the wavelength of the X-ray source ($\lambda_{Cu\ K\alpha}$ =1.541Å) are

known, the lattice constant of ZnSe in the epilayer can be calculated from the average angular separation, $\Delta\theta$.

$$d_{ZnSe(epi)} = \frac{\lambda}{2\sin\theta_{ZnSe(epi)}} = \frac{\lambda}{2\sin(\theta_{GaAs} - \Delta\theta)} \quad (8)$$

ZnSe films thinner than 1μm suffer two-dimensional compressive stress due to a lattice mismatch of 0.27% [Yao *et al.*, 1987]. Stress developed due to lattice mismatch becomes fully or partially relaxed by forming misfit dislocation above the 0.15μm critical thickness of the ZnSe epilayer. Thicker films (>1μm) are normally under tensile stress at room temperature due to thermoelastic strain, because the thermal expansion coefficient of ZnSe ($6.8X10^{-6}K^{-1}$ @RT) is larger than that of GaAs ($5.8X10^{-6}$ K^{-1} @RT). ZnSe tends to shrink more than GaAs when ZnSe/GaAs cools from growth temperature to room temperature.

The strain component normal to the surface, e_3, may be defined as

$$\varepsilon_3 = \frac{\Delta d_{ZnSe}}{d_{ZnSe(bulk)}} = \frac{d_{ZnSe(epi)} - d_{ZnSe(bulk)}}{d_{ZnSe(bulk)}} = \frac{\sin\theta_{ZnSe(bulk)}}{\sin\theta_{ZnSe(epi)}} - 1 \quad (9)$$

Assuming that GaAs is in plane stress condition, the stress-strain relation gives :

$$\sigma_1 = \frac{E}{1-\nu}\varepsilon_1 = -\frac{E}{2\nu}\varepsilon_3 \quad (10)$$

where E and ν are Young's modulus and Poisson's ratio of ZnSe, respectively. The angular separation ranges measured in the 3μm thick ZnSe epilayer on GaAs were 330 ~ 400 arcsec, and corresponds to e_3, ranging from $1X10^{-4}$ to $6.22\ X10^{-4}$. From the equation the tensile stress (σ_1) developed in the ZnSe films ranges

from $1X10^8$ to $6.22X10^8$ dyne/cm^2, using values of Young's modulus and Poisson's ratio from Lee *et al*, [1970].

The lattice constants normal to the ZnSe surface obtained by double crystal diffractometry are plotted as a function of growth temperature in Figure 3.19. The lattice constant dependence on T_G results from the thermoelastic strain due to the thermal expansion mismatch between ZnSe and GaAs. The lattice parameter variation in Figure 3.19 can be explained by a model for lattice deformation of ZnSe layer grown on (100) GaAs proposed by Shibata *et al*, [1988c]. The lattice parameter at measuring temperature (T_O) deviates from that of the bulk ZnSe because the epitaxial film contracts in a direction parallel to the interface at the same rate as the GaAs substrate during the temperature interval $\Delta T = T_G - T_O$. The lattice constant at the measuring temperature may be written as

$$a = a_1 (1+\Delta)$$
$$a = a_2 (1-2\Delta) \qquad (11)$$
$$\text{where } \Delta = K(a_1-a_2)\Delta T + (K-1)(a_1-a_2)/a_1$$

Here, a_1 and a_2 are lattice constants at the measuring temperature for bulk ZnSe and GaAs, respectively. The parameter K represents the degree of lattice relaxation. K=0 corresponds to the coherent growth which is realized for very thin film and K=1 corresponds to fully relaxed growth realized for sufficiently thick films. The calculated lattice constants are shown by solid lines using the lattice constants at room temperature. The calculated values with the lattice relaxation parameter of K= 0.85 agree well with the measured ones.

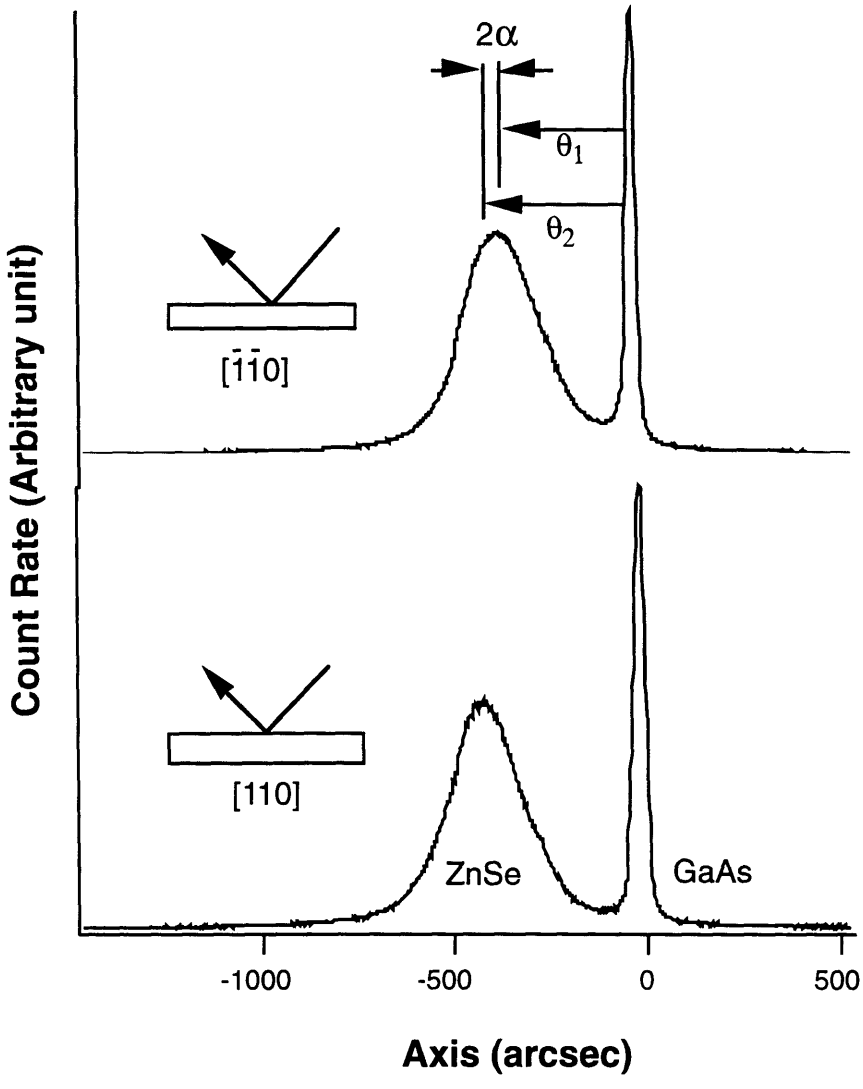

Figure 3.18 Typical DCD rocking curves showing relative misorientation between ZnSe layer and GaAs substrate

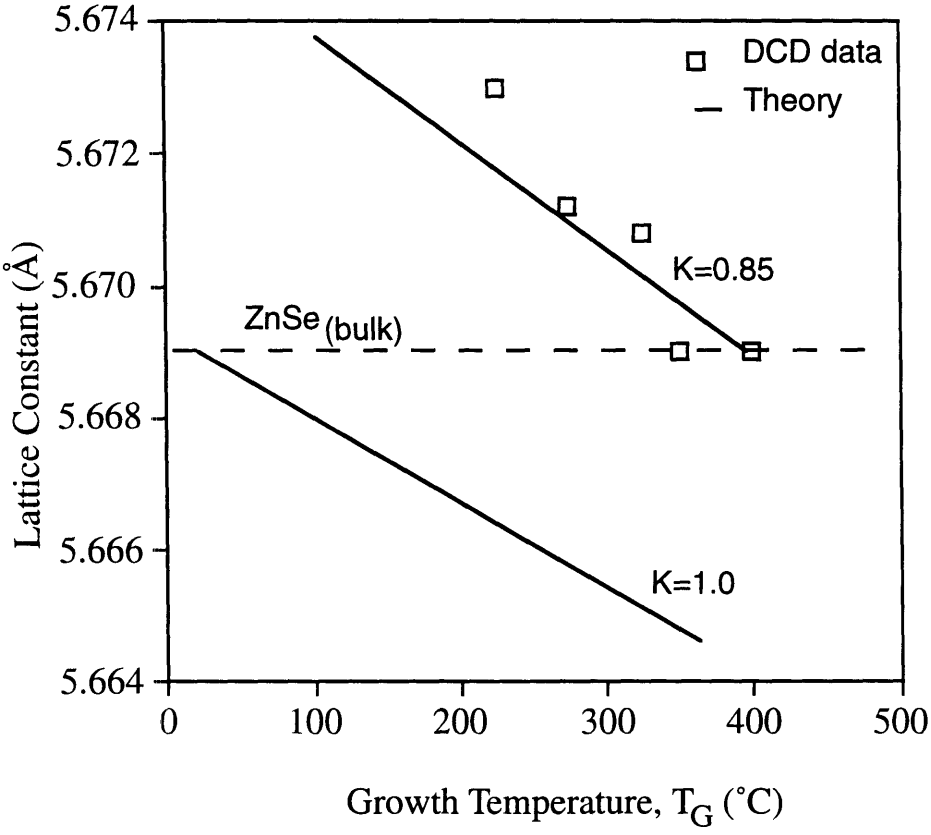

Figure 3.19 Lattice parameter normal to ZnSe measured by double crystal diffractometry as a function of growth temperature. Solid lines indicate calculated values.

3.3.7. GaAs Surface Pretreatment

One of the obstacles preventing preparation of high-quality epilayers is the GaAs substrate surface which has a nonstoichiometric native oxide. In the present case of ZnSe/GaAs heteroepitaxy, the removal of the GaAs surface oxide layer has been performed at ~600°C with Se overpressure, resulting in a rough GaAs surface because of the formation of Ga_2Se_3 clusters at the interface as well as the probable re-evaporation of As. Reports of the passivation of the GaAs surface with $(NH_4)_2S_x$ solution state that sulfur passivation reduces the surface density of GaAs [Sandroff *et al.*, 1987]. GaAs surfaces pretreated by the $(NH_4)_2S_x$ solution appears to be terminated by Ga-S or As-S bonds of sub- or mono-layer [Oigawa *et al.*, 1989; Wu *et al.*, 1991]. Here, preliminary results are presented on OMVPE growth of ZnSe on GaAs substrates pretreated with a $(NH_4)_2S_x$ solution.

In order to investigate the sulfur passivation effect on the growth processes, two different methods of GaAs surface pretreatment have been employed before growth. The first is conventional pretreatment: degreasing and etching followed by loading into the chamber and deoxiding at 600°C with Se overpressure . The second method is sulfur passivation treatment: dipping into $(NH_4)_2S_x$ for 4 minutes, loading and heating at 400°C to desorb the excess sulfur after degreasing and etching.

The optical properties for the different samples were investigated through photoluminescence measurements. Figure 3.20 shows the 10K PL spectrum of a ZnSe epilayer grown on S-pretreated GaAs substrate. The spectrum (see also inset of Figure 3.20) is dominated by intense and narrow free excitonic emission (E_x^{lh}) and donor bounded excitonic peaks (I_x^{lh} and I_x^{hh}). The peak appearing at

2.782eV (I_1^d) is related to Zn vacancies (V_{Zn}). Compared to the PL spectra in Figure 3.16 corresponding to conventional pretreatment, the sulfur pretreatment yields similar features. Moreover, the dominant peak in the epilayer from the S-pretreated substrate is the free excitonic emission (E_x^{lh}), which gives less compensation during p-type doping, and the deep level emissions are greatly reduced in the spectrum in Figure 3.20. The sulfur pretreatment process has the further advantages of being carried out at lower temperature, which will lead to reduced defect incorporation. Thus, these preliminary investigation indicate that the optical properties of ZnSe layers grown on the $(NH_4)_2S_X$-treated GaAs substrate are as good as those grown on a substrate pretreated in the conventional way.

3.4. Doping

3.4.1. Introduction

The real issue for immediate application of current technology is whether true p-type ZnSe can be obtained. The best results have been obtained with nitrogen as the intentional dopant. Therefore, research efforts were focused on the understanding the electrical and optical properties of ZnSe:N as well as enhancing incorporation since its solubility of N in ZnSe poses a fundamental limitation.

The successful p-type doping of ZnSe by nitrogen through the use of radio frequency plasma sources in molecular beam epitaxy (MBE) systems, and the related development of quantum well devices [Park *et al.*, 1990; Xie *et al.*, 1992]

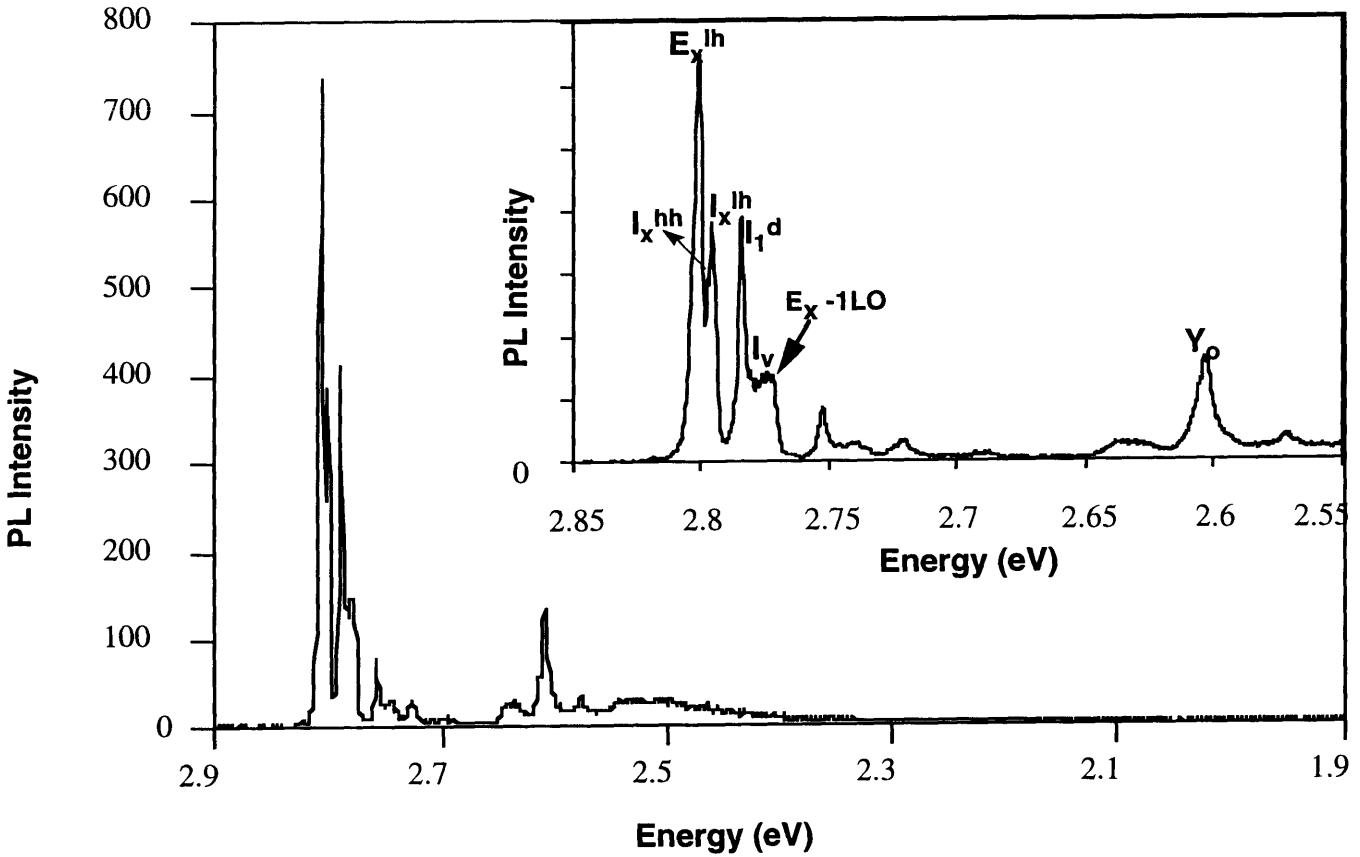

Figure 3.20 The 10K photoluminescence spectrum for S-pretreated ZnSe. The inset of this figure is enlargement of the near-band-edge luminescence of spectrum. The dorminant peak is E_x^{lh}, free bound exciton peak.

have renewed interest in thin film deposition of II-VI compound semiconductors. The advances made in MBE have yet to be mirrored by OMVPE, which would have advantages for manufacturing large area devices. There have been several reports of apparent p-type doping of ZnSe by lithium and nitrogen [Mitsuhashi *et al.*, 1990; Ohki *et al.*, 1990; Yashuda *et al.*, 1988], but although significant nitrogen incorporation levels have been measured (~10^{18} cm^{-3}), the p-type conductivity has been very low, if at all detectable (~10^{15} cm^{-3}).

New sources of nitrogen and new ideas concerning the cracking of nitrogen compounds to form N radicals need to be investigated. OMVPE has advantage of offering flexibility of source manipulation. Here a microwave discharge cavity is used to pre-crack NH_3 molecules into active nitrogen in the inlet section of the OMVPE reactor. DMZn:NEt_3-H_2Se is again the source combination.

3.4.2. Experimental

An Evenson 1/4-λ microwave cavity, energized by a 100W, 2.45GHz power supply, was installed around the quartz tube immediately upstream of the substrate for generation of a NH_3 plasma. A 2.45GHz microwave power generator with separate power meters for simultaneous monitoring of forward and reflected powers (MPG-4, Optos Instruments, Inc.) and with coupling via a 50W transmission line was used to transfer the microwave power to the microwave cavity. The Evenson cavity [Fehsenfeld and Evenson, 1965], which were positioned 2cm from the substrate, were used in the generation of microwave discharge. The criteria for the selection of material for the discharge tube was its recombination efficiency. Low wall recombination in the transport

zone is necessary to assure that the concentrations of reactive species reaching the substrate were not seriously attenuated. A quartz tube was used as the discharge tube for NH_3/H_2 plasmas.

The microwave plasma was created by means of absorption of microwave energy in an ionized gas. The plasma was excited simultaneously with the power input by appropriate selection of gas pressure (collision frequency), gas flow, and power coupling conditions. A Tesla coil was used to provide "seed" electrons. The efficiency of energy transfer depended upon an impedance match of all the components of the system. The coupling device was usually a coaxial cable with a probe or a loop extending into the cavity. When the impedances were matched and the resonant frequency of the cavity was tuned to that of the magnetron of the power supply, the power reflected from the cavity was minimal. The characteristics of the plasma changed with pressure, flow rate, and different gases. Therefore, it was necessary to provide both tuning and matching adjustments to obtain maximum power efficiency over a wide range of discharge conditions.

3.4.3. Microwave Plasma Decomposition

A plasma is defined as partially ionized gas consisting of a variety of highly reactive species ions, free electrons, neutrals and free radicals. The plasma type used for the fabrication of microelectronic devices is referred to as a glow discharge. A glow discharge is non-equilibrium plasma in which the electrons have a greater average energy than ions and neutrals [Chapman, 1980]. The non-equilibrium characteristics provide the plasma processing advantage i.e., making reactive radicals to enhance doping efficiency. In this work, the microwave

plasma is used to increase the incorporation of reactants which do not easily dissociate thermally. Remote plasmas are being investigated to activate selectively and more controllably specific reactants. The remote plasmas have been particularly useful in the growth of ZnSe where doping efficiency is the most critical issue.

In the microwave frequency range from 300 MHz to 300 GHz, the most commonly used microwave frequency in microwave plasma processing is 2.45 GHz, which gives a free space wavelength of 12.24cm. Plasmas generated by a microwave field differ significantly from DC and rf discharges in many respects. Microwave discharges provide a higher density of excited species having high excitation threshold energy, and higher concentration of electrons, ions and chemically reactive species than the conventional direct-current (DC) and rf discharges. The microwave plasma can be generated over a wide range of pressures 10^{-6} to 10^{3} Torr. Moreover, the absence of an internal electrode eliminates a possible source of contamination from sputtering of the electrodes.

Ammonia (NH_3) is a clean source of nitrogen for OMVPE environments and could be used as a suitable reagent for nitrogen-doping. The plasma decomposition of NH_3 is inferred [Hirose, 1985; d'Agostino *et al.*, 1981; Donnelly *et al.*, 1979] to occur through the following primary step:

NH_3 ----------> $NH + H_2$ (ΔH=3.9eV)

NH_3 ----------> NH_2 +H (ΔH=4.5eV)

Secondary reactions between the neutral fragments and reactants gas also take place in the plasma. The abstraction reaction by atomic hydrogen rapidly creates radicals through exothermic process such as:

$H + NH_3$ ----------> $NH_2 + H_2$ (ΔH= -0.04eV)

Radical-molecule reactions also take place :

$$NH + NH_3 \text{ ----------> } N_2H_4 \ (\Delta H = -2.4 \text{ eV})$$

High-energy electron impact with molecules can produce light-emitting species such as H^*, H_2^*, NH^* and N_2^*. These radicals are transferred through the diffusional mass transport toward the growing surface where the deposition occurs.

3.4.4. Results and Discussion

The above growth and characterization results demonstrate that it is feasible to deposit high quality ZnSe at low pressures through the use of the new adduct source. This mode of operation then provides the opportunity for exploring microwave plasma stimulated doping, in addition to admitting the usual advantages of low pressure operation, such as improved uniformity and reduced natural convection effects [Giapis *et al.*,1990; Fotiadis *et al.*,1990].

The quality of ZnSe films and optimum operation condition at lower pressure are determined on the basis of surface morphology and PL spectra. Figure 3.21 shows the surface morphology of films at different pressures and T_G=275°C. The hillock structure was persistent from P_G=30 Torr to P_G=5Torr. At the pressure of P_G=3 Torr, the surface shows randomly oriented criss-crossing structure. At lower pressure (P_G=0.8 Torr), the surface becomes smooth and dense. The low temperature PL spectra shown in Figure 3.22, of the films grown at different reactor pressure reveal similar good optical characteristics, dominant near-band-edge (NBE) emission peaks and negligible deep level defects.

The remote microwave plasma source was used to precrack NH_3 upstream of the substrate and to avoid plasma cracking of the Se and Zn

reagents. Initial investigations showed that feeding the reagents through the plasma zone resulted in excessive precracking and poor quality ZnSe films. With the remote plasma source, the ZnSe growth characteristics were similar to those described above.

Figure 3.23 compares PL spectra for undoped ZnSe (a), NH_3 doped ZnSe (b), and microwave plasma doped ZnSe (c), all grown at 275°C. The delivery rate of DMZn:NEt_3 is 15μmol/min while that of H_2Se and NH_3 is fixed at 120μmol/min and 300μmol/min. This growth temperature was chosen to balance a low I_x^{lh} / E_x^{lh} intensity ratio, which is achieved at high temperatures (Figure 3.17), against the presence of deep levels, which favor low growth temperature. The PL spectrum for undoped ZnSe (a) has a dominant donor bound exciton peak, I_x^{lh}, with negligible donor-acceptor pairs having the zero phonon peak appear at 2.695 eV. The acceptor bound excitonic transition I_1 at 2.7906 eV , as seen in Figures 9(b) and 9(c), further indicates that nitrogen has been incorporated into the ZnSe. The PL spectra 9(c) resulting from remote plasma precracking of NH_3 show a structure similar to that in 9(b), with an increased acceptor bound peak suggesting additional nitrogen incorporation.

The ac impedance technique was used to measure the resistance of the ZnSe:N doped sample. Resistance measurements were made from 1000 Hz to 10 MHz by capacitively coupling using Au contacts deposited by evaporation. At high frequencies, the impedance due to the capacitance is negligible compared to that due to sample resistance. With this technique, the doped sample shows low resistance of 100Ω. However, the films did not display measurable p-type conductivity, as also reported in other nitrogen doping investigations of ZnSe [Ohki *et al.*, 1990]. The lack of measurable p-conductivity of ZnSe when doping

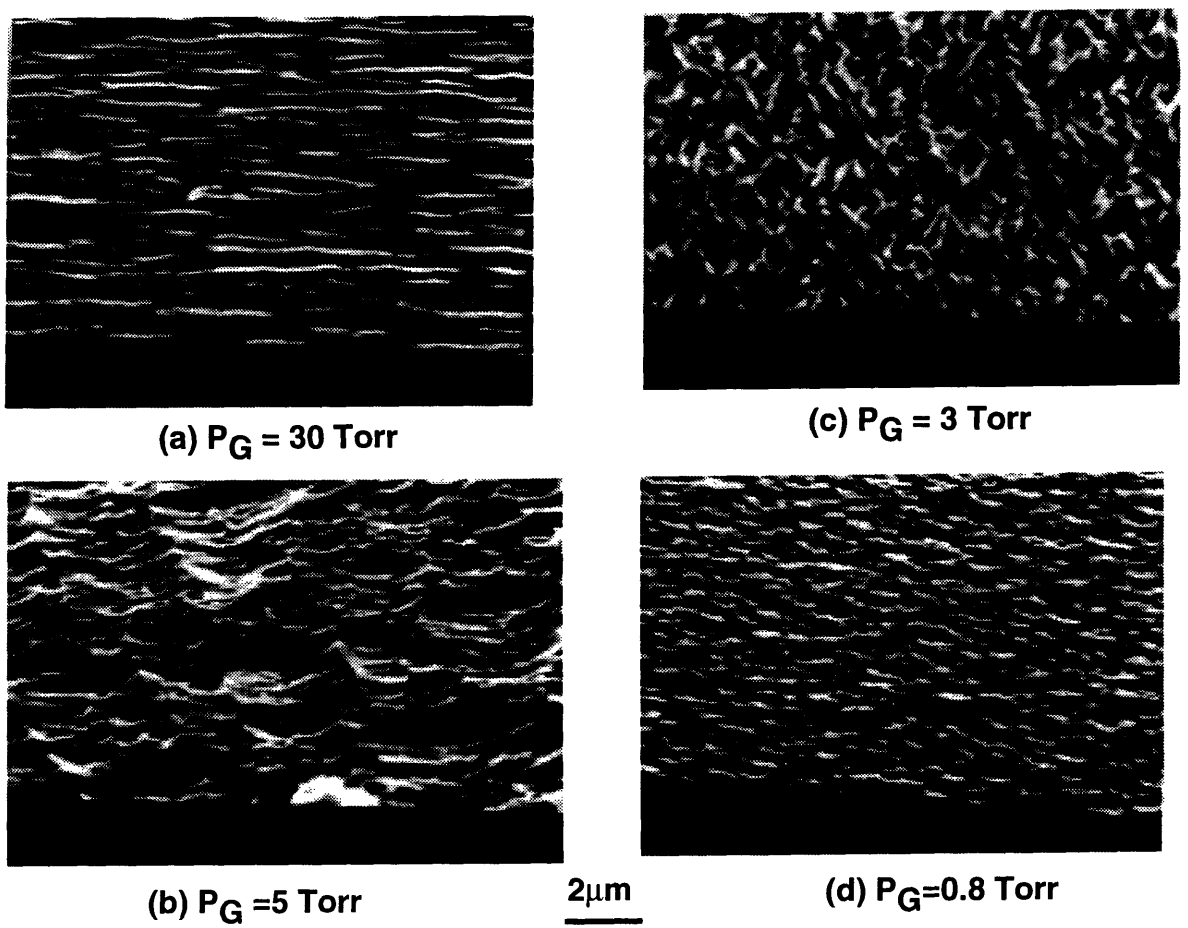

Figure 3.21 SEM micrographs of ZnSe grown with H_2Se/DMZn:NEt_3 at different pressures. (DMZn:NEt_3=15μmol/min, [VI]/[II]=10 and T_G=275°C)

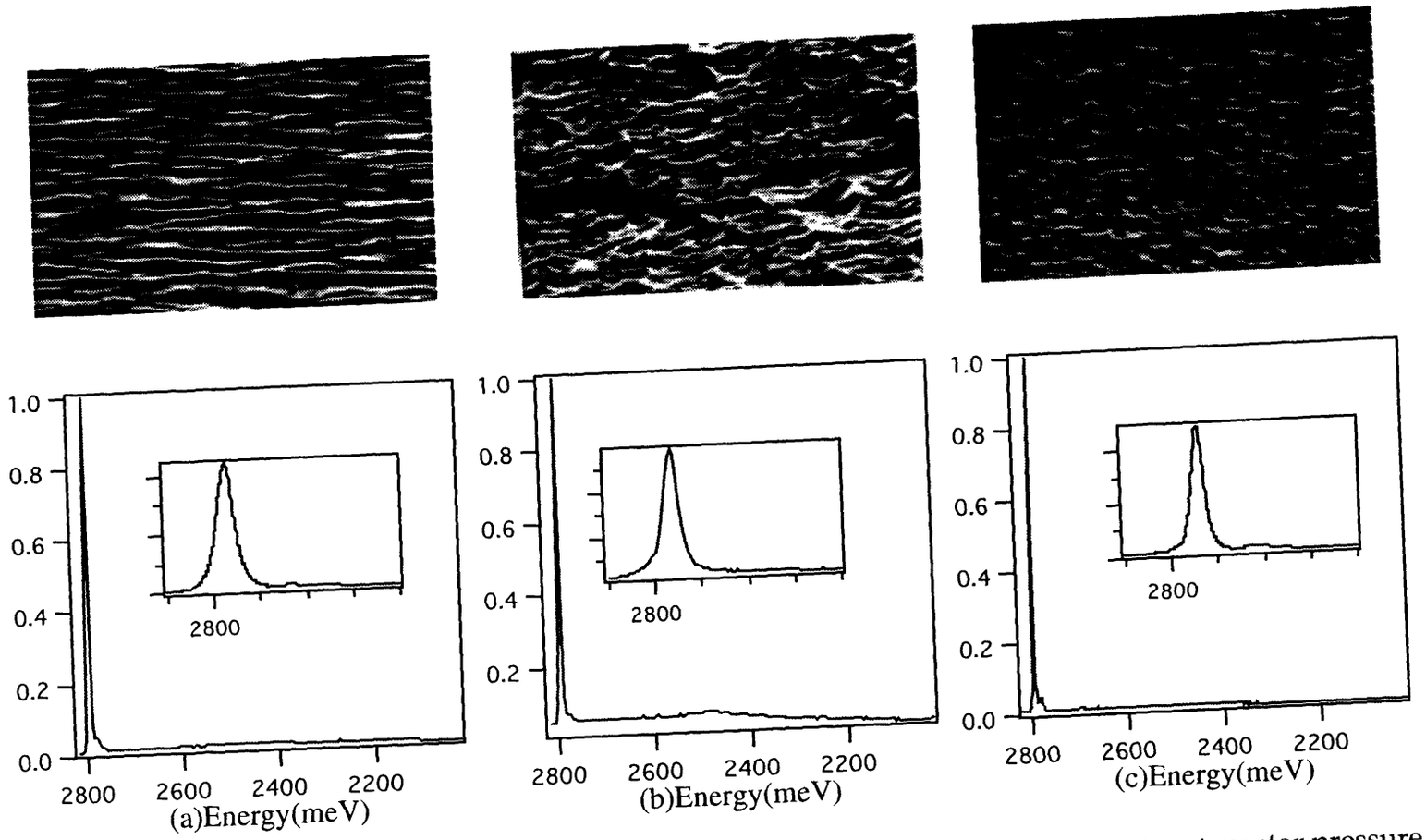

Figure 3.22 The pressure effect on surface morphology and photoluminescence spectra at reactor pressure of (a) 30 Torr, (b) 5Torr and (c) 0.8Torr

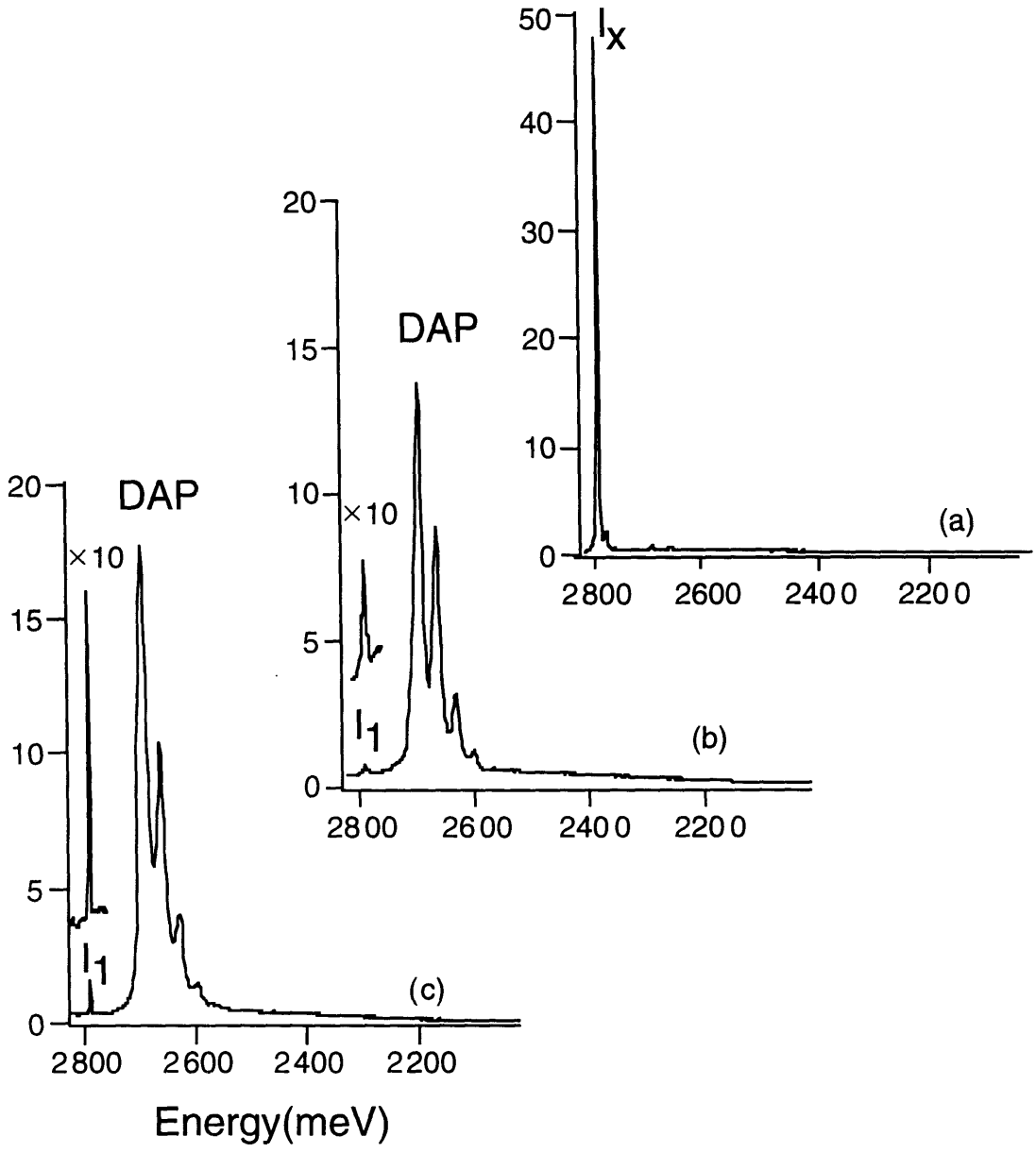

Figure 3.23 PL spectra of (a) undoped, (b)NH_3 doped and (c) plasma assisted NH_3 doped ZnSe. H_2Se (15μmol/min), DMZn:NEt_3 (120μmol/min) and NH_3 (300μmol/min)

with NH_3 raises questions as to the role of hydrogen in the ZnSe films since hydrogen is known to influence electronic properties of many compound semiconductors [Pajot *et al.*, 1991]. The possible sources of H in the growth process include the ues of (1) H_2Se as a Se cource, (2) NH_3 as the dopant source and (3) H_2 as a carrier gas. The passivation effect of N acceptors in OMVPE grown ZnSe by hydrogen was proposed at Lawrence Berkeley Laboratory with spcetroscopic evidence. N-H local vibration modes in ZnSe:N samples were found at the peak of 3194 cm^{-1} using 9K Fourier transform infra-red spctrometer [Wolk *et al.*, 1993].

A simple plug flow model may be used to estimate the fraction of radicals generated in the plasma that make it to the growth interface without undergoing recombination reactions in the gas-phase. Studies of NH_3 plasmas indicate that NH is the radical species in highest concentration [Nicholas *et al.*, 1986]. At room temperature, NH recombines with itself with a rate constant of $2.1X10^{12}$ $cm^3/mol/s$ and reacts with NH_3 and H_2 with rate constants of $4.8X10^7$ $cm^3/mol/s$ and $3.6X10^2$ $cm^3/mol/s$, respectively [Westley *et al.*, 1992]. Based on these rate parameters, the fraction of NH reaching the surface may be estimated to be at least 1%. To substantially increase the fraction of radicals reaching the surface an order of magnitude reduction of the growth pressure would be needed.

3.5. Conclusions

Investigations of low pressure OMVPE of ZnSe with the adduct reagent DMZn:NEt_3, and H_2Se show that use of the adduct minimizes the extent of

detrimental prereactions commonly observed with DMZn. The effect of the adduct is attributed to not just a simple blocking of reactions between DMZn and H_2Se, but also a stabilization of an intermediate preventing the formation of ZnSe-organic-oligomers. Growth data demonstrate that use of the adduct reagent is particularly effective at lower temperatures (< 300°C) and pressures (< 30 Torr). At these conditions growth rates are higher when using DMZn:NEt_3, and the surface morphology is improved relative to films synthesized with DMZn. Hall measurements and photoluminescence spectra of the grown films further show that DMZn:NEt_3 produces material with comparable electronic and optical properties to films grown with DMZn. Additional improvements in electronic properties of ZnSe may be expected, since the adduct is more easily purified than is DMZn [Jones, 1989]. The low pressure growth opens the possibility for microwave stimulated doping in OMVPE. Initial experiments with NH_3 show promising results for this approach, but the deposition pressure will have to be reduced further to increase the concentration of radicals at the growth surface. This also allow the replacement of NH_3 by N_2 as the doping source in order to circumvent hydrogen passivation of N acceptors.

Chapter 4.

Zinc Selenide from Several Organometallic Se Precursors

4.1 Introduction

High quality epitaxial layers of ZnSe whose doping can be controlled have great potential for photonic and electronic applications such as blue light emitting diodes and optical recording systems. Lowering the growth temperature is also of particular importance in order to reduce the formation of native defects, improve dopant incorporation and control stoichiometry at heterojunctions. Growth temperature below 350°C can be obtained with H_2Se as a selenium precursor in combination with zinc alkyls [Giapis *et al.*, 1989]. However, the premature gas phase reaction between group II alkyl and group VI hydride adversely affects surface morphology and film thickness uniformity (see Chapter 3). Combined with its high volatility and flammability, H_2Se constitutes a health threat with a threshold limit value (TLV) of only 50ppb [Sax,1979]. In addition, H_2Se is relatively unstable in humid atmospheres, rapidly decomposing to form selenium oxides which are equally toxic and cannot be detected by existing state-of-the-art hydride monitors.

Safety concerns and parasitic prereactions have already motivated the development of alternative Se sources which would be less likely to participate in

parasitic reactions and be less hazardous [Mitsuhashi *et al.*, 1986]. The use of alkyl selenide has been shown to produce films with good surface morphology and photoluminescence spectra, but a high growth temperatures above 450°C is necessary for acceptable growth rate [Mitsuhashi *et al.*, 1985]. From the general stability trend of metalorganics, the metal carbon bond is expected to weaken with the stability of the leaving radical [Stringfellow, 1989]. Hence, the low temperature growth of ZnSe would be possible with *tertiary*butyl- or allyl- based selenium compounds. Recent growth experiment with methylallyl selenide (MASe) has showed to reduce growth temperature at 400-450°C, but also to lead to extensive carbon incorporation [Giapis *et al.*, 1989].

Novel Se precursors, *tertiary*-butyl allyl selenide (tBASe), bicyclic selenocyclohexene (bCpSe), diisopropyl selenide (DIPSe) and diallyl selenide (DASe) have been employed in conjunction with DMZn:NEt_3 or DMZn. The structure of these sources were shown in Figure 4.1. Successful identification of superior source reagents represent a significant step toward the commercialization of OMVPE grown ZnSe base devices. Not only is the use of Se precursors expected to aid in solving the technical problems of prereaction, poor morphology and high growth temperature but a major increase in safety result from elimination of highly toxic H_2Se. These new Se sources should be a liquid source to easy to handle, show low reactivity toward the Zn source at an ambient temperature, have relatively high vapor pressure, acceptable toxicity, a suitable pyrolysis mechanism for negligible carbon incorporation and a reduced potential for hydrogen incorporation in order to avoid passivation effects in N-doping.

(a) DIPSe

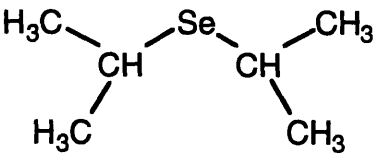

(b) DASe

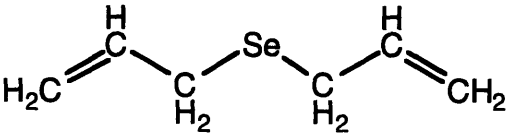

(c) tBASe

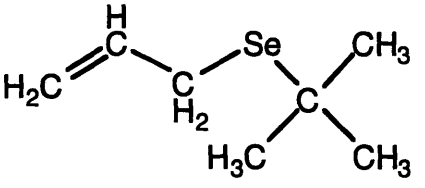

(d) bCpSe

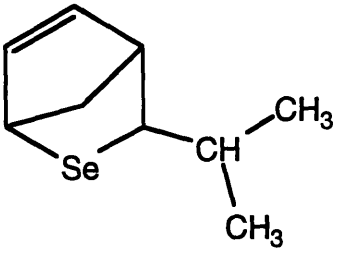

Figure 4.1 Chemical structures of novel Se sources (a)Diisopropyl selenide (b) Diallyl selenide (c) *tertiary*-butyl allyl selenide and (d) 2-selena-3-(methylethyl)-bicyclo[2.2.1]hept-5-ene.

4.2. Experimental

The ZnSe films were grown in a vertical downflow OMVPE reactor equipped with a laser interferometer for *in-situ* growth rate measurements. Electronic grade DMZn:NEt3 (Epichem) or DMZn was used as a Zn precursor in conjunction with novel organometallic Se sources, diallylselenide (DASe), tertiarybutylallylselenide (tBASe), 2-selena-3-(methylethyl)-bicyclo[2.2.1]hept-5-ene (bCpSe) (Advanced Technology Materials, Inc). Substrates were semi-insulating (100) GaAs, misoriented 2° toward <110> and were prepared according to standard procedures [Stutius, 1981]. The deposition sequence was initiated with native oxide removal in 0.4 slm H_2 flow with Se overpressure (150μmol/min of H_2Se) in order to suppress As desorption. The films were grown at 300 Torr with a total flow rate of 1 slm of H_2 through the reactor. The growth temperature varied between 325 - 425°C. The DMZn:NEt3 delivery rate was maintained at 20μmol/min while the delivery rate of Se sources were varied between 10-120μmol/min. In the case of the bCpSe source, a reduced pressure of 30Torr with a total flow rate of 0.4 slm H_2 was employed because of the relatively low vapor pressure of the source.

The surface morphology of ZnSe films was examined by scanning electron microscopy (SEM). Rutherford backscattering spectrometry through channeling was employed to verify that the layers grown were epitaxial. He ions accelerated to 2MeV was employed. The lattice parameter of the ZnSe epilayer was measured by a double crystal diffractometer (model 300, BEDE Scientific, Inc.) with $Cu_{K_{\alpha 1}}$ radiation from a rotating anode X-ray generator (Model RU-200, Rigagu). Symmetric ZnSe (004) rocking curves were recorded and full widths at

half maximum (FWHM) were compared for quantitative evaluation of the quality of epitaxy.

Measurement of carbon impurity levels in ZnSe was performed by secondary ion mass spectrometry (SIMS) with a detection limit for ^{12}C around $5X10^{17}cm^{-3}$. Undoped ZnSe films grown from $H_2Se/DMZn:NEt_3$ and showing no detectable carbon impurities were implanted with ^{12}C to provide an internal standard for SIMS measurement of the carbon concentration in ZnSe films. The implant had a peak ^{12}C concentration of $1X10^{19}cm^{-3}$. The SIMS measurements were carried out by J.Turner at HP with a Cameca IMS-4f spectrometer using Cs^+ primary ion beam with an incident energy of 10keV and ion current of 33nA, rastered over an area 100X100 μm^2. Negative secondary ions were monitored. Depth scales for the SIMS profiles were determined from measurements of the crater depths with a calibrated profilometer.

Photoluminescence (PL) spectra were obtained at 4K by using He-Cd laser (λ=325nm) at low power density (<10mW/cm^2) and analyzed using a 0.85m SPEX 1404 double grating monochrometer and GaAs photon multiplier tube. Spectral resolution in the range of interest was better than $0.5cm^{-1}$.

The vapor pressure of novel precursors were determined with a high vacuum system equipped with a MKS Baratron (10 Torr range). The stainless steel container with the sample was carefully degassed by several freeze-pump-thaw cycles and then immersed into a temperature controlled bath. The vapor pressures were measured at temperatures in the range of 19-45°C. All connection lines, including the pressure sensor, were maintained at a temperature 10°C higher than the temperature of the bath. After each measurement, a portion of

the gas-phase was pumped off and the equilibrium was allow to establish again to eliminate a presence of any permanent gas.

4.3. Diisopropyl selenide (DIPSe)

Diisopropyl selenide (DIPSe) has been used for high quality ZnSe growth in OMVPE. In order to reduce growth temperature, methyl or ethyl radical has been replaced with isopropyl radical since the metal-radical bond strength is considerably reduced.

4.3.1. Growth Rate

Growth rates were measured as a function of growth temperatures in Figure 4.2. The growth rate is controlled by chemical kinetics below 470°C with apparent activation energy of 20kcal/mol and become constant at higher temperatures which is indicative of mass controlled region. Figure 4.3 gives the growth rate dependence on the molar flow rate of DIPSe source at 450°C. The delivery rate of DMZn is constant with 20μmol/min. The growth rate is increasing linearly with DIPSe flow rate at the kinetic limited region of T_G=450°C.

4.3.2 Surface Morphology

The morphology of ZnSe epilayers grown from DMZn/DIPSe reveals a highly faceted morphology, which shows different reflectivity from the specific plane. The surface morphology of ZnSe grown at two different temperature is

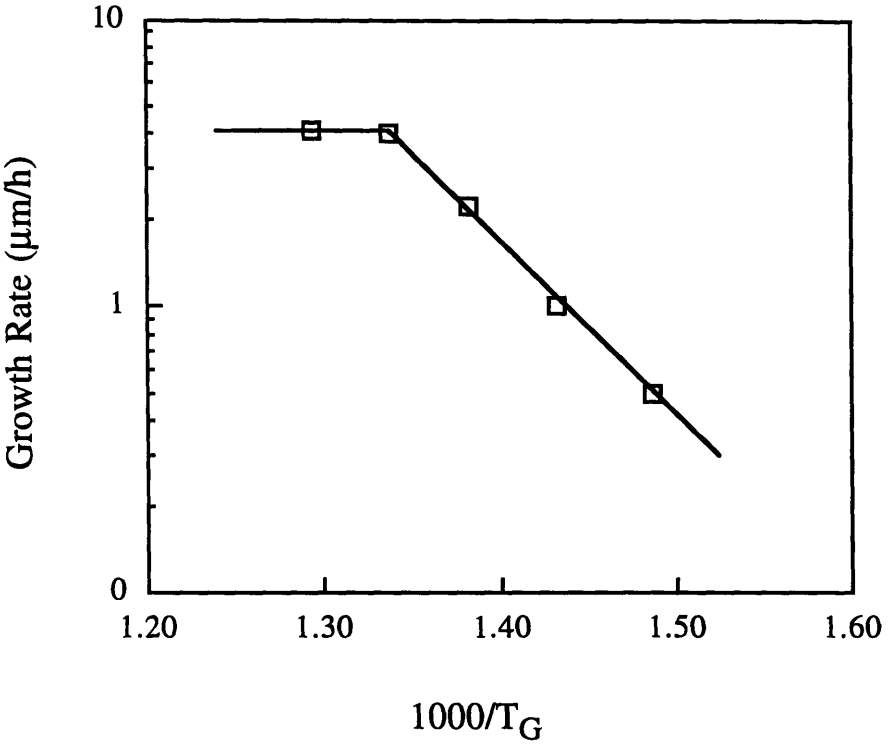

Figure 4.2 The effect of temperature on the growth rate of ZnSe from DIPSe/DMZn. (DMZn=20μmol/min, VI/II=2)

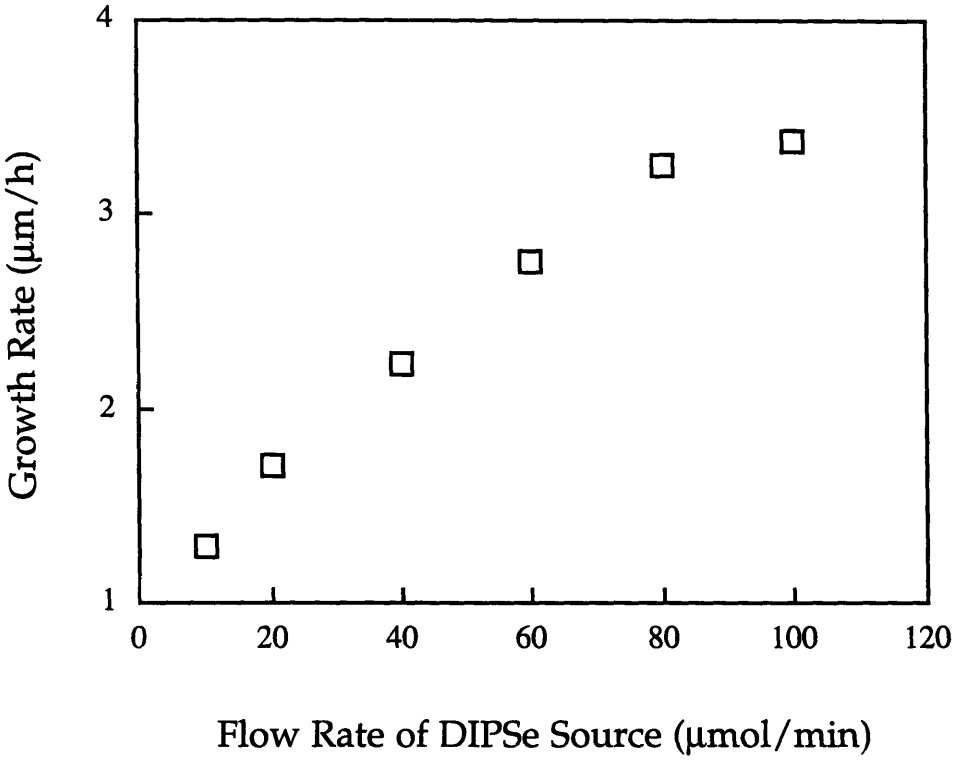

Figure 4.3 The growth rate of ZnSe as a function of DIPSe source flow rate at 450°C (DMZn=20μmol/min)

shown in Figure 4.4, The size of the hexagonal shaped structure is increased at higher temperature (450°C).

4.3.3. Materials Characterization

ZnSe films grown from DIPSe do not show any detectable carbon incorporation (below detection limit, $5X10^{17}$ atoms/cm^3) even at high molar ratio of VI/II=4.

The structural properties of the ZnSe epilayer was examined through RBS channeling experiments. The RBS channeling yields are low enough to indicate good crystallinity of the films but the backscattering yields exceeds those from grown with tBASe and bCpSe to be discussed below. All ZnSe layers grown from DIPSe at 450°C appear to be highly resistive as determined by Hall effect measurements. The films do not show any resolvable near-band-edge spectra in low temperature photoluminescence measurement, presumably because of contamination of the DIPSe precursor.

4.4. DASe (Diallyl selenide)

The increased stability of the allyl radical compared to the methyl and ethyl radicals makes allyl-based organometallic compounds thermally less stable. This in turn implies that organometallic Se sources involving allyl ligands have potential for lower temperature growth of ZnSe.

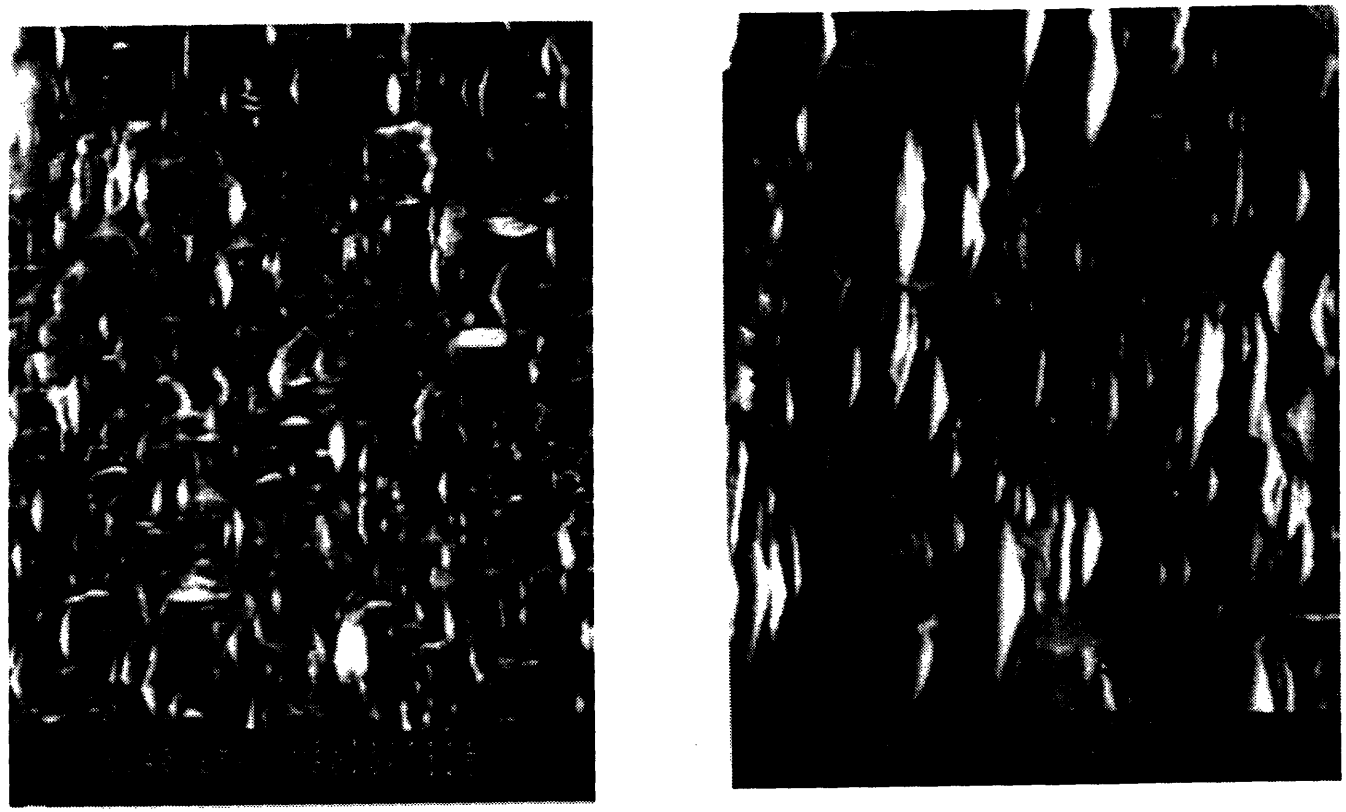

(a) 400°C (b) 450°C

Figure 4.4 Surface morphology of ZnSe from DIPSe/DMZn at two different growth temperatures

4.4.1. Growth Rate

Figure 4.5 shows the measured growth rate as a function of the reciprocal growth temperatures for ZnSe growth from DASe. This DASe source also exhibits two different temperature regimes for growth: a kinetic limited region at lower temperatures and a mass transfer controlled region at high temperatures. The growth is limited by chemical kinetics below 425°C with an apparent activation energy of 25kcal/mol. The effect of the molar flow rate of the Se precursor is shown in Figure 4.6 for growth from DASe at T_G=400°C. The delivery rate of DMZn:NEt_3 flux is fixed at 20μmol/min. The growth rate increases linearly with a DASe flow rate of T_G=400°C (kinetic limited region), which is indicative of the DASe source being the rate-limiting minority reactant.

4.4.2. Surface Morphology

The morphology of the ZnSe epilayers grown from DASe showed a pronounced variation in surface morphology with the VI/II ratio and growth temperature. SEM micrographs of the films grown at different growth temperatures with a VI/II ratio of 2 are shown in Figure 4.7. For a growth temperature of 350°C, the films were specular and mirror-like to the naked eye. Even under high magnification observation by SEM (20,000 X), the film surface was devoid of any features (Figure 4.7a). The layer grown at 375°C showed a randomly oriented criss-cross structure. At higher temperatures (above 400°C), the films became rough.

SEM micrographs of the surface of films grown at a temperature, T_G= 400°C with different VI/II ratios, are shown in Figure 4.8. At low VI/II ratios,

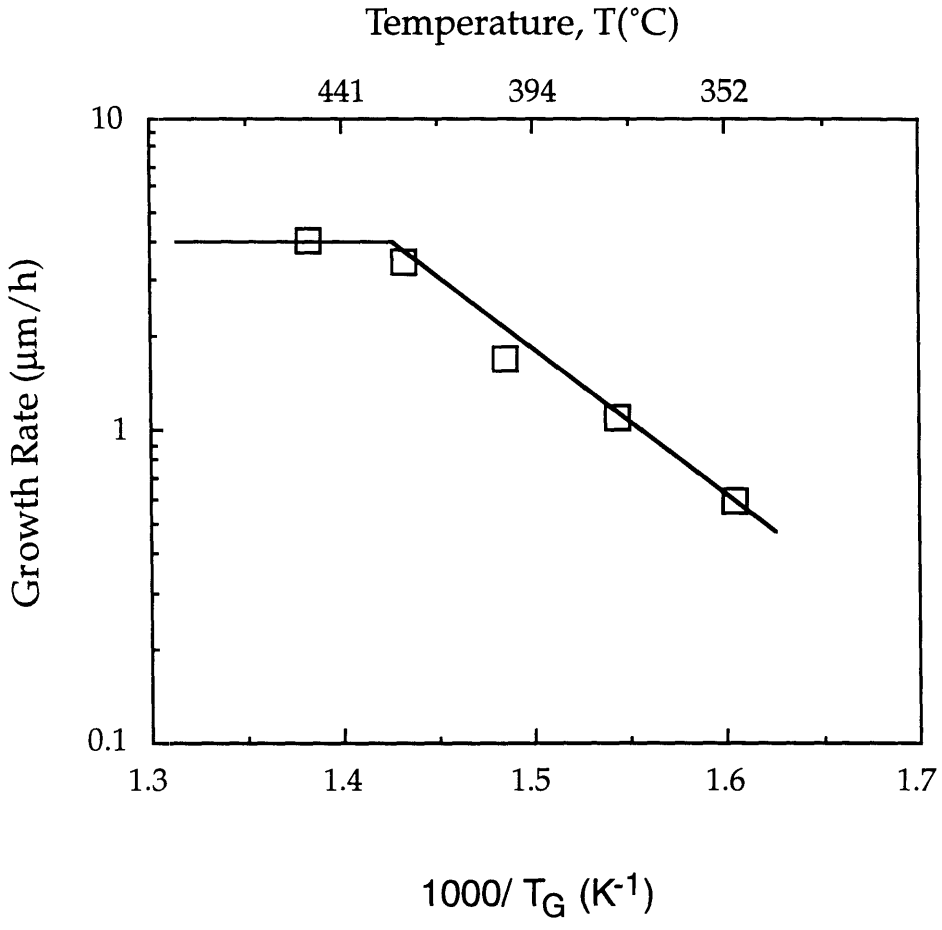

Figure 4.5 The effect of temperatur e on the growth rate of ZnSe from DMZn:NEt_3/DASe (DMZn:NEt_3= 20μmol/min, VI/II=2,)

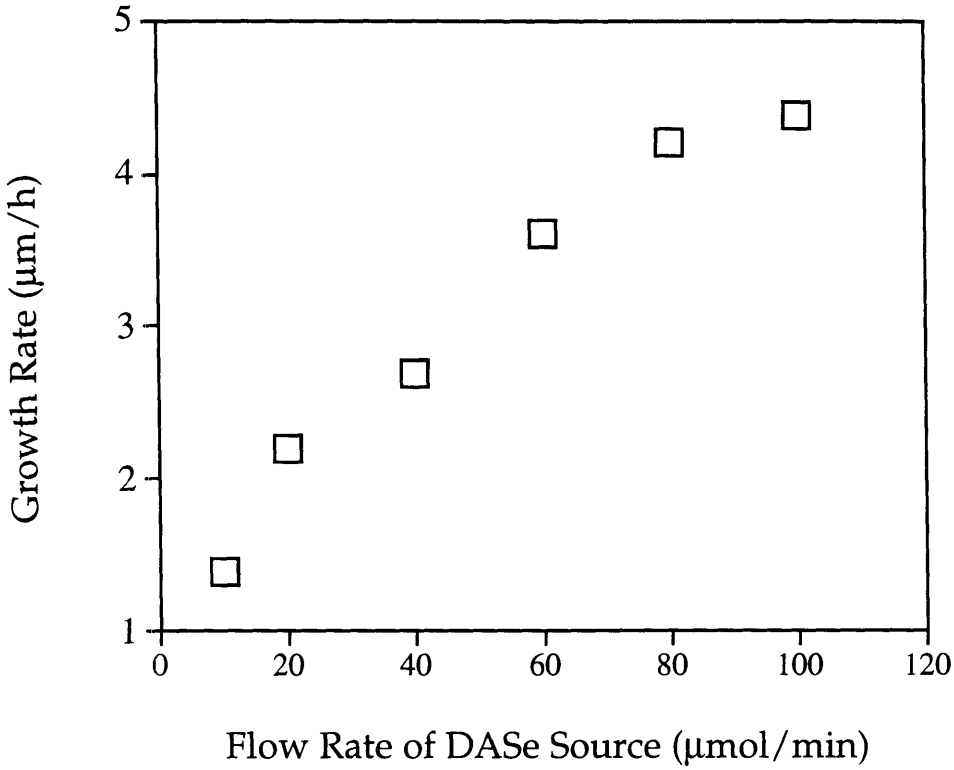

Figure 4.6. The growth rate of ZnSe as a function of DASe source flow rate at T_G=400°C. (DMZn:NEt_3=20μmol/min)

the films appeared a dull bluish-gray. The surface showed a cylindrical island structure of small size (~0.4μm), probably resulting from a Se deficiency in the vapor phase. Films grown with VI/II = 2 had a large number of hexagonal shapes of nearly uniform size (approximately 0.5μm). Upon further increasing the VI/II ratio above 3 the films still appeared shiny and reflecting but the surface became rough with short, randomly oriented criss-crossing structures visible by SEM (Figure 4.8c and d).

4.4.3. Materials Characterization

SIMS depth profiles of the ^{12}C peak are shown in Figure 4.9 for ZnSe films grown from DASe at 400°C with different VI/II ratios. When the delivery rate of DASe is increased relative to that of DMZn:NEt_3 the carbon concentration in the films becomes detectable and, even at a low molar ratio of VI/II=1, the carbon level is three orders of magnitude above the detection limit (10^{20} -10^{21} atoms/cm^3), as illustrated by the depth profile in Figure 4.9. All the ZnSe layers grown from DASe at 400°C and at various VI/II ratios were highly resistive according to the Hall effect measurement.

4.5. Gas phase pyrolysis of MASe and DASe

A gas phase pyrolysis study on MASe and DASe has revealed that allyl precursors decompose by a combination of a homolysis and a retro-ene rearrangement pathway as shown in Figure 4.10 [Sanjay *et al.*, 1993]. 1,5-hexadiene is the predominant decomposition product of the bond homolysis pathway. The rearrangement mechanism involves a H atom shift in a six

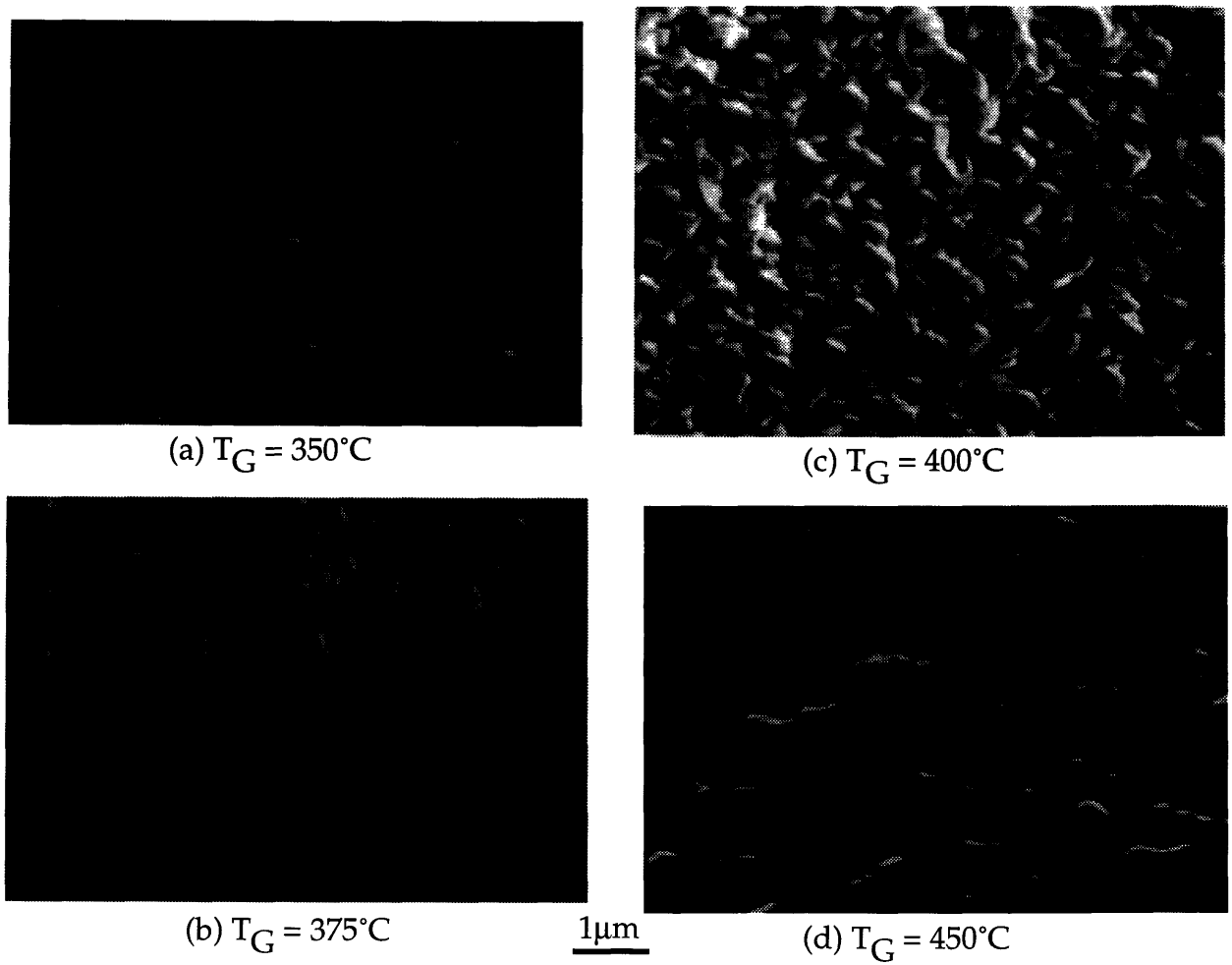

Figure 4.7 SEM micrographs of ZnSe grown from DASe/DMZn combination at different temperatures (PG=300 Torr, VI/II=2)

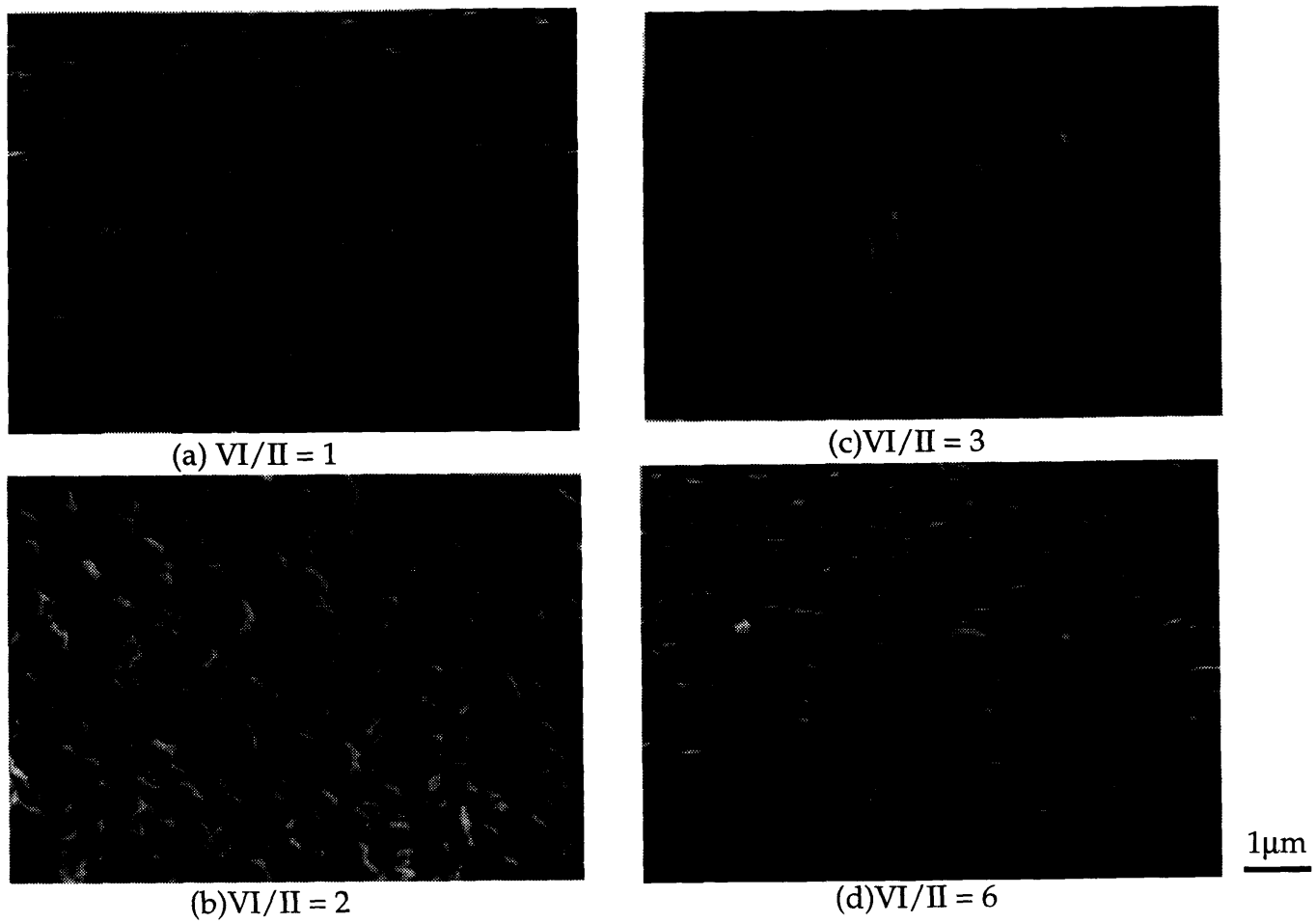

Figure 4.8 SEM micrographs of ZnSe grown from DASe/DMZn combination at different VI/II ratios. (P_G=300 Torr, P_G=400°C)

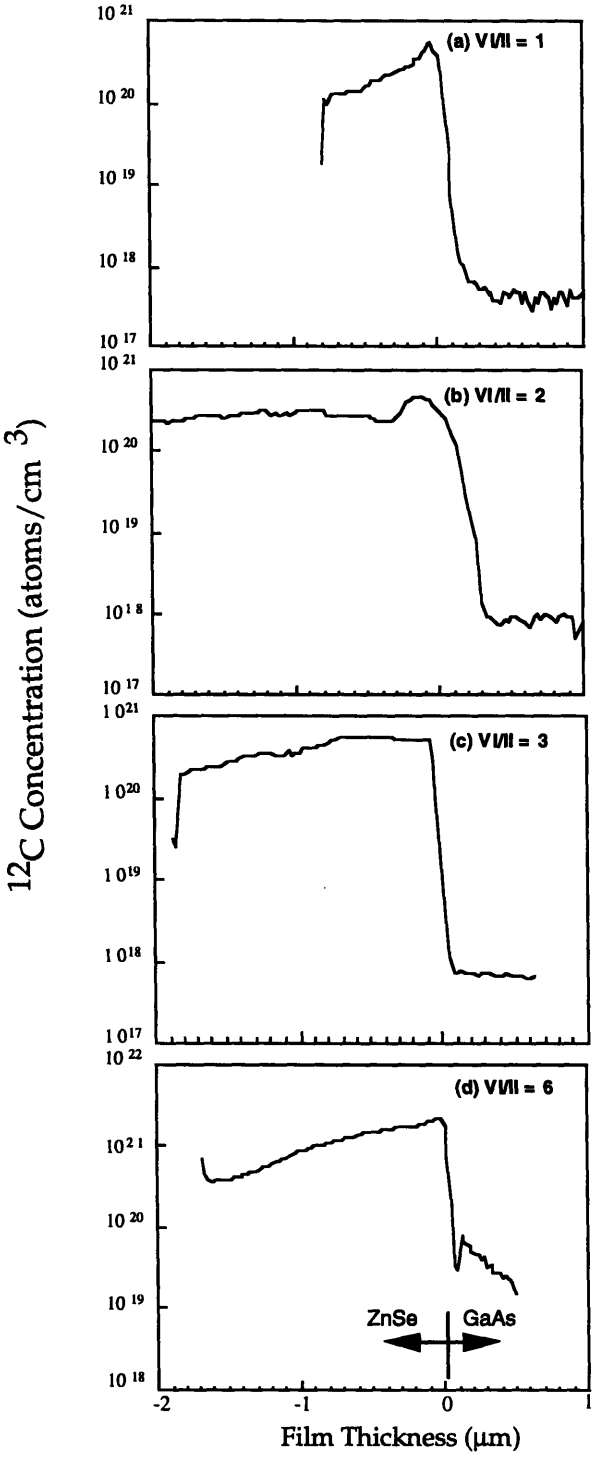

Figure 4.9 ^{12}C depth profiles in ZnSe films gr own from DASe/DMZn combination at different VI/II ratios

centered ring transition state and produces primarily propene(CH_3-CH=CH_2) and selenoaldehydes (R=Se).

The latter pathway is conjectured to lead to lead to increased carbon incorporation. The relative intensities of the peaks at m/e =67, corresponding to a fragment of 1,5-hexadiene and at m/e=42, corresponding to propene, were measured in order to probe the competition between the homolysis and rearrangement pathway in the decomposition of the allyl compounds. The intensities of these two peaks, normalized by the maximum intensity of the peak at m/e=67, are plotted as a function of temperature in Figures 4.11 (a) and (b) for the decomposition of MASe and DASe, respectively. The relative intensity of the m/e=42 (propene) peak is greater for DASe as compared to MASe, indicating that the rearrangement pathway is more facile in DASe. The Se-bearing products of the pyrolysis, R=Se from rearrangement and RSe$^\bullet$ from homolysis, were not observed in the mass spectrometer. The selenoaldehydes (R=Se) are expected to be unstable and would tend to oligomerize and to deposit out on the reactor walls. The RSe$^\bullet$ radicals can be expected to recombine to produce diselenides that may decompose to produce stable monoselenides On incorporation at the growth interface the selenoaldehydes is less likely to lose its organic ligand and thus a likely source of carbon in the ZnSe films grown from allyl selenides. One could expect to see a large degree of carbon incorporation with DASe and MASe, for which the rearrangement decomposition pathway is dominant. This is confirmed by the SIMS measurements of ^{12}C incorporation in ZnSe films form DASe and MASe reported in Figure 4.18.

(a) Homolysis

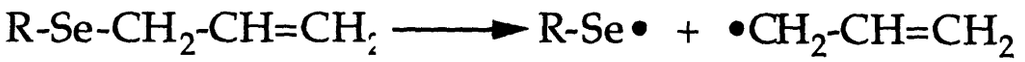

(b) Rearrangement

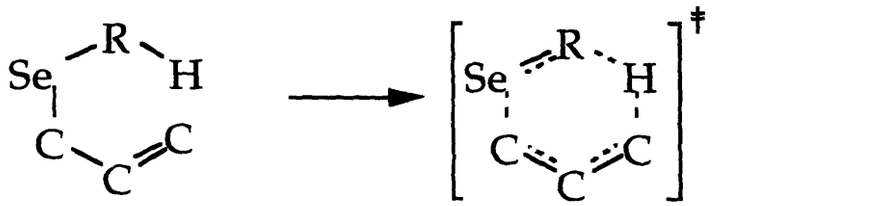

Figure 4.10 Decomposition pathways for allyl based sources (a) homolysis and (b) retro-ene r earrangement

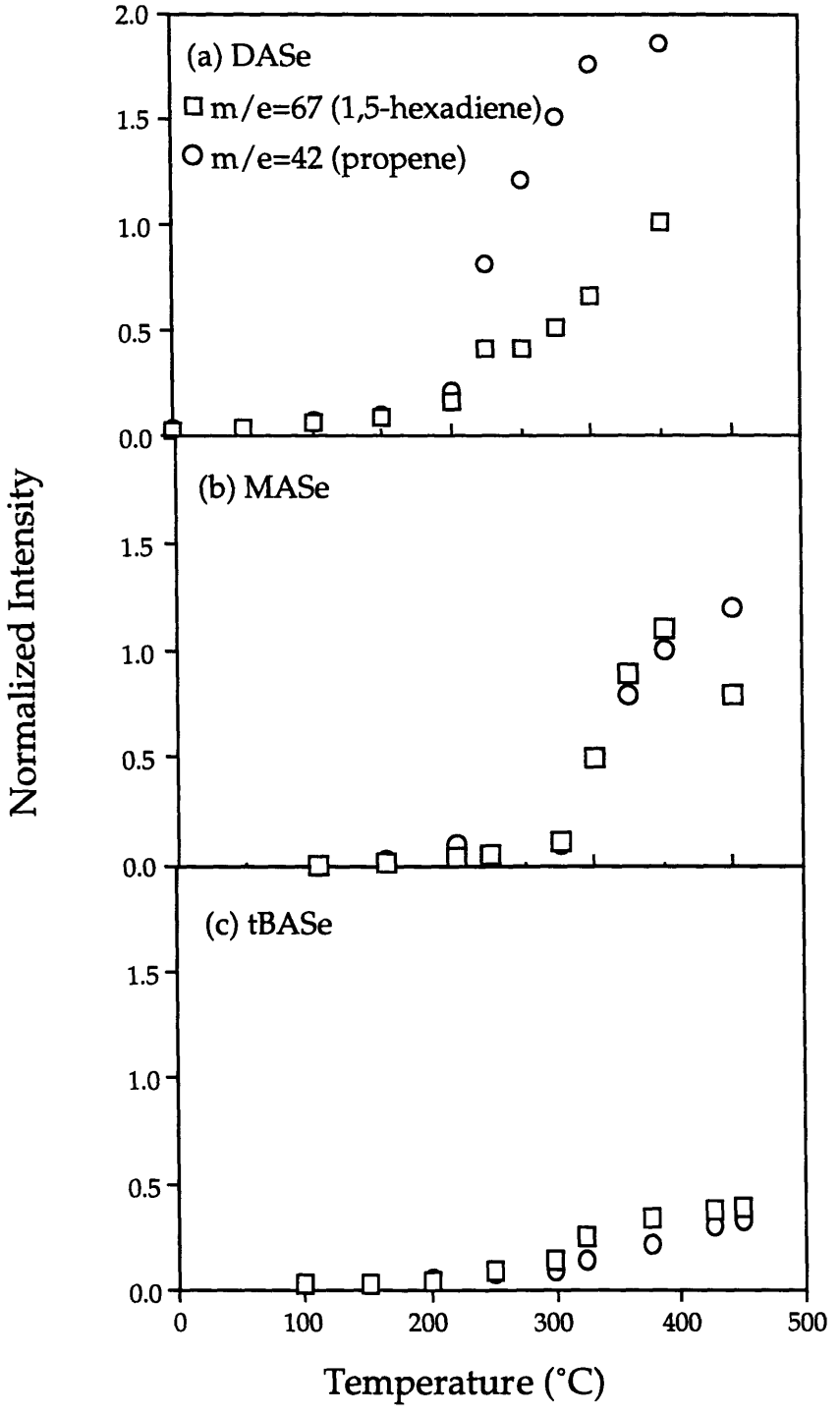

Figure 4.11 Intensity of peaks at m/e=67 (□) and at m/e=42 (O) as a function of temperature for pyrolysis of (a) DASe, (b)MASe and (c)tBASe in H_2 carrier gas.

4.6. *tertiary*-Butyl allyl selenide (tBASe)

To reduce the carbon incorporation experience with DASe and MASe, a novel allyl-based selenium source, *tertiary*-butyl allyl selenide (tBASe) was used in conjunction with DMZn:NEt_3 for low temperature OMVPE growth of high quality ZnSe. Since the *tertiary*-butyl ligand are expected to sterically hinder the retro-ene rearrangement and the corresponding formation of the selenoaldehydes, the carbon incorporation in the films should be significantly reduced compared to those grown from MASe and DASe (see Section 4.5). It will be shown below that SIMS does indeed show negligible carbon concentration (10^{17} atoms/cm^3) in the ZnSe films grown even at high VI/II ration. The high thermodynamic stability of allyl and *tertiary*-butyl free radicals should furthermore favor low temperature homolysis. Moreover, the films shows high optoelectronic quality, comparable to those grown from H_2Se at 325°C [Huh *et al.*, 1993].

4.6.1. Vapor Pressure

Accurate knowledge of source precursor vapor pressure is a critical factor for performing an OMVPE process. It is necessary to estimate this vapor pressure so that the delivery rate of the precursor can be calculated for the growth.

Since vapor pressure of the precursors are expected to be low, one can assume the validity of the Clausius-Clapeyron equation;

$$\ln P_{vapor} = A + \frac{B}{T} \qquad (1)$$

Based on the experimental measurements in Figure 4.12, the vapor pressures of the tBASe source may be expressed as:

$$ln(p[Torr]) = 18.065 - 4981.6/(T[°K]), R = 0.99685 \qquad (2)$$

4.6.2. Growth Rate

Figure 4.13 shows the growth rate as a function of the reciprocal growth temperature for two different reactor pressures. Growth with this organometallic Se source exhibits two distinct temperature regimes for ZnSe growth (as did MASe and DASe). At lower temperatures growth is kinetically limited with Arrhenius temperature dependence, while a growth rate plateau at higher temperatures is indicative of a mass transfer controlled deposition process. The growth is limited by chemical kinetics below 395°C with apparent activation energies of 21 kcal/mol. When the reactor pressure is reduced from 300Torr to 30 Torr, the onset of mass transferred growth is shifted from 395°C to 440°C.

Figure 4.14 shows the variation in growth rate with VI/II ratio at different growth temperatures. The delivery rate of DMZn:NEt3 flux is fixed at 20μmol/min. At 400°C (mass transfer limited region in Figure 4.13), the growth rate increases linearly with the tBASe flow rate and saturates at flows greater than 40μmol/min, corresponding to a VI/II ratio of 2. At 350°C (kinetic limited region) the growth rate increases linearly with the tBASe flow rate. This result indicates that the Se source is the rate-limiting minority reactant.

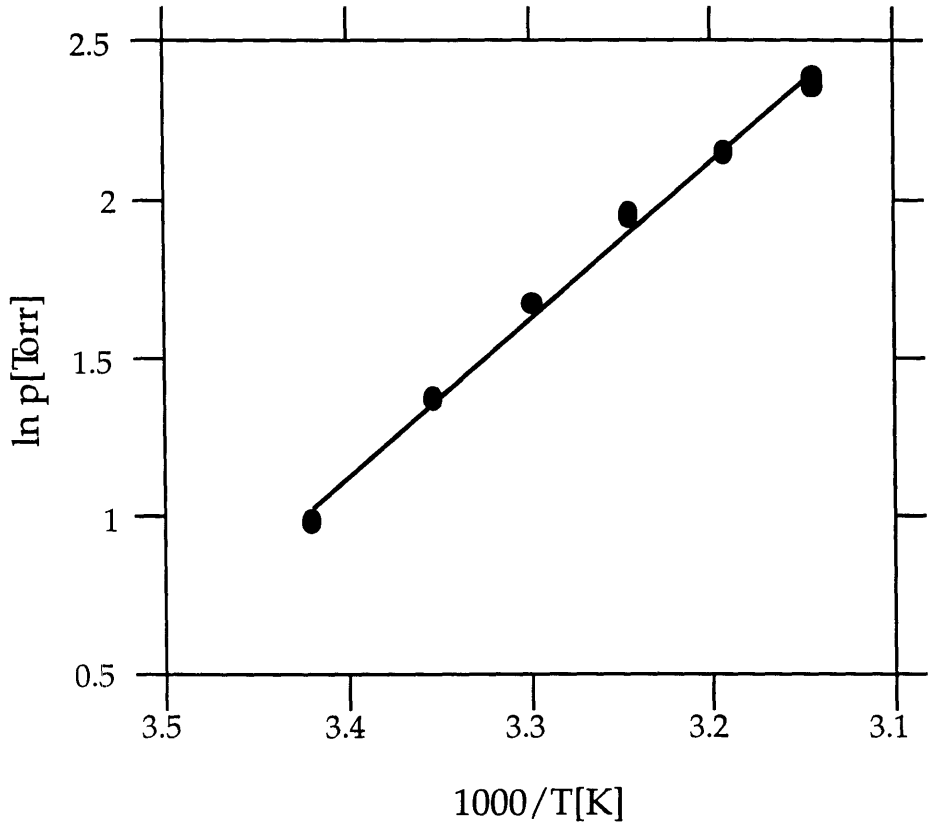

Figure 4.12 Vapor pressure curve for tertiary-butyl allyl selenide

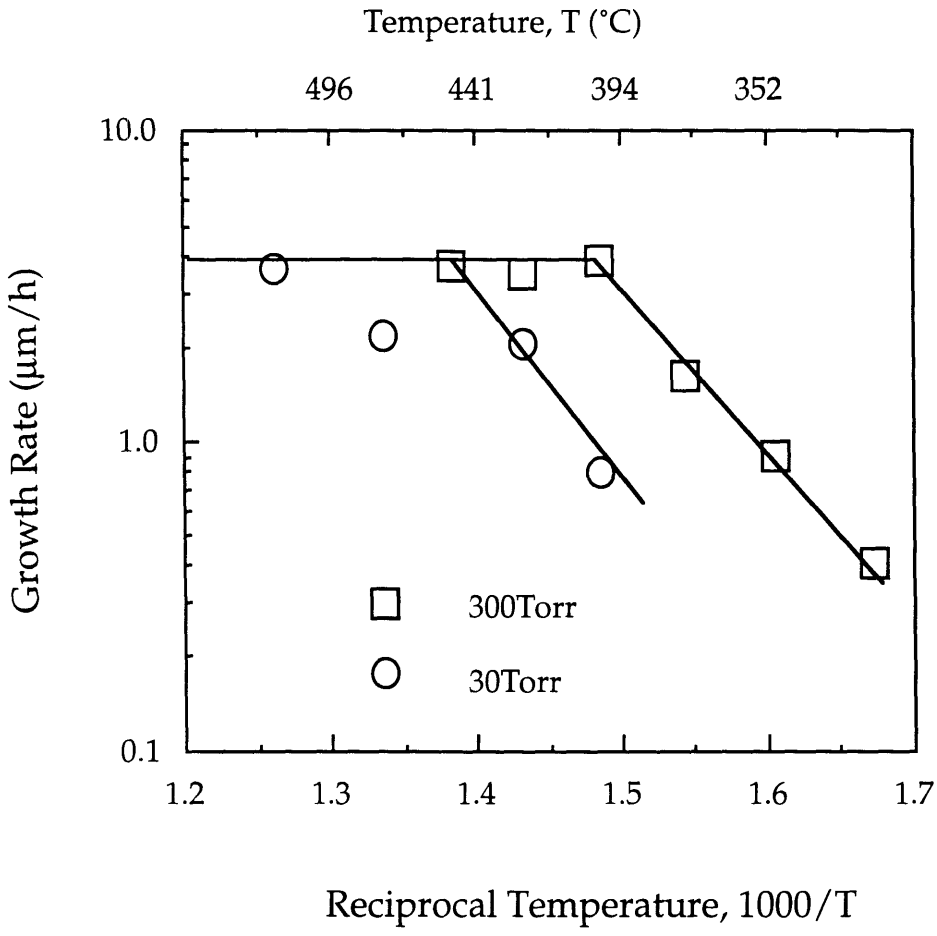

Figure 4.13 The effect of gr owth temperature on the deposition rate of ZnSe from DMZn:NEt3/tBASe at two differ ent reactor pressures (DMZn:NEt_3=20μmol/min, VI/II=2)

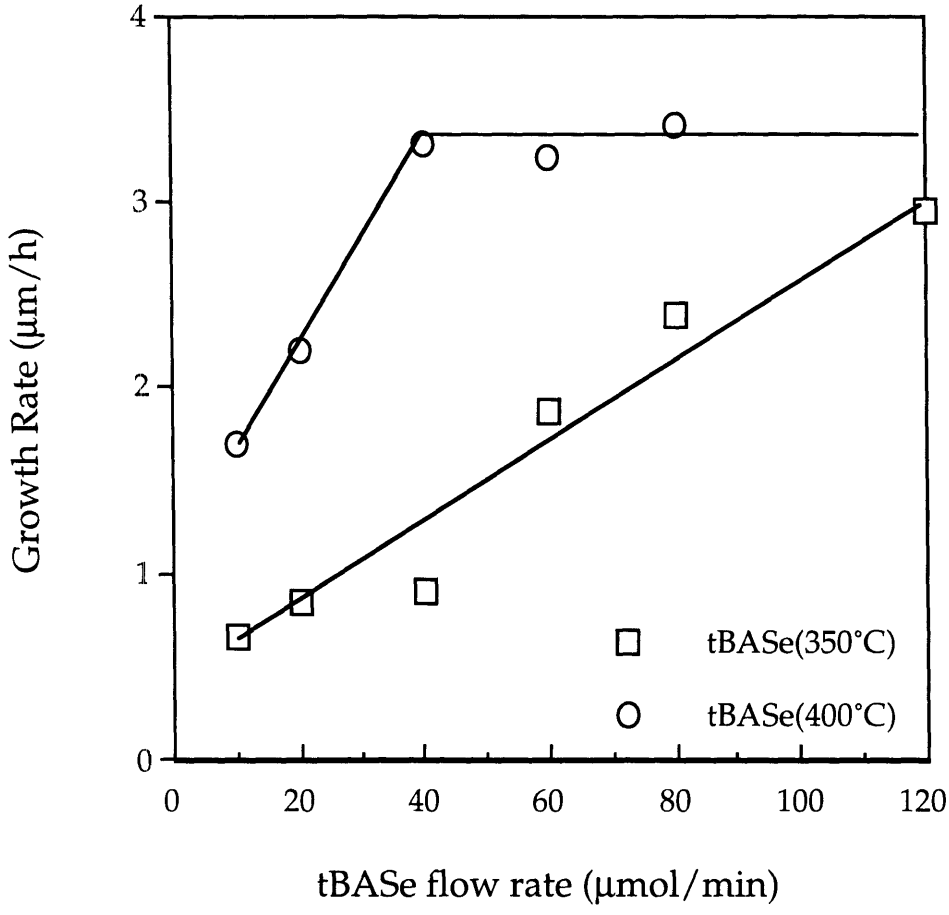

Figure 4.14 Growth rate variation with tBASe flow rate
at two different growth temperatures (P_G=300Torr, VI/II=2)

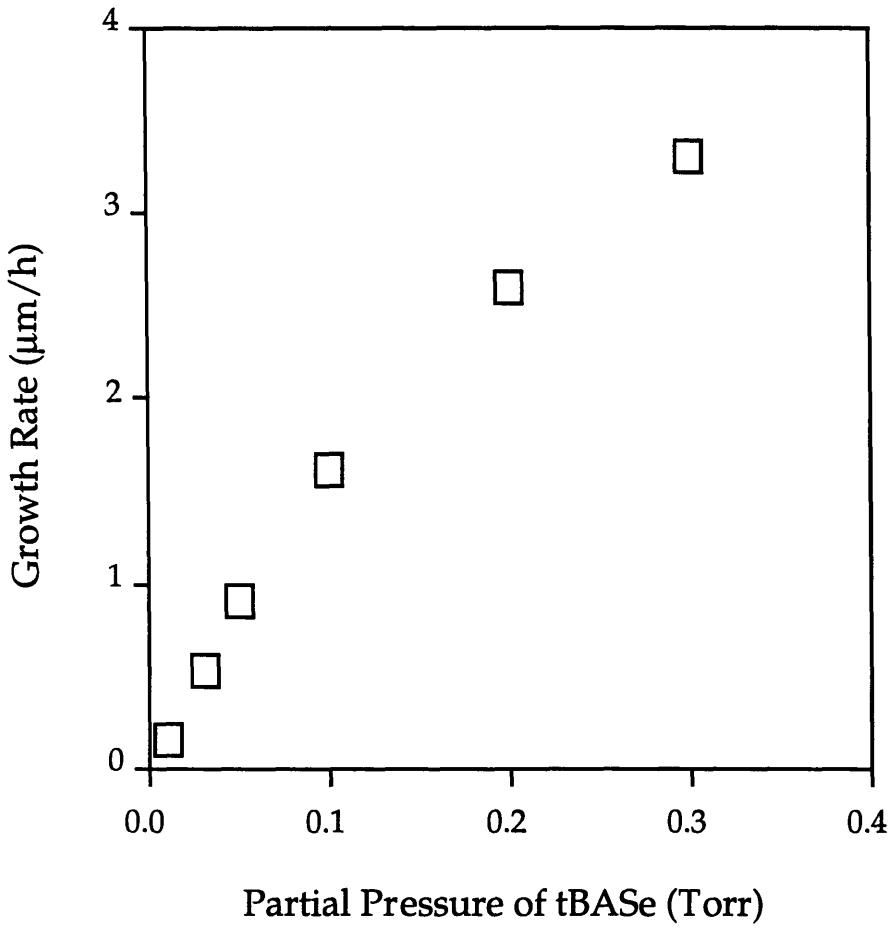

Figure 4.15. The effect of partial pr essure of Se source on the growth rate of ZnSe from tBASe/DMZn:NEt_3 (T_G=350°C,DMZn:NEt_3=20µmol/min, VI/II=2)

Finally, the effect of partial pressure of the Se source on the growth rate of ZnSe from the DMZn:NEt3/tBASe combination is shown in Figure 4.15.

4.6.3. Surface Morphology

Films grown with tBASe showed a pronounced variation in surface morphology with growth temperature (Figure 4.16) but no surface morphology changes with different VI/II ratios. At a lower temperature (325°C), films were specular and shiny to the naked eye. Layers grown at 350°C showed smooth surfaces interspersed with small gaps. At higher temperature (400°C) the films appeared dull bullish-gray and the surface was composed of a large number of hexagons of nearly uniform size (approximately 0.2μm long).

4.6.4. Materials Characterization

SIMS profiles of tBASe/DMZn:NEt3 grown ZnSe films are shown in Figure 4.17 with the ion, $^{12}C^-$ for carbon detection and the mass 138, representing $ZnSe^-$ in the epilayer and Ga_2^- in the substrate. The $^{12}C^-$ signal shows a sharp increase of carbon concentration in a region near the ZnSe/GaAs interface. Saito *et al.* [1986] attributed the carbon peak at the interface to possible carbon residues present on the substrate surface, even though the substrate were carefully etched with H_2SO_4 mixture solution and rinsed with deionized water. This carbon interface peak is detectable in the ZnSe films which have grown from a wide range of Se precursors including H_2Se.

Figure 4.18 compares SIMS depth profiles for ^{12}C for ZnSe films grown with different allyl selenide sources. The ^{12}C concentration in the bulk of the ZnSe films grown from DASe always stays above 10^{20}atoms/cm^3 and those

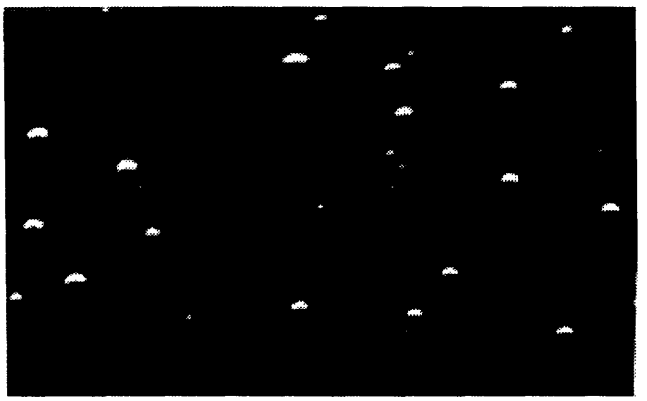

(a) T_G = 325°C

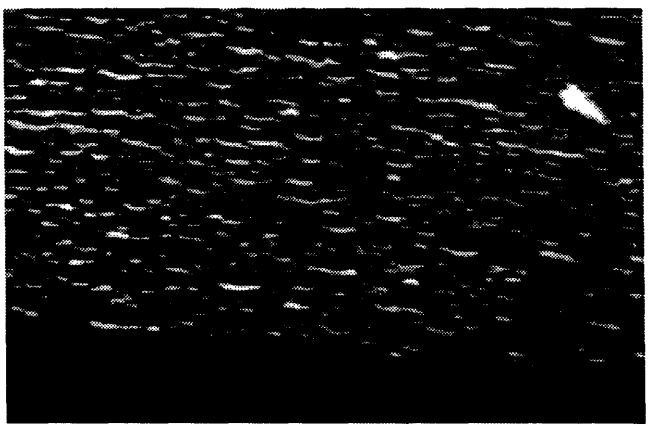

(b) T_G = 350°C

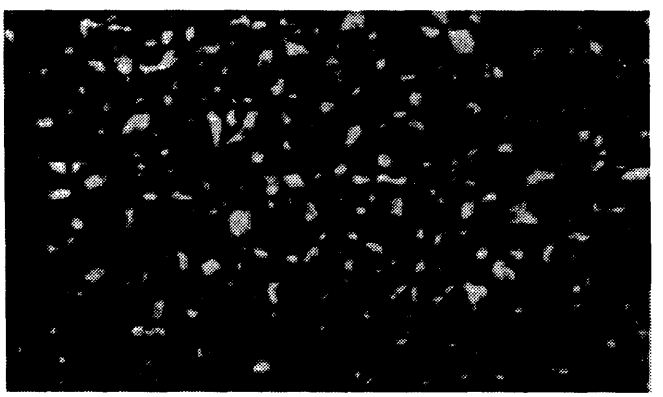

1μm

(c) T_G = 400°C

Figure 4.16 SEM micrographs of ZnSe grown from tBASe/DMZn:NEt3 at different growth temperatures

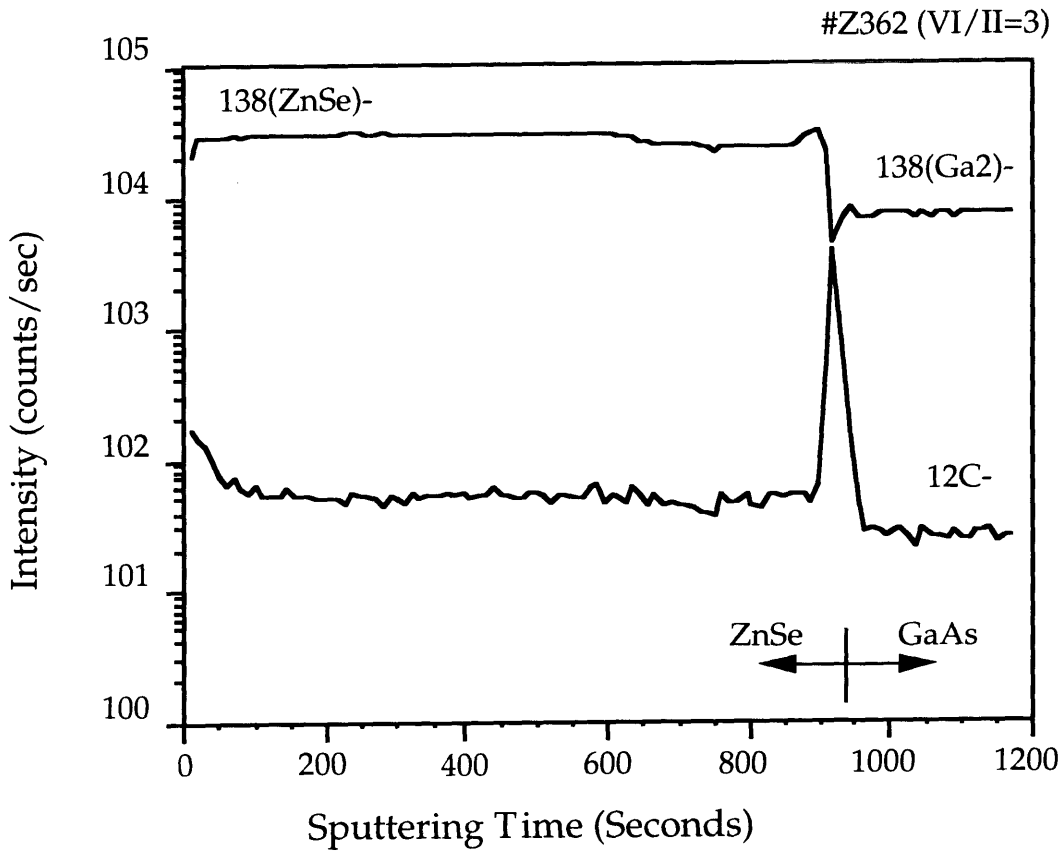

Figure 4.17 SIMS depth profiles for carbon (^{12}C) in ZnSe grown on GaAs. Mass 138 represents $ZnSe^-$ in the epilayer and Ga_2^- in the substrate

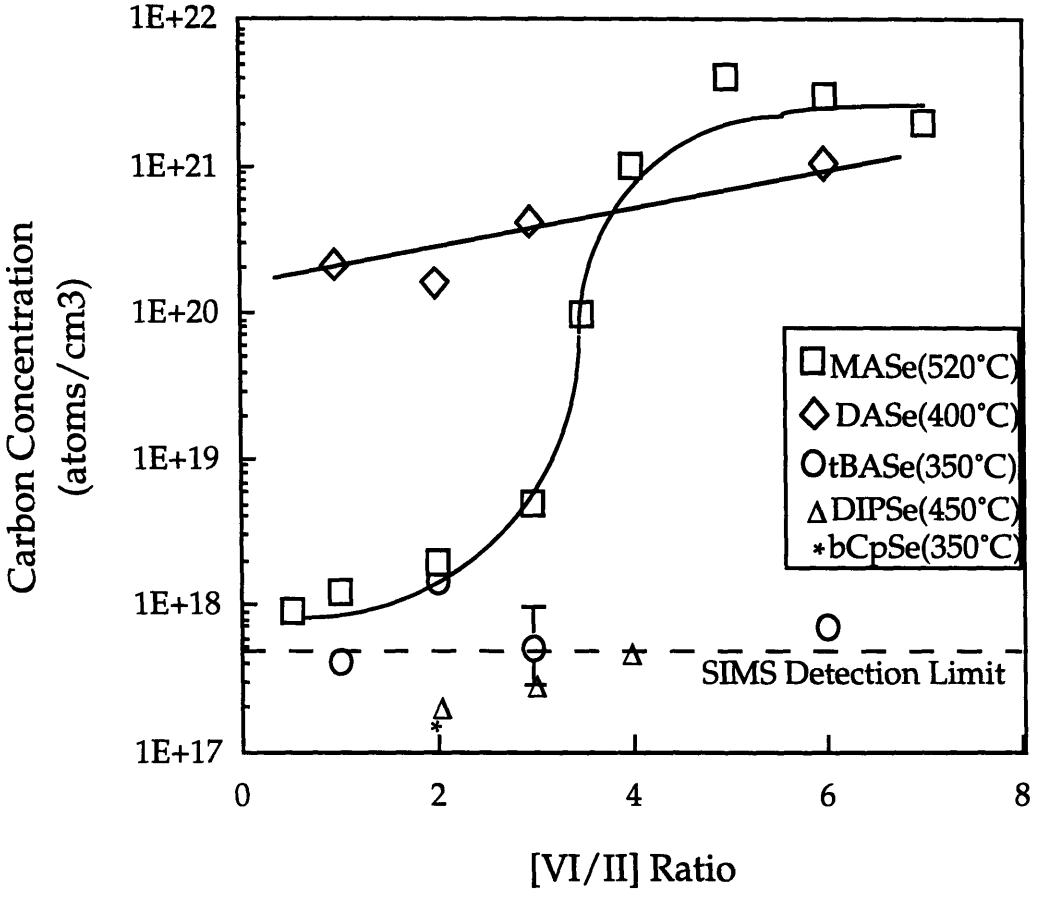

Figure 4.18 Dependence of ^{12}C concentration as determined by SIMS on the VI/II ratiofor ZnSe films gr own from tBASe ( ) at 350°C, DASe( ) a 400°C, MASe ( ) at 520°C, DIPSe (Δ) at 450°C and bCpSe (*) at 350°C.

from MASe goes up to 10^{21} atoms/cm^3, when the [VI]/[II] ratio increases above 3. In contrast, the bulk ZnSe films from tBASe show no significant carbon incorporation (below detection limit, 5X10^{17} atoms/cm^3) even at high VI/II ratio of 6. This dramatic difference in carbon concentration in ZnSe films from DASe, and MASe *vs.* tBASe suggests that different decomposition mechanisms are responsible for carbon incorporation [Danek *et al.*, 1993]. In fact, mass spectroscopy studies show that the retro-ene rearrangement pathway is much reduced relative to the case of DASe and MASe (see Figure 4.11).

The ZnSe films were investigated by the nondestructive Rutherford backscattering spectrometry (RBS). To clarify the random spectrum profiles, the schematic random spectra calculated from the parameters for each atom, such as the kinematic factor, stopping cross section and scattering cross section [Chu *et al.*, 1978] are shown with actual random spectrum of 1.2μm ZnSe/GaAs in Figure 4.19. The random spectrum reflects the interface profile, from which film thickness information may be obtained. The abrupt change in RBS yield at the ZnSe/GaAs interface is caused by misfit dislocation and diffusion of active impurities.

The RBS channeling yield for the three different thickness are shown in Figure 4.20. The result may be interpreted in terms of relaxation of the ZnSe film through dislocation formation. The critical thickness, h_c [Mattews and Blakeslee, 1974], below which the film is pseudomorphic, may be expressed by minimizing the sum of energies associated with strain and edge dislocation.

$$h_c = \frac{b}{8\pi f}\frac{(1-\nu\cos^2\alpha)}{(1+\nu)\cos\lambda}\left(\ln\frac{h_c}{b}+1\right) \qquad (3)$$

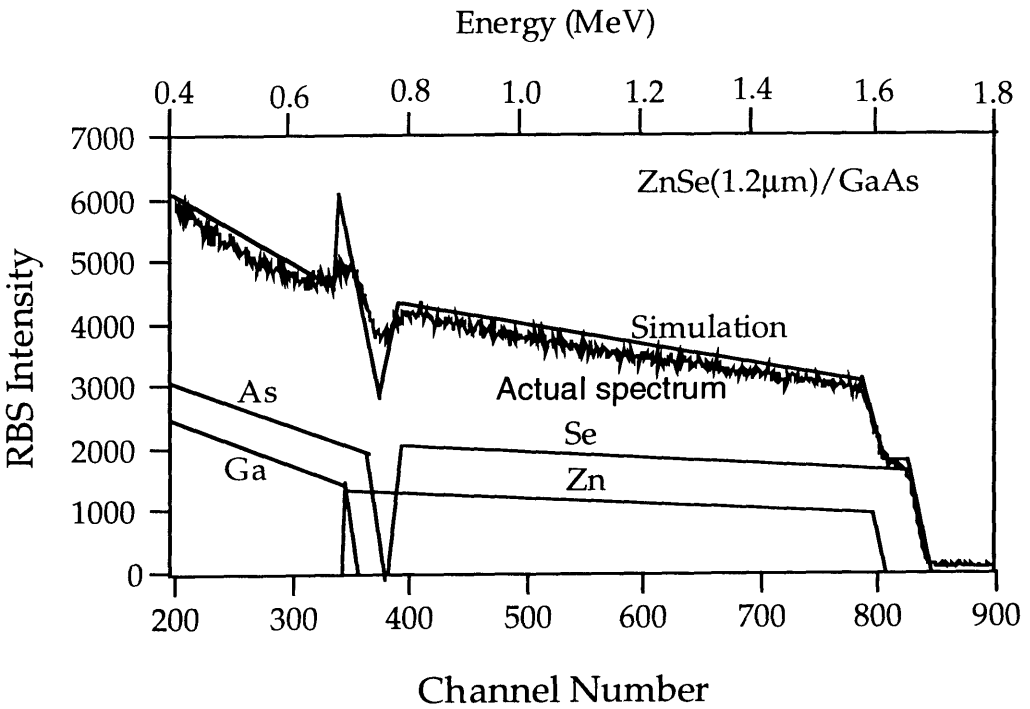

Figure 4.19. Schematic RBS random spectrum calculated from the kinematic factor, stopping cross section and scattering cross section for 1.2 μm thick ZnSe/GaAs(100).

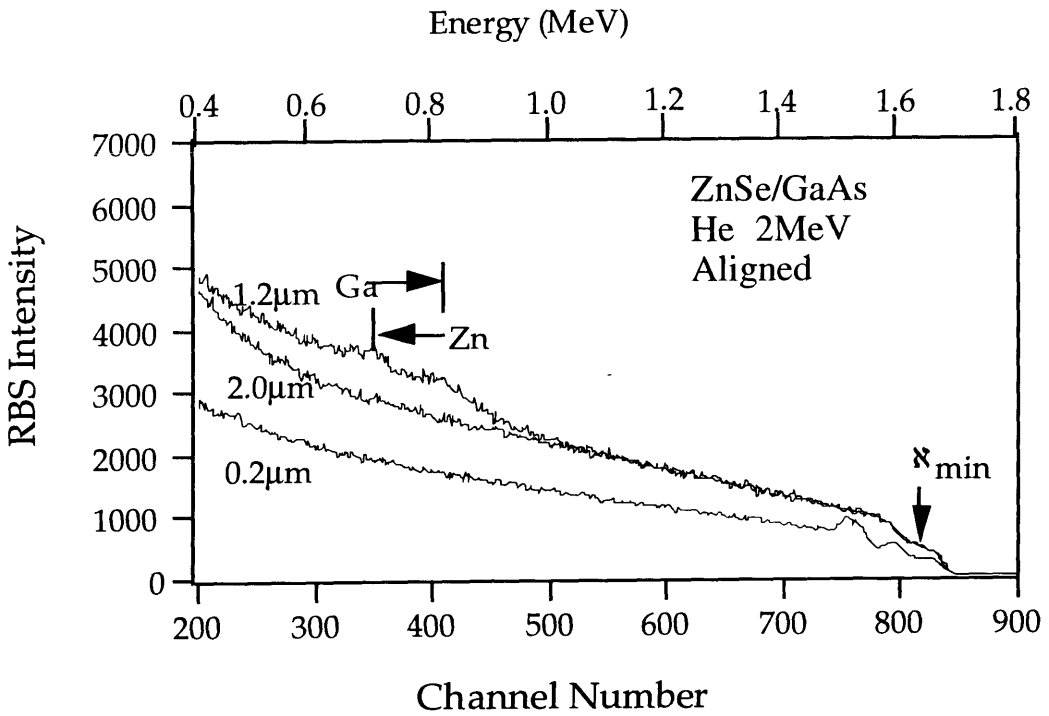

Figure 4.20. RBS Intensity measured in channeling for ZnSe/GaAs(100) samples. The Ga and Zn arrows indicate the distribution edge of each atom estimated from RUMP.

Here, b (=4.008Å) is the magnitude of Burger's vector, ν (=0.376) is Poisson's ratio and f (=2.72X10^{-3}) is the absolute value of the misfit. For the ZnSe/GaAs system, $h_c \cong$ 450Å. Lattice relaxation is actually observed around 1500 - 2000Å from X-ray diffraction measurements [Mitsuhashi *et al.*, 1986]. The lowest yield for the 0.2μm thick sample in the whole spectrum range indicates good crystalline property of the film as well as the interface. The increase of the minimum background yield χ_{min} [Ohmi *et al.*, 1988] measured at the surface from 6.6 % to 11.1% with the increase in the ZnSe film thickness from 0.2μm to 1.2μm, respectively, indicates the clear degradation of ZnSe films above the critical thickness. With the further increase of layer thickness, the background yield becomes almost the same and is estimated according to the lattice-mismatched dislocations. At the heterointerface, the RBS yield, in particular, is seen to have increased comparably because of lattice imperfections. The Ga and Zn arrows in Figure 4.20 indicate the distribution edge of each atom estimated from the kinematic factor and stopping cross section from the Rutherford Universal Manipulation Program (RUMP).

The lattice parameters of the ZnSe epilayer on the GaAs substrate were measured by double crystal X-ray diffractometry. Figure 4.21 shows the lattice spacing of ZnSe epilayers perpendicular to the heterointerface. Above an experimental critical thickness of 1500Å the lattice spacing start to decrease, indicating the rapid relieving of the mismatch lattice strain due to the formation of dislocations. The vertical lattice constant of the ZnSe layer with 0.2μm thickness is 5.6808±0.0005Å, which is larger than the lattice parameter of bulk ZnSe (a_0=5.6694Å). The lattice spacing becomes almost the same as that of bulk ZnSe when the film thickness reaches 1μm, and becomes smaller than bulk ZnSe

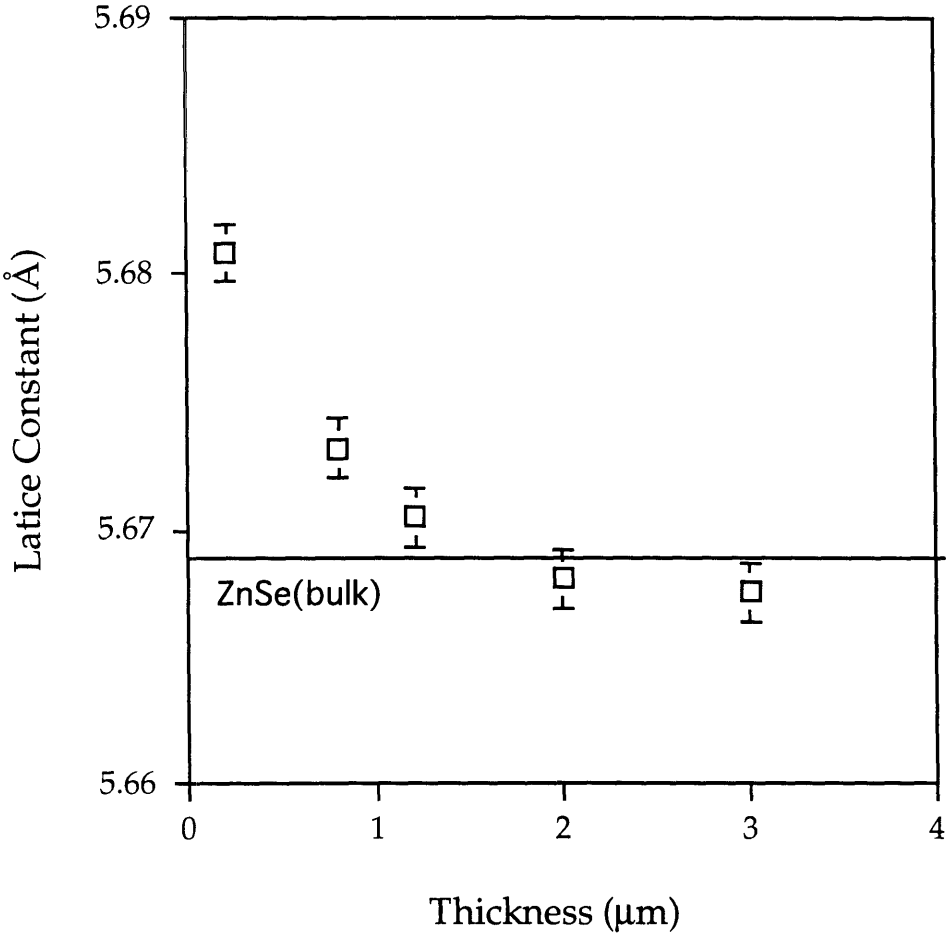

Figure 4.21 Lattice parameter normal to the ZnSe surface measured by DCD as a function of the film thickness

for films thicker than 1μm, implying that the ZnSe layer suffers two-dimensional tensile stress. This tensile stress is mostly likely induced by the difference in thermal expansion coefficients between the ZnSe epilayer ($6.8X10^{-8}$ K^{-1} at RT) and the GaAs substrate ($5.7X10^{-6}$ K^{-1}).

In Figure 4.22 (004) reflection of ZnSe films with different VI/II ratio are shown. There is no degradation of crystalline quality in ZnSe epilayers with different VI/II ratio. The FWHM of the layer reflection is found to vary from 220 to 400 arc sec depending on the samples, while the FWHM of the GaAs substrate reflection remains constant (40 ~ 60 arc sec). The quality of the ZnSe layer is comparable to that of the best ZnSe film from H_2Se, which showed 150 arc sec of FWHM from layer reflection.

The low temperature (10 K) photoluminescence (PL) spectrum of the ZnSe sample grown at VI/II=2 is shown in Figure 4.23. The near-band-edge PL spectra are similar to those previously reported for DMZn:NEt_3/H_2Se [Huh *et al.*, 1993]. The PL consists of strong signals of two donor bound excitonic peak (I_2^{lh} and I_2^{hh}) at 2. 7954eV and 2.7970eV and free excitonic peaks (E_x^{lh} and E_x^{hh}) at 2.8004eV and 2.8026eV. The deep level emission due to self-activated centers appears around 2.3eV and probably originates from residual impurities in the tBASe precursor.

Most of the ZnSe epilayers grown from tBASe were highly resistive. However, one sample grown at low temperature at 325°C resulted in slightly n-type conductivity with room temperature mobility of 105 cm^2/Vs. This high resistivity indicates a high concentration of electron traps or scattering centers, limiting electronic transport in the films. Highly resistive layers have also been reported when DESe was used as a Se precursor [Giapis *et al.*, 1990].

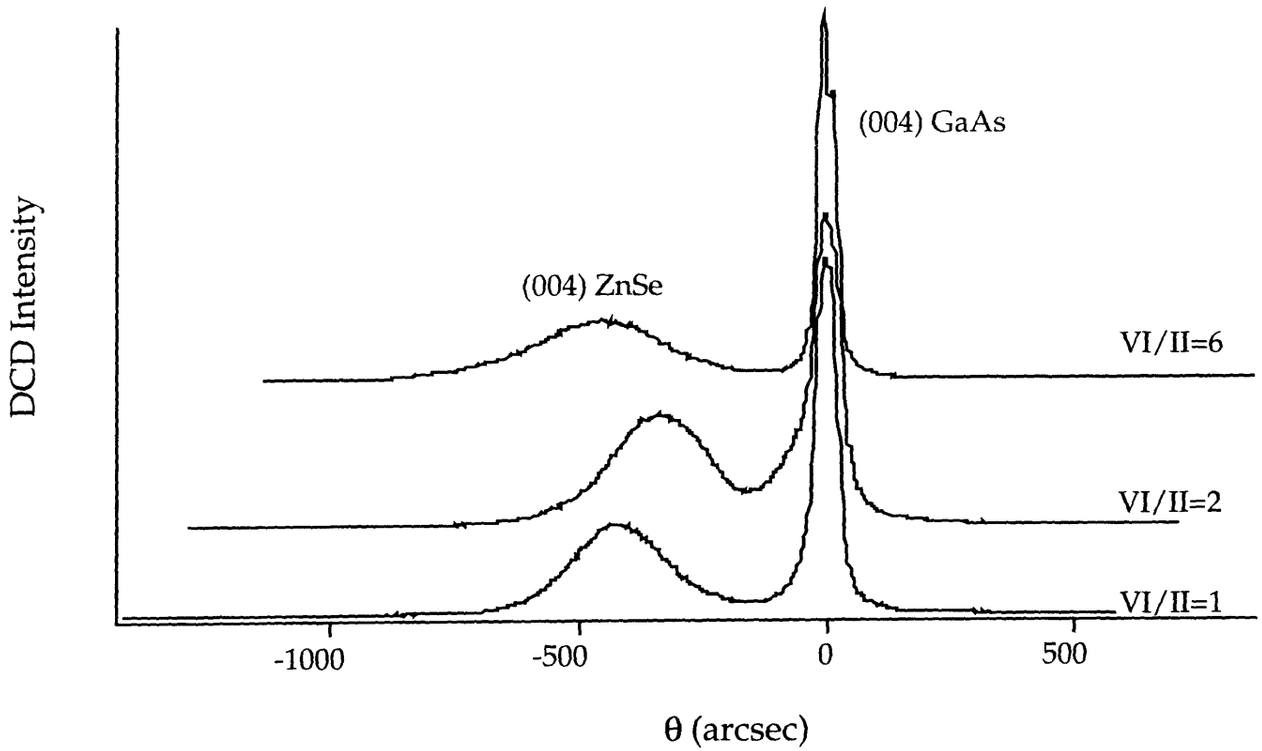

Figure4. 22. Rocking curves for the (004) r eflection of ZnSe/(001)GaAs grown with different VI/II ratios.

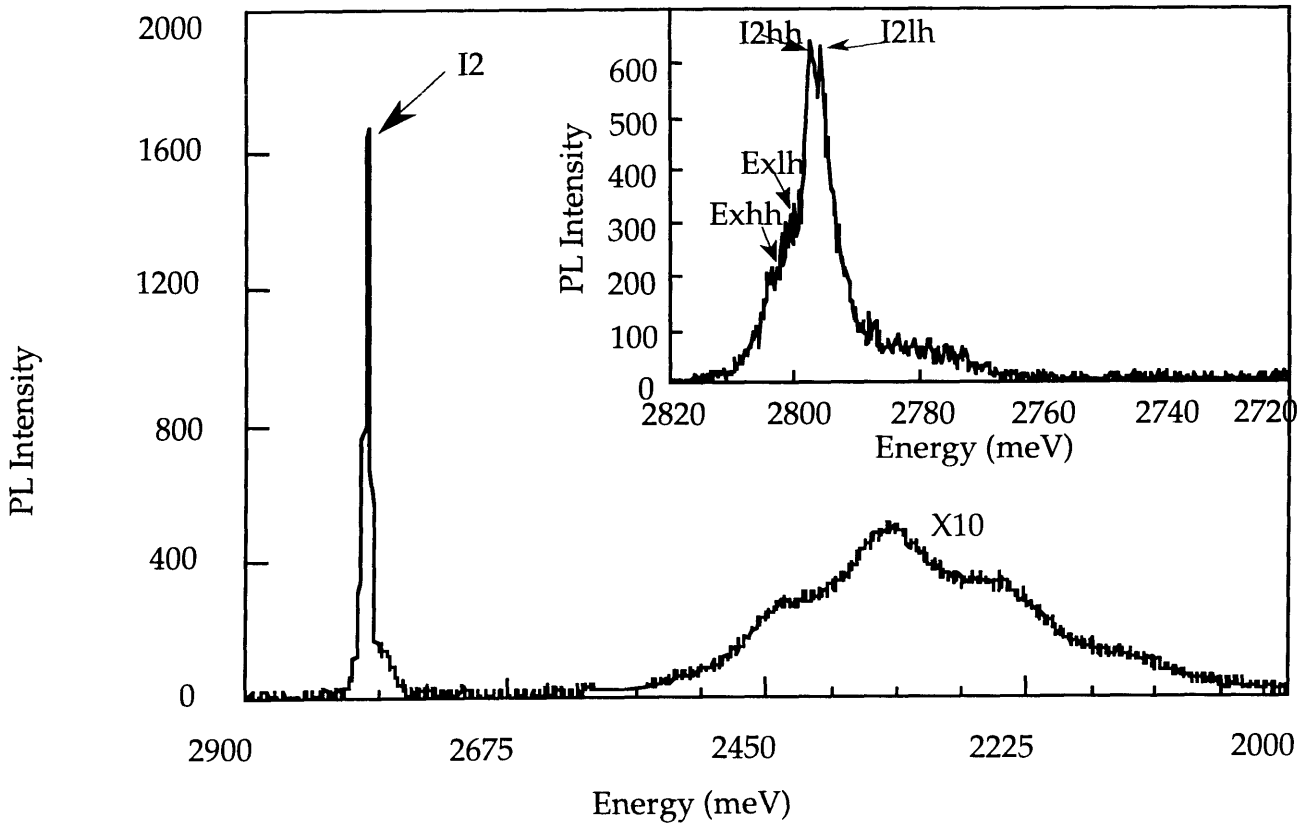

Figure 4.23 10K Photoluminescence spectra of ZnSe grown with tBASe/DMZn:NEt_3 conditions (T_G=350°C, P_G=300Torr, VI/II=2, tBASe=40μmol/min)

4.7. 2-Selena-3-(1-methylethyl)-bicyclo [2.2.1] hept-5-ene. (bCpSe)

Another novel Se source, 2-Selena-3-(1-methylethyl)-bicyclo [2.2.1] hept-5-ene (bCpSe), was employed in conjunction with DMZn:NEt3 for low temperature OMVPE growth. In order to prevent the rearrangement pathway, the Se atom is placed in a ring so that the compound cannot attain the conformation needed for rearrangement reaction which requires that alpha hydrogen atom be in proximity to the terminal carbon of the double bond. The new cyclic compound decomposes at a relatively low temperature of 300°C and the predominant volatile byproduct is cyclopentadiene [Gordon, 1993].

4.7.1. Growth Rate

The vapor pressure of bCpSe was measured by the simple experimental procedure described in Chapter 4.2. In Figure 4.24 the vapor pressure of bCpSe source is shown as follows.

$$ln(p[Torr]) = 19.887 - 6435.7/(T[K]), R = 0.99881 \qquad (4)$$

The vapor pressure of bCpSe is relatively low because of its precursor structure. The ZnSe films were therefore grown at a lower pressure (P_G=30Torr) to maintain the same delivery rate of the bCpSe source as that of tBASe.

The growth rates were measured as a function of the reciprocal growth temperature (see Figure 4.25). The growth was limited by chemical kinetics below 400°C with apparent activation energies of 16 kcal/mol and became

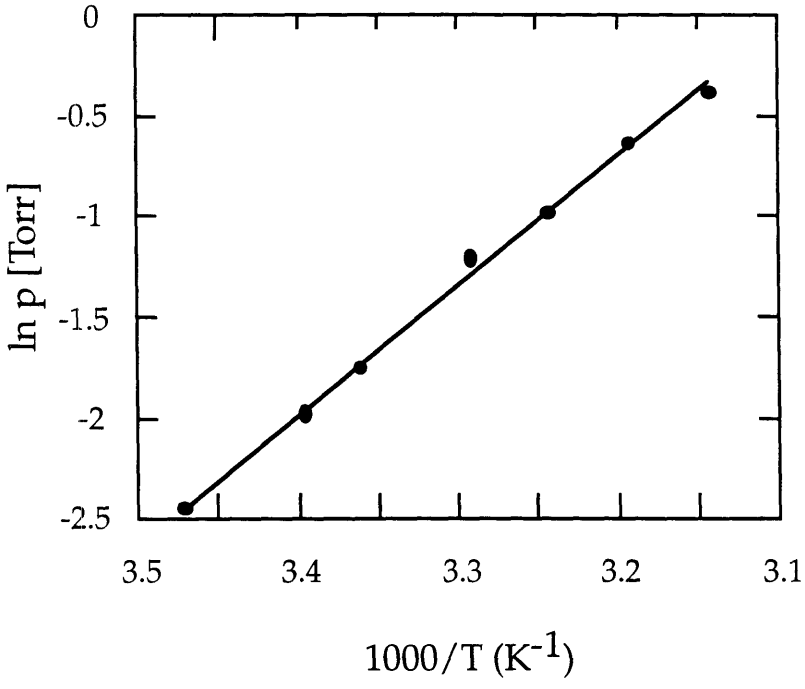

Figure 4.24 Vapor pressure of bCpSe source

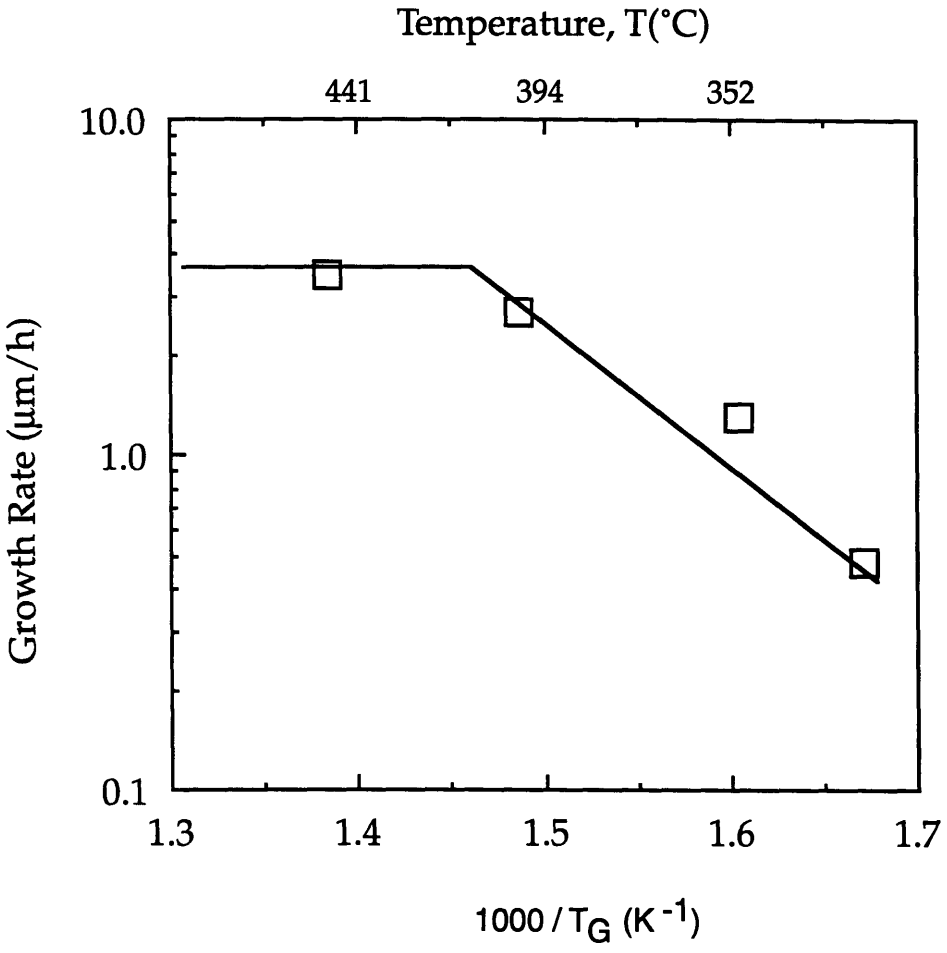

Figure 4.25. Growth rate of ZnSe fr om DMZn:NEt_3/bCpSe as a function of temperature (DMZn:NEt_3=20µmol/min, VI/II=2, P_G=30 Torr)

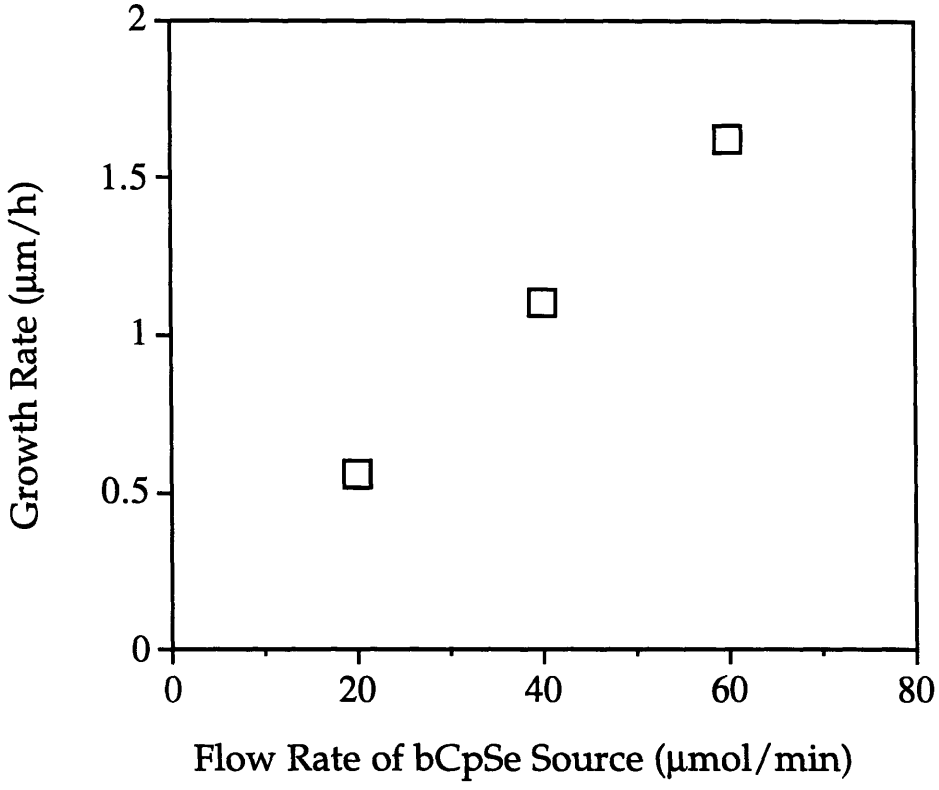

Figure 4.26 Growth rate of ZnSe as a function of bCpSe source flow rate at T_G=350°C. (DMZn:NEt_3=20μmol/min)

constant at higher temperatures which is indicative of a mass controlled deposition process. In Figure 4.26, the growth rate dependence on different VI/II ratio is shown with the bCpSe source at the growth temperature of 350°C. The delivery rate of DMZn:NEt_3 flux was fixed at 20μmol/min.

4.7.2. Surface morphology

Under high magnification observation (20,000 X) by SEM, no hillocks, pinholes or inclusions were detected on the surface. The specular surface exhibited, however, tetrahedral features, like the one shown in Figure 4.27. In this type of overgrowth the tetrahedral symmetry of the lattice is preserved. We note here that SEM observation of these films was difficult because their high resistivity caused charging of the surface and subsequent blurring of the image.

4.7.3. Materials Characterization

The carbon concentration, as measured by SIMS, in the ZnSe films grown from bCpSe at 350°C was not detectable (*i.e.*, below the detection limit, $5X10^{17}$ atoms/cm^3). The lattice parameters of ZnSe/GaAs were investigated by double crystal diffractometry. The FWHM of the (004) reflection of the ZnSe samples appeared around 200-250 arcsec, which is indicative of good quality of ZnSe epilayer on a GaAs substrate. The ZnSe films were also evaluated by RBS. The RBS channeling yields were low, again showing a good crystalline property of the film and interface.

The low temperature (4 K) photoluminescence (PL) spectrum of the ZnSe film grown from the DMZn:NEt_3/bCpSe combination at VI/II=2 is shown in Figure 4.28. With close inspection of the expanded near-band-edge spectrum in

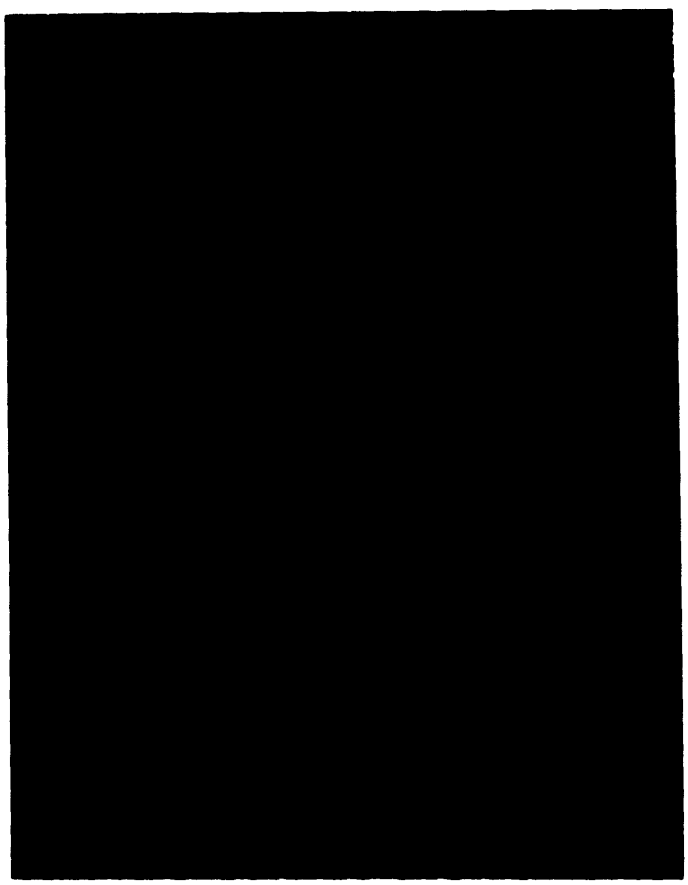

Figure 4.27 SEM micrographs of ZnSe grown from bCpSe and DMZn:NEt_3 source. (VI/II=2, T_G=350°C and P_G=30 Torr)

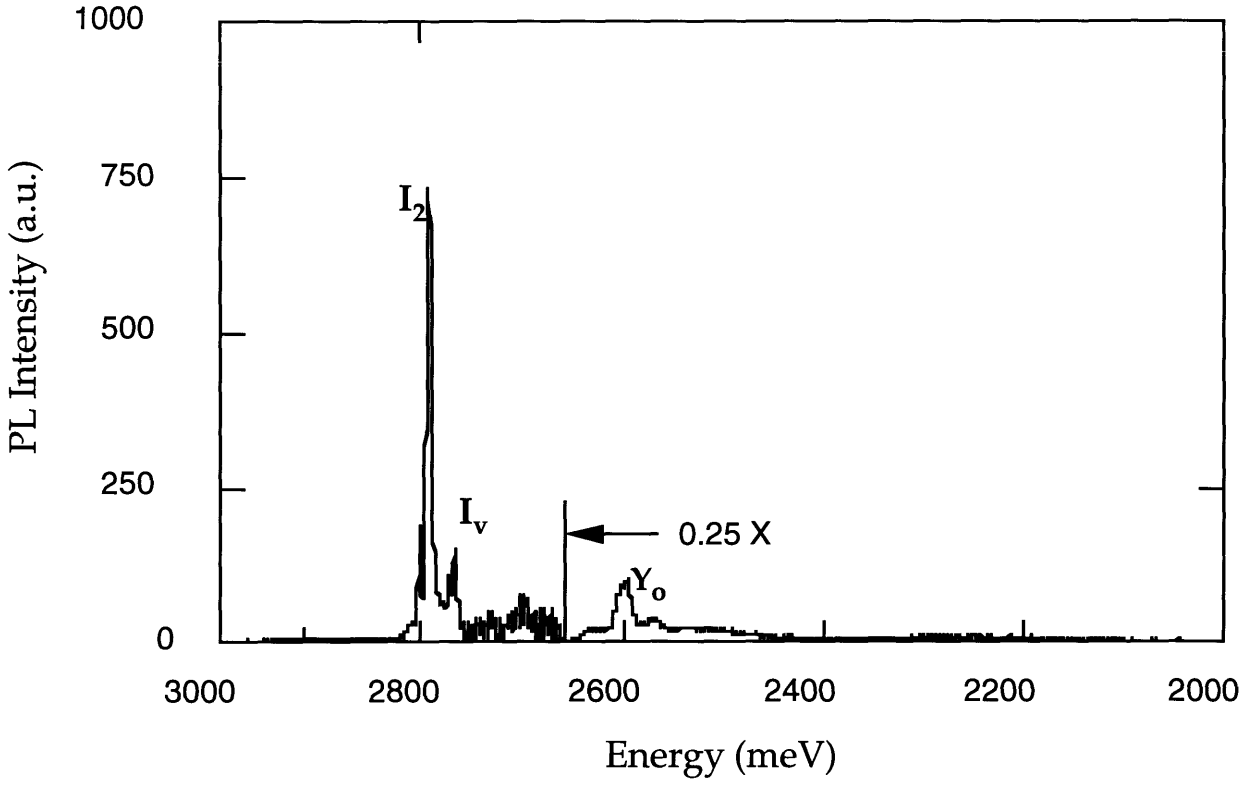

Figure 4.28 The photoluminescence spectra of ZnSe from bCpSe/DMZn:NEt_3.

the insert, donor-bound excitons are apparent at 2.7967 eV (I_2^{hh}) and 2.7945 eV (I_2^{lh}). At lower energies, the peak at 2.773eV (I_v) has been suggested to be the result of recombinations involving selenium-site-related defects [Shahzad *et al.*, 1989]. At 2.6004 eV, a Y_o peak, attributed to recombination of excitons at structural and other extended defects [Dean, 1984], is noticeable. The relatively weak intensity of the Y_o peak is an indication of good crystalline quality of the film.

4.8 Conclusions

The results of the above investigations allow the comparison of organometallic Se sources developed for low temperature growth of ZnSe. Table 4.1 lists critical characteristics. The first criterion is vapor pressure. It is desirable that at room temperature vapor pressures is more than 5 Torr since this avoids the necessity of using extremely high carrier gas flow rates through the bubbler, and heating of the downstream lines. In this regard, bCpSe is at a disadvantage (0.2 Torr at RT). The second consideration is growth temperature, which dependence on growth rate are shown in Figure 4.29. Lower growth temperature is particularly important to limit native defects and improve dopant incorporation. In order to get low desirable growth temperature of 300-350°C, the Se source must pyrolyze at relatively low temperature and must remain stable at room temperature. The tBASe and bCpSe sources maintain lower growth temperature than other Se sources such as DESe, MASe, DIPSe and DASe. The third major consideration is related with purity. The sources should be easily purified without decomposing and must produce no detectable carbon

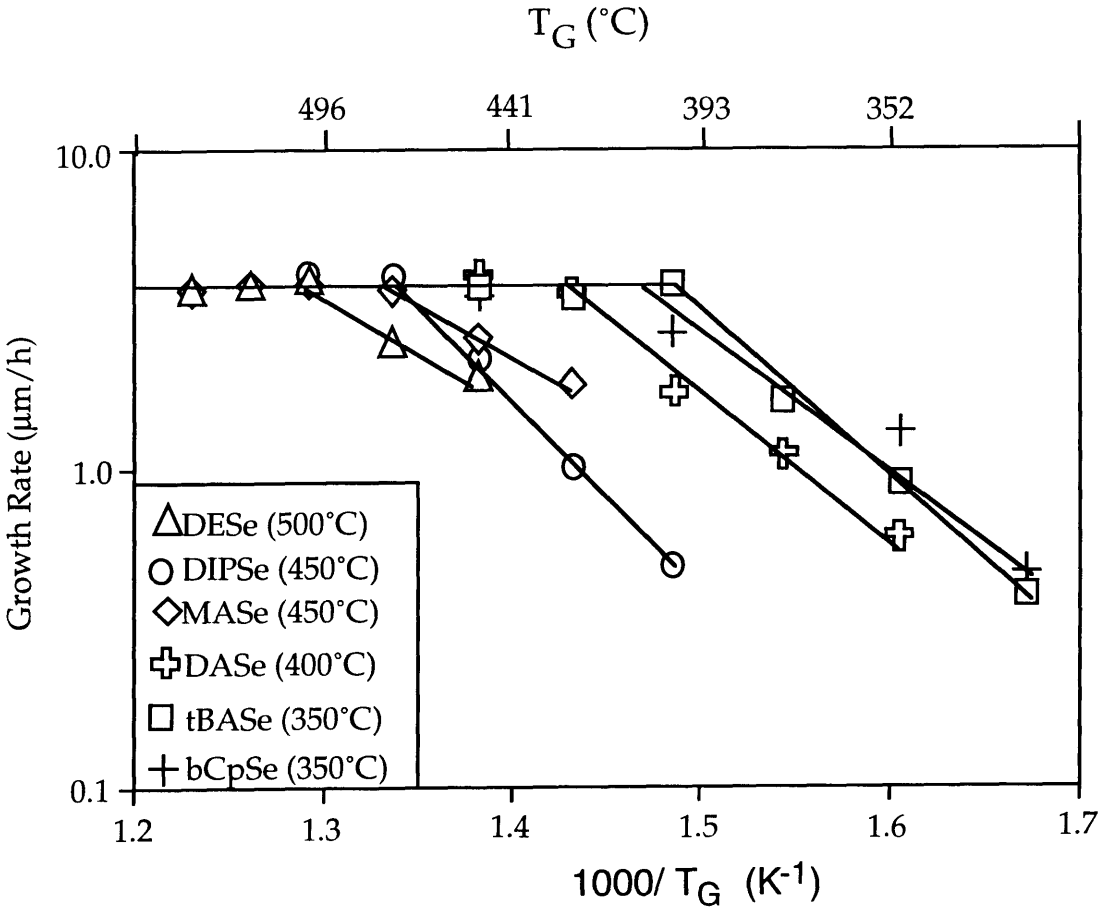

Figure 4.29 Growth temperature effect on growth rate with several or ganometallic Se sources (DESe,DIPSe, MASe, DASe, tBASe and bCpSe)

Table 4.1 Comparison of basic characteristics of Se sources for O MVPE

Source	Vapor Pressure (25°C)	Growth Temperature	Carbon Contamination (atoms/cm^3)	Hazard (TLV-TWA)
H_2Se		300°C	+++	0.05ppm (0.02μg/m^3)
DESe	28 Torr	500°C	+	(0.2mg/m^3)*
DIPSe	10.5 Torr	450°C	+	(0.2mg/m^3)*
MASe	20 Torr	450°C	1e21 (VI/II>3)	(0.2mg/m^3)*
DASe	2.5 Torr	430°C	1e21	(0.2mg/m^3)*
tBASe	3.9 Torr	350°C	+	(0.2mg/m^3)*
bCpSe	0.2Torr	350°C	+	(0.2mg/m^3)*

+ signifies no detectable carbon concentration.

* estimated from toxicity of elemental Se.

contamination in the resultant epitaxial layer. The allyl based compounds (DASe and MASe) give unacceptably high background carbon concentrations ($1X10^{21}$ atoms/cm^3), whereas the carbon incorporation appears to be sterically hindered for tBASe. Finally, the toxicity should be considered as an extremely important issue in precursor selection.

Considering all these factors, tBASe appears to be optimum choice as a H_2Se replacement. The ZnSe films from tBASe did not show any noticeable carbon incorporation (<$5X10^{17}$ atoms/cm^3) while other allyl based selenides (MASe and DASe) were found to have high levels of carbon incorporation ($10^{21}cm^{-3}$) at VI/II $\geq$ 3. The epitaxial quality of the ZnSe/GaAs layers and interfaces were confirmed by DCD and RBS. The RBS channeling spectra revealed a ZnSe/GaAs interface which is comparable to high quality ZnSe films grown from H_2Se/DMZn:NEt_3. Although these films appeared resistive, photoluminescence showed a sharp near-band-edge (NBE) peak. Thus, the OMVPE growth with novel Se precursors has yielded new routes for achieving reasonable quality ZnSe films.

Chapter 5

Conclusions and Future Work

Investigations of low pressure OMVPE of ZnSe with the adduct precursor DMZn:NEt_3 and H_2Se show that use of the adduct minimizes the extent of detrimental prereactions commonly observed with DMZn and H_2Se. The effect of the adduct is attributed to not only a simple blocking of reactions between DMZn and H_2Se, but also a stabilization of an intermediate preventing the formation of ZnSe-organic-oligomers. Growth data demonstrate that use of the adduct reagent is particularly effective at lower temperatures (< 300° C) and low pressures (< 30 Torr). At these conditions growth rates are higher when using DMZn:NEt_3, and the surface morphology is improved relative to films synthesized with DMZn. Hall measurements and photoluminescence spectra of the grown films further show that DMZn:NEt_3 produces materials with comparable electronic and optical properties to films grown with DMZn. Additional improvements in electronic properties of ZnSe may be expected since the adduct is more easily purified than DMZn [Jones, 1989].

Low temperature (~325°C) growth of ZnSe films by OMVPE was achieved from DASe, DIPSe, tBASe or bCpSe in the combination of DMZn:NEt_3 or DMZn as the Zn source. The films were evaluated in terms of growth rates, surface morphology and optoelectronic properties. ZnSe films from tBASe did not show any noticeable carbon incorporation ($<5X10^{17}$ atoms/cm^3) while other allyl

based selenides (MASe and DASe) were found to have high levels of carbon incorporation ($10^{21}cm^{-3}$) at VI/II $\geq$ 3.

The low pressure growth opens the possibility for microwave stimulated doping in OMVPE. Initial experiments with NH_3 showed promising results for this approach, but the deposition pressure will have to be reduced further to increase the concentration of radicals at the growth surface. This should also allow the replacement of NH_3 by N_2 as the doping source. For reducing the reactor pressure mm Torr range, the present mechanical pump should be replaced with a high efficiency turbomolecular pump. It is critical to increase the fraction of plasma radicals reaching the surface of the films, since the mean free path of radicals are strongly dependent on the reactor pressure.

Other direction to get a high quality p-type ZnSe is the utilization of dopant chemistry with nitrogen dopant sources like an azidotrimethylsilane ($Si(CH_3)_3N_3$). Once the chemical pathway, leading to the growth of ZnSe and affecting its doping from different sources, is understood, the chance of modifying the doping mechanism leading to increased incorporation of one or another impurity can be significantly increased.

It is most important to develop methods to activate electrically impurities in the films. One of the main difficulties in preparing a low-resistivity p-type ZnSe is the amphoteric behavior of the incorporated acceptor impurities. It is known that acceptor-type impurities in the interstitial and substitutional sites behave as donors and acceptors, respectively, and compensate each other [Neumark, 1980]. For this reason, a method for *site-selective impurity doping* should be developed through the rapid thermal annealing, laser annealing or δ-doping with fast quenching. The other difficulty of getting p-type ZnSe comes

from hydrogen passivation in N-doped ZnSe samples. In order to alleviate passivation effect, hydrogen containing sources should not be employed. The tBASe is a possible replacement of H_2Se and appropriate dopant source without hydrogen incorporation effect could be searched.

Bibliography

Akram,S., I.B.Bhat and A.A.Melas, "Nitrogen Doping of ZnSe by OMVPE Using a Novel Organometallic Precursor", *J.Electronic Mater.*, to be published

Aldermann, L.C. and J.J.Birgin, "Hydrogen Selenide Poisoning: An Illustrative Case with Review of the Literature", *Archives of Environmental Health*, 41.354-358, (1986)

Anderson,S.G., F.Xu, M.Vos, J.H.Weaver and H.Cheng, "Schottky-Barrier Formation and Atomic Mixing at Au/ZnSe (100) and Co/ZnSe (100) Interfaces with Co and Au Interlayers", *Phys.Rev.*, B39, 5079-5090, (1989)

Akimoto,K., H.Okuyama, M.Ikeda and Y.Mori, "Isoelectronic Oxygen in II-VI semiconductors", *Appl.Phys.Lett*, 60, 91-93, (1991)

Akimoto,K., T.Miyajima and Y.Mori, "Injection Luminescence in Oxygen-Doped ZnSe grown by MBE", *J.Cryst.Growth*, 101, 1009-1012, (1990)

Besomi,P. and W.Wessels, "High-Conductivity Heteroepitaxial ZnSe Films", *Appl.Phys.Lett.*, 37, 955-957, (1980)

Bhargava,R.N., "Optoelectronic Devices from Wide Band GaP II-VI Semiconductors", *Growth and Optical Properties of Wide-Gap II-VI Low Dimensional Structures*, eds T.C.McGill and Gebharbt, Plenum Press, 1-9 (1989)

Bhargava,R.N., R.J.Seymour, B.J.Fitzpatrick and S.P.Herko, "Donor-Acceptor Pair bands in ZnSe", *Phys.Rev.*, 2407-2419, (1979)

Blanconnier,P., M. Cerlet, P.Henoc and A.M. Jean-Louis, "Growth and Characterization of Undoped ZnSe Epitaxial Layers Obtained by Organometallic Chemical Vapor Deposition", *Thin solid films*, 55 , 375-386 (1978)

Brooks,H., in *Advances in Electrons and Electron Physics*, eds by L.Marton, 158-165, Academic Press, New york, (1958)

Coates,G.E., M.L.H.Green and K.Wade, *"Organometallic Compounds"*, Vol. 1 121-141 (1967)

Cockayne,B. and P.J.Wright, "The Growth of Thin Layers by MOCVD of wide Bandgap II-VI Compounds", *Growth and Optical Properties in Wide-Gap II-VI Low Dimensional Structures*, Plemun Press, 75-85 (1989)

Cockayne,B., P.J.Wright, A.J.Armstrong, A.C.Jones and E.D.Orrell, "MOCVD Layer Growth of ZnSe Using a New Zinc Source", *J.Cryst.Growth*, 84, 552-554, (1987)

Cockayne,B. and P.J.Wright, "Metalorganic Chemical vapor Deposition of Wide Band Gap II-VI Compounds", *J.Cryst.Growth*, 68, 223-230, (1984)

Chapman, B., *Glow Discharge Processes: Sputtering and Plasma Etching*", Wiley-Interscience Publication, New York, (1980)

Cheng,H., J.M.DePuydt, J.E.Potts and M.A.Haase, "Growth of p- and n-type ZnSe by MBE", *J.Cryst. Growth*, 95, 512-516, (1989)

Cheng,H., J.M.DePuydt, J.E.Potts and T.L.Smith, "Growth of p-type ZnSe:Li by MBE", *Appl.Phys.Lett.*, 52, 147-149, (1988)

Chu,W.K., J.W.Mayer and M.A.Nocolet, "*Backscattering Spectrometry*", Academic Press, New York, (1978)

d'Agostino,R., F.Cramarossa, S.De Benedictis and G.Ferraro, "Kinetic and Spectroscopic Analysis of NH3 Decomposition Under R.F.Plasma at Moderate Pressures", *Plasma Chemistry and Plasma Processing*, 1, 19-35, (1981)

Danek,M., J.-S.,Huh, K.F.Klavs, D.C.Grodon, W.P.Kosar, "Low Temperature OMCVD Growth of ZnSe and Gas-Phase Pyrolysis Study with *Tertiary*-butyl Allyl Selenide", *Chemistry of Mater.*, to be published

Dean,P.J. "Comparison of MOCVD-Grown with Conventional II-VI Materials Parameters for EL Thin Films", *Phys.Stat.Sol.(a)*, 81, 625-646, (1984)

DePuydt,J.M., M.A.Haase, H.Cheng and J.E.Potts, "Electrical characterization of p-type ZnSe", *Appl.Phys.Lett.*, 55, 1103-1105, (1989)

Donnelly, V.M., A.P.Baronavski and J.R.McDonald, "ArF Laser Photodissociation of NH_3 at 193nm", *Chem.Phys.*, 43, 271-281, (1979)

Dreifus,D.L., B.P.Sneed, J.Ren, J.W.Cook,Jr., and J.F.Schetzina, "ZnSe Field-Effect Transistors", *Appl.Phys.Lett.*, 57, 1663-1665, (1990)

Fan,G. and J.O.Williams, "On the Growth of ZnSe on (100)GaAs by Atmospheric Pressure MOVPE", *Mater.Lett.* 3, 453-456, (1985)

Faulkner,R.A., "Toward a Theory of Isoelectronic Impurities in Semiconductors", *Phys.Rev.*, 175, 991-1009, (1968)

Feldman,L.C and J.W.Mayer, *Fundamental of Surface and Thin Film Analysis*, North-Holland, New York, (1986)

Fortiadis,D.I., S.Kieda and K.F.Jensen, "Transport Phenomena in Vertical Reactors for Metalorganic Vapor Phase Epitaxy", *J.Cryst.Growth* , 102, 441-470, (1990)

Fujita,S., T.Sakamoto, M.Isemura and S.Fujita, "Use of Methylselenol for Organometallic Vapor-Phase Epitaxy of ZnSe", *J.Cryst.Growth*, 87, 581-584, (1988)

Fujita,S., Y.Matsudand A.Sasaki, "Blue Luminescence of a ZnSe-$ZnS_{0.1}Se_{0.9}$ Strained-Layer Superlattice on a GaAs Substrate grown by Low-Pressure Organometallic Vapor Phase Epitaxy", Appl.Phys.Lett., 47, 955-957, (1985)

Fujita,S., Y.Matsuda and A.Sasaki, "Growth and Properties of Undoped n-type ZnSe by Low-Temperature and Low-Pressure OMVPE", *Jpn.J.Appl.Phys.*, 23, L360-362, (1984)

Gaines,J.M., R.R.Drenten, K.W.Haberern, T.Marshall, P.Mensz and J.Petruzzzello "Blue-Green Injection Lasers containing Pseudomorphic $Zn_{1-x}Mg_xS_ySe_{1-y}$ Cladding Layers and operating up to 394K", *Appl.Phys.Lett.*, 62, 2462-2464, (1993)

Giapis,K.P., K.F. Jensen, J.E.Potts and S.J.Pachuta, "Investigation of Carbon Incorporation in ZnSe : Effects on Morphology, Electrical and Photoluminescence Properties", *J. Electron. Mater.* ,19, 453-462 (1990)

Giapis,K.P., D.C.Lu, D.I. Fotiads and K.F. Jensen, "A New Reactor System for MOCVD of ZnSe : Modeling and Experimental Results for Growth from Dimethylzinc and Diethylselenide", *J. Crystal Growth*,, 104, 629-640 (1990)

Giapis,K.P., D.C.Lu and K.F.Jensen, " High-Quality Epitaxial ZnSe and relationship between Mobility and Photoluminescence Characteristics", *Appl.Phys.Lett.*, 54, 353-355, (1989a)

Giapis,K.P., D.C.Lu and K.F.Jensen, "Effects of the Selenium Precursors on the Growth of ZnSe by Metalorganic Chemical Vapor Deposition", *MRS Proceedings*, Vol. 131, 63-69 (1989b)

Giapis,K.P., D.C.Lu, K.F.Jensen, J.E.Potts and S.J.Pachuta, "Carbon Incorporation in ZnSe grown by Metalorganic Chemical Vapor Deposition ", *Appl.Phys.Lett.*, 55, 463-465, (1989c)

Gimmeiss, H.G., C.Ovren and R.Mach, "Electrical and Optical properties of the 'Cu-Red' Center in ZnSe", *J.Appl.Phys.*, 50, 6328-6333 (1979)

Goldstein,J.I., eds. "*Scanning Electron Microscopy and X-ray microanalysis*", New York, (1981)

Gordon,C.D., private communication

Gotoh, J., H.Fujiwara, H.Shirai, J.Hanna and I.Shimizu, "Low-Temperature Growth of ZnSe-based Pseudomorphic Structures by hydrogen-Radical-Enhanced Chemical Vapor Deposition", *J.Cryst.Growth*, 117, 85-90, (1992)

Gotoh, J., H.Shirai, J.Hanna and I.Shimizu, "Improvement of Photoluminescence Properties of ZnSe Film grown by Hydrogen Radical-Enhanced Chemical Vapor Deposition Using lternate Gas Supply and Substrate Bias Application", *Jpn.J.Appl.Phys.*, 30, L1241-1243, (1991)

Gotoh, J., T.Kobayashi, H.Shirai, J.Hanna and I.Shimizu, "Coherent Growth of ZnSe Thin Film at Low Growth temperature by Hydrogen Radical Enhanced Chemical vapor Deposition", *Jpn.J.Appl.Phys.*, 29, L1767-L1770, (1990)

Gunshor, R., A.Nurmikko and M.Kobayashi, "II-VI Semiconductors come of age", *Physics World*, 46-50, (1992)

Haase,M.A., J.Qiu, J.M.DePuydt and H.Cheng, "Blue-Green Laser Diodes", *Appl.Phys.Lett.*, 59, 1272-1274, (1991a)

Haase,M.A., J.M.DePuydt, H.Cheng and J.E.Potts, "Electromigration in p-type ZnSe:Li", *Appl.Phys.Lett.*, 58, 1173-1175, (1991b)

Hails,J.E. and S.J.C.Irvine, "Screening of Organotellium compounds for Use as MOVPE Precursors", *J.Cryst.Growth*, 107, 319-324, (1991)

Hamata,T., T.Hariu and S.Ono, "Plasma Assisted Epitaxial Growth of p-type ZnSe in Nitrogen-Based Plasma", *Jpn.J.Appl.Phys.*, 32, 674-677, (1993)

Hartmann,H., R.Mach and B.Selle, "Wide Gap II-VI Compounds as electronic Materials", *Current Topics in Materials Science*, Vol.9, (1982)

Heiman,D., "Fiber Optics for Low-Temperature Spectroscopy: Applications to Photoluminescence from (Cd,Mn)Te", *Rev.Sci.Instrum.* 56, 684-687 (1985)

Helms,C.R., Possible New Mechanism of Acceptor Character for Oxygen in ZnSe and Other II-VI Semiconductors", *Jpn.J.Appl.Phys.*, 32, 1558-1561, (1993)

Hess,K.L. and R.J.Riccio, "Integrated Safety system for MOCVD Laboratory", *J.Cryst.Growth*, 77, 95-100, (1986)

Hirata,S., S.Fujita, S.Fujita and M.Isemura, "OMVPE Growth of ZnSe and ZnS_xSe_{1-x} Using Methylselenol As a Selenium Source", *J.Cryst.Growth*, 104, 521-526, (1990)

Hirose,M., "Plasma-Deposited Films:Kinetics of Formation,Composition and Microstructure", in *Plasma Deposited Thin Films* eds. by Mort,J. and F.Jansen, 21-45, CRC Press,Inc., (1985)

Hopfield, H.H., D.G.Thomas and R.T.Lynch, "Isoelectronic Donors and Acceptors", *Phys.Rev.Lett.*, 17, 312-315, (1966)

Huh,J.S., S.Patnaik and K.F.Jensen, "Low Pressure OMVPE of ZnSe with Hydrogen Selenide and Dimethylzinc-Triethylamine", *J.Electron. Mater.*, 22, 509-514, (1993)

Isshiki,M., T.Yoshida, K.Igaki, W.Uchida and S.Suto, "Photoluminescence Spectra of High Zinc Selenide Single Crystal", *J.Cryst.Growth*, 72, 162-166, (1985)

Jensen,K.F., A. Annapragada, K.L Ho, J.S. Huh, S. Patnaik and S. Salim, "Metallogranic Chemical Vapor Deposition :Examples of the Influence of Precursor Structure on Film Properties", *J. de Physique II*, 1 C2:243 -C2:252 (1991)

Jeon,H., J.Ding, A.V.Nurmikko, W.Xie, D.C.Grillo, M.Kobayashi, R.L.Gunshor, G.C.Hua and N.Otsuka, "Blue and Green Diode Lasers in ZnSe-based Quantum Wells", *Appl.Phys.Lett.*, 60, 2045-2047, (1992a)

Jeon,H., J.Ding, A.V.Nurmikko, W.Xie, M.Kobayashi, R.L.Gunshor, "ZnSe based Multilayer p-n junctions as Efficient Light Emitting Diodes for Display Applications"", *Appl.Phys.Lett.*, 60, 892-894, (1992b)

Jeon,H., J.Ding, A.V.Nurmikko, W.Xie, D.C.Grillo, M.Kobayashi, R.L.Gunshor, "Blue-Green Injection Laser Diodes in (Zn,Cd)Se/ZnSe Quantum Wells", *Appl.Phys.Lett.*, 59, 3619-3621, (1991a)

Jeon,H., J.Ding, A.V.Nurmikko, H.Luo, N.Samarth and J.Furdyna, "Low Threshold Pulsed and Continuous-wave Laser Action in Optically Pumped (Zn,Cd)Se/ZnSe Multiple Quantum Well Lasers in the Blue-Green Range", *Appl.Phys.Lett.*, 59, 1293-1295, (1991b)

Johnson,E., R.Tsui, D.Convey, N.Mellen and J.Curless, "A MOCVD Reactor Safety System for a Production Environment", *J.Cryst.Growth*, 68, 497-501, (1984)

Jones,A.C., "Metalorganic Precursors for VApor Phase Epitaxy", *J.Cryst.Growth*, 129, 728-773, (1993)

Jones,A.C., P.J.Wright and B.Cockayne, "Precursors for II-VI Semiconductors : Requirements and Developments", *J.Cryst.Growth*, 107, 297-308, (1991)

Kamata,A., T.Uemoto, M.Okajima, K.Hirahara, M.Kawachi and T.Beppu, "Superiority of Group VII Element over Group III Elements as Donor Dopants in MOCVD ZnSe", *J.Cryst.Growth*, 86, 285-289 (1988)

Kamata,A., Y.Zota, M.Kawachi, T.Sato, M.Okajima, K.Hirahara and T.Beppu, "Deep level Characterization for Al Doped ZnSe grown by MOCVD", *18th International Conference on Solid State Device Materials*, Tokyo, 651-654, (1986)

Kanda,T., I.Suemune, Y.Kan and M.Yamanishi, "Thermal Stability of Nearly Lattice-Matched ZnSSe/GaAs Interface grown by MOVPE", *J.Cryst.Growth*, 93, 662-666 (1988)

Khan,O.F.Z., P.O'Brien, P.A.Hamilton and J.R.Walsh, "Investigation of some adducts of Dimethyl Cadmium and Dimethyl Zinc, in the Vapor Phase, by Infrared Spectroscopy", *Chemtronics*, 244-247 (1989)

Kosai,K., B.J.Fitzpatrick, H.G.Grimmeiss, R.N.Bhargava and G.F.Neumark, "Shallow Acceptors and p-type ZnSe", *J.Cryst.Growth*, 91, 639-646, (1988)

Kroger,F.A., *The Chemistry of Imperfect Crystals*, North-Holland (1964)

Kukimoto,H., "Conductivity Control of Wide Gap II-VI Compounds", *Growth and Optical Properties of Wide-Gap II-VI Low Dimensional Structures*, eds T.C.McGill and Gebharbt, Plenum Press, 119-127 (1989)

Lansari,Y., J.Ren, B.Sneed, K.A.Bowers, J.W.Cook,Jr., and J.F.Schetzina, "Improved Ohmic Contacts for p-type ZnSe and Related p-on-n Diode Structures", *Appl.Phys.Lett.*, 61, 2554-2556, (1992)

Lansari,Y., Z.Yu, J.Ren, C.Boney, J.W.Cook,Jr., and J.F.Schetzina, "Integrated Heterostructure Devices (IHDS): A New Approach For the Fabrication of

High-Efficiency Blue/Green Light Emitters based on II-VI Materials", *MRS Fall Conference*, (1992)

Lee B.H., "Elastic Constants of ZnTe and ZnSe between 77°-300°K", *J.Appl.Phys.*, 41, 2984-2987, (1970)

Lilley,P., M.R.Czerniak, J.E.Nicholls and J.IDavies, "Control of Optoelectronic Properties of ZnSe Films grown on GaAs by VPE", *J.Cryst.Growth*, 59, 161-166, (1982)

Ludowise,M.J., "Metalorganic Chemical Vapor Deposition of III-V Semiconductors", *J.Appl.Phys.*, 58, R31-55, (1985)

Lum,R.M., J.K.Klingert and B.V.Dutt, "An Integrated Laboratory-Reactor MOCVD Safety System", *J.Cryst.Growth*, 75, 421-428, (1986)

Manasevit,H.M. and W.I.Simpson, "The Use of Metal-Organics in the Preparation of Semiconductor Materials -II-VI Materials", *J. Electrochem. Soc.*, 118, 644-647, (1971)

Matsumoto,T., T.Iijima, and H.Goto, "LP-VPE of In-doped ZnSe with Controlled Electrical Properties", *J.Cryst.Growth*, 99,427-431 (1990)

Matsumoto,T., T.Iijima, Y.Katsumata and T.Ishida, "Electrical and Luminescent Properties of In-doped ZnSe grown by LP-Vapor Phase Epitaxy", *Jpn.J.Appl.Phys.*, 26, L1736-1739, (1987)

Matthews, J.W. and A.E.Blakeslee, "Defects in Epitaxial Multilayers", *J.Cryst.Growth*, 32, 265-273, (1976)

Matthews,J.W. and A.E.Blakeslee, "Defects in Epitaxial Multilayers: Misfit Dislocations", *J.Crystal Growth* , 27 118-125 (1974)

Marfaing,Y., "Self-Compensation in II-VI Compounds", *Prog.Cryst.Growth Charact.*, 4, 317-343, (1981)

Mino,N., M.Kobayashi, M.Konagai and K.Takahashi, "Plasma-Assisted Metalorganic Chemical Vapor Deposition of ZnSe Films", *J.Appl.Phys.*, 59, 2216-2221, (1986)

Mitsuhashi, H., I.Mitsuishi and H.Kukimoto, "Growth Kinetics in the MOVPE of ZnSe on GaAs Using Zinc and Selenium Alkyls", *J.Cryst.Growth*, 77, 219-222, (1986)

Mitsuhashi, H., I.Mitsuishi, M.Mizuta and H.Kukimoto, "Coherent Growth of ZnSe on GaAs by MOCVD", *Jpn.J.Appl.Phys.*, 24, L578-580, (1985)

Mullin,J.B., D.J.Cole-Hamilton, S.J.C.Irvine, J.E.Hails, J.Giess and J.S.Gough, "MOVPE of Narrow and Wide Gap II-VI Compounds", *J.Cryst.Growth*, 101, 1-13, (1990)

Myhajlenko,S., J.L.Batsone, H.J.Hutchinson and J.W.Steeds, "Luminescence Studies of Individual Dislocations in II-VI (ZnSe) and III-V (InP) Semiconductors", *J.Phys.C:Sol.State Phys.*, 17, 6477-6492, (1984)

Nagai, H., "Structure of Vapor-Deposited $Ga_XIn_{1-X}As$ Crystals", *J.Appl.Phys.*, 45, 3789-3794 , (1974)

Nakanishi,K., I.Suemune, Y.Fuji, Y.Kuroda and M.Yamanishi, "High Output Power (>20W) and High Quantum Efficiency in a Photopumped ZnSe/ZnSSe Blue Laser Operating at Room Temperature, *Jpn.J.Appl.Phys.*, 30, L1399-1401, (1991)

Nelson,W.A., *Active Nitrogen*, Academic Press, New York, (1968)

Neumark,G.F., "Electrical Properties of Twinned ZnSe;p-type ZnSe and the Role of Twinning", *Materials Science Forum*, 38-41, 513-518, (1989a)

Neumark,G.F. "Achievement of Low-Resistivity p-type ZnSe and the role of Twinning", *J.Appl.Phys.*, 65, 4859-4863, (1989b)

Neumark,G.F., "Achievement of Well Conducting Wide-Band-Gap Semiconductors: Role of Solubility and Non-equilibrium Impurity Incorporation", *Phys.Rev.Lett.*, 62, 1800-1803, (1989c)

Neumark,G.F. and S.P.Herko, "Li-Doped ZnSe and Problems of p-type Conduction", *J.Cryst.Growth*, 59, 189-195, (1982)

Neumark,G.F., "Are Impurities in II-VI Compounds in Large-Band-Gap Semiconductors?", *J.Appl.Phys.*, 51, 3383-3387 (1980)

Nishimura,K., Y.Nagao and K.Sakai, "Metalorganic Vapor Phase Epitaxy of ZnSe Using Tertiarybutylselenol at Selenium Source Precursor", *Jpn.J.Appl.Phys.*, 32, L428-L430, (1993)

O'Brien, P., "Chemical Considerations in the design and Use of Precursors for the Deposition of II-VI Materials of II/VI Materials by MOCVD and Related Methods", *Chemtronics*, 5, 61-70, (1991)

Ohmi,K., I.Suemune, T.Kanda, Y.Kan, M.Yamanishi, F.Nishiyama and H.Hasai, "Stability and Interdiffusion at MOCVD grown ZnSe/GaAs Interfaces", *J.Cryst. Growth*, 86 467-470 (1988)

Ohmi,K., I.Suemune, T.Kanda, Y.Kan and M.Yamanishi, "Lattice-Mismatched Enhanced Diffusion at a ZnSe/GaAs Interface - Increase of Thermal Stability in a Lattice-Matching System" *Jpn.J.Appl.Phys.*, 26, L2072-2075, (1987)

Ohkawa.K., A.Ueno and T.Mitsuyu, "MBE growth of p-type and n-type ZnSe homoepitaxial layers", *J.Cryst.Growth*, 117, 375-384, (1992)

Ohkawa.K. and T.Mitsuyu, "p-type ZnSe homoepitaxial layers grown by MBE with nitrogen radical doping", *J.Appl.Phys.*, 70, 439-441, (1991a)

Ohkawa.K., T.Karasawa and T.Mitsuyu, "Doping of Nitrogen Acceptors into ZnSe using a radical beam during MBE growth", *J.Cryst. Growth*, 111, 797-801, (1991b)

Ohkawa.K., T.Karasawa and T.Mitsuyu, "Characteristics of p-type ZnSe Layers grown by MBE with Radical Doping", *Jpn.J.Appl.Phys.*, 30, L152-155, (1991c)

Ohkawa,K., T.Mitsuyu and O.Yamazaki, "Effcet of Biaxial Strain on Exciton Luminescence of Heteroepitaxial ZnSe Layers", *Phys.Rev.B.*, 38, 12465-12469 (1988)

Ohki,A., Y.Kawaguchi, K.Ando and A.Katsui, "Acceptor compensation mechanism by midgap defects in nitrogen-doped ZnSe films", *Appl.Phys.Lett.*, 59, 671-673, (1991)

Ohki,A., "High Concentration Nitrogen Doping in MOVPE grown ZnSe", *J.Cryst.Growth*, 99, 413-417 (1990)

Ohki,A., N.Shibata, K.Ando and A.Katsui, "Nitrogen-Doped p-Type ZnSe Films grown by MOVPE", *J.Cryst.Growth*, 93, 692-696 (1988)

Oigawa,H., J.Fan. Y.Nannichi, K.Ando, K.Saiki and A.Koma, "Studies on an $(NH_4)_2S_x$- Treated GaAs Surface Using AES,LEEls and RHEED",*Jpn.J.Appl.Phys.*, 28, L340-344 (1989)

Pankove,J.I., Optical Processes in Semiconductors, 107-159, Dover Publication, New York, 1971

Parbrook,P., A.Kamata and T.Uemoto, "CdZnSe-ZnSe Multilayers by Metalorganic Vapor Phase Epitaxy Using Dimethylselenide", *Jpn.J.Appl.Phys.*, 32, 669-673, (1993)

Park,R.M., M.B.Troffer, E.Yablonovitch and T.J.Gmitter, "Noncontact electrical characterization of low-resistivity p-type ZnSe:N grown by MBE", *Appl.Phys.Lett.*, 59, 1896-1899, (1991)

Park,R.M., M.B.Troffer, C.M.Rouleau, J.M.DePuydt and M.A.Haase, "p-type ZnSe by nitrogen atom beam doping during molecular beam epitaxial growth", *Appl.Phys.Lett.*, 57, 2127-2129, (1990)

Patnaik,S., K.L.Ho, K.F. Jensen D.C.Gordon, R.U.Kirss and D.W.Brown, , "Decomposition of Allylselenium Sources in the Metalorganic Chemical Vapor Deposition of ZnSe", *Chem. Mater.* 5, 305-310 (1993)

Patnaik,S., K.F. Jensen and K. P. Giapis, "MOVPE of ZnSe Using Organometallic Allyl Selenium Precursors", *J. Crystal Growth,*, 107, 390-395 (1991)

Price,S.J. and A.F.Trotman-Dickenson, "Metal-Carbon Bonds: Part2-The Pyrolysis of Dimethyl Zinc", *Trans.Faraday Soc.*, 53, 1208-1213 (1957)

Qiu,J., J.M.DePuydt, H.Cheng and M.A.Haase, "Heavily doped p-type ZnSe:N grown by MBE", *Appl.Phys.Lett.*, 59, 2992-2994, (1991)

Ren,J., K.A.Bowers, J.W.Cook,Jr., and J.F.Schetzina, "Properties of ZnS_xSe_{1-x}--$Zn_{1-y}Cd_ySe$ Quantum Well Structures", *J.Vac.Sci. Technol.*, B10, 909-911, (1992a)

Ren,J., K.A.Bowers, J.W.Cook,Jr., and J.F.Schetzina, "Properties of ZnSe-$ZnS_{0.9}Te_{0.1}$ and ZnSe-$Zn_{0.9}Cd_{0.1}Se$ Multilayers", *J.Cryst.Growth*, 117, 510-514 (1992b)

Ren,J., K.A.Bowers, B.Sneed, F.E.Reed, J.W.Cook,Jr., and J.F.Schetzina, "Blue ZnSe and Green $ZnS_{0.9}Te_{0.1}$ Lighting Emitting Diodes", *J.Cryst.Growth*, 111, 829-832 (1991)

Ren,J., K.A.Bowers, B.Sneed, D.L.Dreifus, J.W.Cook,Jr., and J.F.Schetzina, " ZnSe Lighting Emitting Diodes", *Appl.Phys.Lett* 57, 1901-1903 (1990)

Robbins,D.J., P.J.Dean, P.E.Simmonds and H.Tews, "The Optoelectronic Properties of Copper in Zinc-Cation II-VI Compound Semiconductors", *Deep Centers in Semiconductors*, eds by S.T.Pandelides, Chapter 11, 717-772, (1986)

Robinson,R.J. and Z.K.Kun, "p-n junction Zinc Sulfo-Selenide and Zinc Selenide Lighting Emitting Diodes", *Appl.Phys.Lett.*, 27, 74-76, (1975)

Ruda,H.E., "A Theoretical Analysis of Electron Transport in ZnSe", *J.Appl.Phys.*, 59, 1220-1231, (1986)

Saito,J., T.Ishikawa, T.Nakamura, K.Nanbu, K.Kondo and A.Shibatomi, "Effect of Thermal Etching on GaAs Substrate in Molecular Beam Epitaxy", *Jpn.J.Appl.Phys.*, 25, 1216-1220 (1986)

Sandroff,C.J., R.N.Nottenburg, J.-C.Bischoff and R.Bhat, "Dramatic Enhancement in the Gain fo a GaAs/AlGaAs Heterostructure Bipolar Transistor by Surface Chemical Passivation", *Appl/Phys.Lett.*, 51, 33-35, (1987)

Sax,N.I., "*Dangerous Properties of Industrial Materials*", 5th ed., New York, Van Norstrand Rheinhold, (1979)

Shahzad,K., D.J.Olego and D.A.Cammack, "Optical Transitions in Ultra-High-Purity Zinc Selenide", *Phys.rev.B.*, 39, 13016-13019, (1989)

Shahzad, K., "Excitonic Transitions in ZnSe Epilayers grown on GaAs", *Phys.Rev.B*, 38, 8309-8312, (1988)

Shibata,N., A.Ohki and S.Zembutsu, "Use of Ethyliodine in Preparation of Low-Resistivity n-Type ZnSe by MOVPE", *Jpn.J.Appl.Phys.*, 27, L251-253, (1988a)

Shibata,N., A.Ohki and A.Katui, "Iodine-Doped Low Resistivity n-type ZnSe Films grown by MOVPE", *J.Cryst.Growth*, 93, 703-707, (1988b)

Shibata,N., A.Ohki., S.Zembutsu. and A.Katsui, "Thermoelastic Strain in ZnSe Films grown on GaAs by Metalorganic Vapor Phase Epitaxy", *Jpn.J.Appl.Phys.*, 27, L487-489, (1988c)

Skromme,B.J., M.C.Tamargo, J.L.de Miguel and R.E.Hahory, "Photoluminescence of Heteroepitaxial ZnSe/GaAs and ZnSe/AlAs grown by MBE", *Mater. Res.Soc.Symp.Proc.*, 102, 577-582, MRS, Pittsburg, (1988)

Sritharan,S., K.A.Jones and K.M.Motyl, "The MOCVD Growth of ZnSe Using Me_2Zn, H_2Se and $SeEt_2$", *J.Cryst.Growth*, 68, 656-664, (1984a)

Sritharan,S. and K.A.Jones, "MOCVD Growth of ZnSe Films Using Diethylselenide", *J.Cryst.Growth*, 66, 231-234, (1984a)

Stanzl,H., K.Wolf, S.Bauer, A.Naumov and W.Gebhardt, "Low Temperature Growth and Characterization of ZnSe Films grown on GaAs", *J.Electron Mater.*, 22, 501-503, (1993)

Stringfellow,G.B., "Organometallic Vapor Phase Epitaxy; Theory and Practice", Acadenic Press, 15-50, (1989)

Stuecheli,N. and E.Bucher, "Low Resistive p-type ZnSe: A Key for Efficient Blue Electoluminescence Device", *J.Electron.Mater.*, 18, 105-108, (1989)

Stutius,W., "Nitrogen as Shallow Acceptor in ZnSe grown by Organometallic hemical Vapor Deposition", *Appl.Phys.Lett.*, 40, 246-248, (1982)

Stutuis,W., "Photoluminescence and Heterojunction Properties of ZnSxSe1-x Epitaxial Layers on GaAs and Ge Grown by Organometallic CVD", *J.Electron.Mater.*, 10, 95-106 (1981a)

Stutius,W., "Preparation of Low-Resistivity n-type ZnSe by Organometallic Chemical Vapor Deposition", *Appl. Phys. Lett.*, 38, 352-354 (1981b)

Stutuis,W., "Organometallic Vapor Phase Epitaxial ZnSe Films on GaAs Substrates", *Appl. Phys. Lett.*, 33, 656-658 (1978)

Suemune,I., H.Masato, K.Nakanishi, Y.Kuroda and M.Yamanishi, "Doping of nitrogen in ZnSe films: improved doping properties in ZnSe/ZnSSe periodic layered structures grown on GaAs by MOVPE", *J.Cryst.Growth* , 107,679-682 (1991)

Suemune,I., K.Yamada, H.Masato, T.Kanda, Y.Kan and M.Yamanishi, " Characterization of Nitrogen-Doped ZnSe and ZnS0.06Se0.94 Films grown by MOVPE", *Jpn.J.Appl.Phys.*, 27, L2195-2198 (1988)

Taskar,N.R., B.A.Khan, D.R.Dorman and K.Shahzad, "Novel technique for p-type nitrogen doped ZnSe epitaxial layers", *Appl.Phys.Lett.*, 62, 270-272, (1993)

Tew.H., H.Venghaus and P.D.Dean, "Excited States of Shallow Acceptors in ZnSe", *Phys.Rev.*, B19, 5178-5184, (1979)

Tu,D.W. and A.Kahn, "ZnSe- and Se-GaAs Interfaces", *J.Vac.Sci.Technol.*, A3, 922-925, (1985)

Van der Pauw,L.J., "A method of measuring specific resistivity and Hall effect of a discs of arbitrary shape", *Philips Res.Reports*, 13, 1-9, (1958)

Vickerman,J.C., A.Brown and N.M.Reed, *Secondary Ion Mass Spectrometry*, Oxford University Press, Oxford, (1989)

Williams,J.O., E.S.Crawford, J.L.Jenkins, B.Cockayne and P.J.Wright, "High Resolution TEM of Epitaxially grown ZnSe/GaAs Interfaces", *J.Mater.Sci.*, 3, 189 (1984)

Wolk,J.A., J.W.Ager III, K.J.Duxstad, E.E.Haller, N.R.Tasker, D.R.Dorman and D.J.Olego, "Local Vibration Mode Spectroscopy of Nitrogen-Hydrogen Complex in ZnSe", *Appl.Phys.Lett.*, to be published.

Wright,P.J., B.Cockayne, P.E.Oliver, A.C.Jones, "Control of Prereaction in the Metalorganic Chemical Vapor Deposition of Zinc- and Cadmium- based Chalcogenides", *J.Crystal Growth*, 108 525-533 (1991)

Wright, P.J., B.Cockayne, P.J.Parbrook, A.C.Jones, P.O'brien and E.D.Orrell, "MOCVD Layer Growth of ZnSe and ZnS/ZnSe Multiple Layers Using Containing Adducts of Dimethylzinc", *J.Cryst.Growth*, 104, 601-619, (1990)

Wright, P.J., P.J.Parbrook, B.Cockayne, A.C.Jones, E.D.Orrell, K.P.O'Donnell and B. Henderson, "The MOCVD Growth without Prereaction of ZnSe and ZnS Layers", *J.Cryst.Growth*, 94, 441-447, (1989)

Wright, P.J., B.Cockayne, A.C.Williams, A.C.Jones, and E.D.Orrell, "MOCVD Layer Growth of ZnSe Using a New Zinc Source", *J.Cryst.Growth*, 84, 552-554, (1987)

Wright, P.J., R.J.Griffiths and B.Cockayne, "The Use of Heterocyclic Compounds in the Organometallic Chemical vapor Deposition of Epitaxial ZnS, ZnSe and ZnO", *J.Cryst.Growth*, 66, 26-34, (1984)

Wu,Y.-H., Y.Kawakami, Shizuo, S.Fujita and S.Fujtta, "Growth and Characterization of $(HN_4)_2S_x$ - treated GaAs Substrates; Effect of GaAs Surface Microstructure on the Growth rate of ZnSe", *J.Cryst.Growth*, 111, 757-761, (1991)

Xie,W., D.C.Grillo, R.L.Gunshor, M.Kobayashi, G.C.Hua, N.Otsuka, H.Jeon, J.Ding and V.Nurmikko, "Blue/Green Injection Lasers and Light Emitting Diodes", *J.Vac.Sci.Technol.*, B10, 921-923 (1992a)

Xie,W., D.C.Grillo, R.L.Gunshor, M.Kobayashi, H.Jeon, J.Ding, V.Nurmikko, G.C.Hua and N.Otsuka, "Room Temperature Blue Lighting Emitting p-n Diodes from Zn(S,Se)-based Multiple Quantum Well Structures", *Appl.Phys.Lett.*, 60, 1999-2001, (1992b)

Xie,W., D.C.Grillo, R.L.Gunshor, M.Kobayashi, G.C.Hua, N.Otsuka, H.Jeon, J.Ding and V.Nurmikko, "Blue/Green p-n junction Electroluminescence from ZnSe-based Multiple Quantum-Well Structures", *Appl.Phys.Lett.*, 60, 463-465 (1992c)

Yamada,Y. and T.Taguchi, "Epitaxial Growth and Photoluminescence of ZnSe:Na Films by LP-MOCVD", *J.Cryst.Growth*, 99, 408-412 (1990)

Yanashima,K., K.Koyanagi, K.Hara, J.Yoshino and H.Kukimoto, "MOVPE Growth of p-type ZnSe Using Dimethylaminolithium as the Dopant", *6thInt.Conf. on MOVPE*, 55-56, Cambridge, MA (1992)

Yasuda,T., I.Mitsuishi and H.Kukimoto, "Metalorganic Vapor Phase Epitaxy of Low-Resistivity p-type ZnSe", *Appl.Phys.Lett.*, 52, 57-59, (1988)

Yao T., Y.Okada., S.Matsui, K.Ishida, and I.Fujimoto, "The Effect of Lattice Deformation on Optical Properties and Lattice Parameters on ZnSe grown on (100)GaAs", *J.Cryst. Growth*, 81, 518-523, (1987)

Yao, T. and K.Yamashita, "Phosphorus Acceptor Levels' in ZnSe grown by MBE". *Jpn.J.Appl.Phys.*, 25, 821-827, (1986)

Yao,T., M.Ogura, S.Matsuoka and T.Morishita, "High Quality ZnSe Thin Films grown by Molecular Beam epitaxy", *Appl.Phys.Lett.*, 43, 499-501, (1983)

Yates,H.M and J.O.Williams, "Purity of Zinc Precursors and the Properties of Epitaxial ZnSe grown by Atmospheric Pressure Metalorganic Chemical Vapor Deposition", *J.Cryst.Growth*, 107, 386-389, (1991)

Yodo,T. and K.Yamashita, "Li-Doped ZnSe epitaxial Layers by Ion Implantation", *Appl.Phys.Lett.*, 54, 1178-1180 (1989)

Yodo,T. and K.Yamashita, "Li-doped ZnSe Epitaxial Layers by Ion Implantation", *Appl.Phys.Lett.*, 53, 2403-2405, (1988)

Yoshikawa, A., S.Matsumoto, S.Yamaga and H.KAsai, "Use of Dimethyl Hydrazine As a Acceptor-Dopant Source in Metalorganic Vapor Phase Epitaxy of ZnSe", *J.Cryst.Growth*, 101, 305-310 (1990)

Yoshikawa,A., S.Muto, S.Yamaga and H.Kasai, "Photoluminescence Properties of Li-doped ZnSe Films grown by MOCVD", *Jpn.J.Appl.Phys.*, 27, L260-L262, (1988a)

Yoshikawa,A., S.Muto, S.Yamaga and H.Kasai, "Growth and Properties of Lithium-doped ZnSe films by AP-MOVPE", *J. Cryst.Growth*, 93, 697-702, (1988b)

Yoshikawa,A., S.Muto, S.Yamaga and H.Kasai, Photoluminescence Properties of Nitrogen-Doped ZnSe films grown by Low-Pressure MOVPE", *Jpn.J.Appl.Phys.*, 27, 992-996, (1988c)

Yoshikawa,A., S.Muto, S.Yamaga and H.Kasai, "The Dependence on Growth Temperature of the Photoluminescence properties of Nitrogen-Doped ZnSe grown by MOCVD", *J.Cryst.Growth*, 86, 279-284, (1988d)

Yoshikawa,A., S.Yamaga and K.Tanaka, "New and Simple MOCVD Technique Using Completely Gaseous MO-Sources Especially Useful for growing Zn-Chalcogenide Films", *Jpn.J.Appl.Phys.*, 23, L388-390, (1984)

Yu,Z., J.Ren, Y.Lansari, B.Sneed, K.A.Bowers, C.Boney, D.B.Eason, R.P.Vaudo, K.J.Gossett, J.W.Cook,Jr., and J.F.Schetzina, " Light Emission from Quantum Well Structures Containing ZnS, ZnSe and Related Alloys", *Jpn.J.Appl.Phys.*, 32, 663-668, (1993)

Yu,Z., J.Ren, B.Sneed, K.A.Bowers, K.J.Gossett, C.Boney, Y.Lansari, J.W.Cook,Jr., and J.F.Schetzina, " High-Resolution Study of Stimulated Emission from Blue-Green Laser Diodes", *Appl.Phys.Lett.*, 61, 1266-1268, (1992)

Zhang,S and N.Kobayashi, "Using Tertiary Butylamine for Nitrogen Diping during Migration-Enhanced Epitaxial Growth of ZnSe", *Jpn.J.Appl.Phys.*, 31, l666-l668, (1992)